

arXiv:gr-qc/0701083v1 15 Jan 2007

Brane world cosmology with Gauss-Bonnet and induced gravity terms

by

Richard A. Brown

THE THESIS IS SUBMITTED IN PARTIAL FULFILMENT OF THE REQUIREMENTS FOR
THE AWARD OF THE DEGREE OF
DOCTOR OF PHILOSOPHY
OF THE
UNIVERSITY OF PORTSMOUTH

November, 2006

Copyright

© Copyright 2006 by Richard A. Brown. All rights reserved.

The copyright of this thesis rests with the Author. Copies (by any means) either in full, or of extracts, may not be made without the prior written consent from the Author.

Declaration

Whilst registered as a candidate for the above degree, I have not been registered for any other research award. The results and conclusions embodied in this thesis are the work of the named candidate and have not been submitted for any other academic award.

To my family and friends.

Edgar Allan Poe (1809-1849) ponders the subject of matter undergoing collapse:

In sinking into Unity, it will sink at once into that Nothingness which, to all Finite Perception, Unity must be—into that Material Nihilism from which alone we can conceive it to have been evoked—to have been created by the Volition of God.

from Eureka - A Prose Poem (1848), written 81 years before Edwin Hubble's observations of the expansion of the universe.

Abstract

In this thesis we investigate certain cosmological brane world models of the Randall-Sundrum type. The models are motivated by string theory but we focus on the phenomenology of the cosmology.

Two models of specific interest are the Dvali-Gabadadze-Porrati (DGP, induced-gravity) model, where the brane action is modified, and the Gauss-Bonnet model where the bulk action is modified. Both of these modifications maybe motivated by string theory.

We provide a brief review of Randall-Sundrum models and then consider the Kaluza-Klein modes on Minkowski and de Sitter branes, in both the two and one brane cases. The spectrum obtained for the de Sitter branes is a new result. We then consider a Friedmann-Robertson-Walker brane in order to investigate the cosmological dynamics on the brane.

We present a brief discussion of the DGP and Gauss-Bonnet brane worlds. We then investigate the Gauss-Bonnet-Induced-Gravity (GBIG) model where the Gauss-Bonnet (GB) bulk term is combined with the induced-gravity (IG) brane term of the DGP model. We present a thorough investigation of cosmological dynamics, in particular focusing on GBIG models that behave like self-accelerating DGP models at late times but at early times show the remarkable feature of a finite-temperature Big Bang. We also discuss the constraints from observations, including ages and Big Bang nucleosynthesis.

Preface

The work of this thesis was carried out at the Institute of Cosmology & Gravitation, University of Portsmouth, United Kingdom.

The following chapters are based on published work:

- Chapter 3 - R. A. Brown, Roy Maartens, Eleftherios Papantonopoulos and Vasilis Zamarias. “A late-accelerating universe with no dark energy-and a finite-temperature big bang”, JCAP 0511 (2005) 008, gr-qc/0508116.
- Chapter 4 - R. A. Brown. “Brane Universes with Gauss-Bonnet-Induced-Gravity”, accepted for publication in “General Relativity and Gravitation”, gr-qc/0602050.

Acknowledgements

First and foremost I would like to thank Roy Maartens without whose support, guidance and infinite patience this thesis would never have been completed. Other people who directly influenced this work and require my thanks include Mariam Bouhmadi-López, Chris Clarkson, Kazuya Koyama and Sanjeev Seahra the Maple Guru. I must also include David Wands and Andrew Mennim for useful discussions. Other people who deserve thanks for their support and making my stay in the ICG more pleasurable are Kishore Ananda, Frederico Arroja, Iain Brown, Chris Byrnes, Dan Carson, Robert Crittenden, Mathew Smith and David Wake. Kishore Ananda deserves special thanks for putting up with me as a flat mate for the three years of my PhD study.

I would also like to thank all the teaching staff in the Physics and Astronomy department at the University of Hertfordshire. Without the foundation degree course provided there I would never have got into cosmology in any practical way.

I must also thank dear friends such as Dan Mee, my connection to the real world outside academia in Portsmouth. Also all the Hatfield guys who are able to make me forget all about work within a few minutes of meeting up. I want to thank all the Haslemere crew as well, whose friendship I know I can rely upon however long it is between meeting up.

Last but not least I must thank my family whose support is one of the few constants in life that can be relied upon however bad things get.

Without all these people, starting, let alone finishing, this project would never have happened.

Table of Contents

Abstract	v
Preface	vi
Acknowledgements	vii
1 Introduction	1
2 RS Brane Worlds	7
2.1 Introduction	7
2.2 Minkowski Branes	7
2.2.1 The background	7
2.2.2 Field equations on the brane	10
2.2.3 Kaluza-Klein Modes	11
2.3 de Sitter Brane Worlds	19
2.3.1 The background	19
2.3.2 Kaluza-Klein modes	22
2.4 Friedmann Equations	26
2.4.1 The GR result	27
2.4.2 RS result	29
2.5 Conclusions	33
3 The DGP, GB and GBIG Brane World Cosmologies	34
3.1 Introduction	34
3.2 DGP Branes	35
3.3 Gauss-Bonnet Brane Worlds	37
3.4 Gauss-Bonnet-Induced Gravity (GBIG) Branes	39
3.4.1 Field Equations	40
3.4.2 DGP brane with GB bulk gravity: combining UV and IR modifi- cations of GR	41

3.4.3	Cosmological Dynamics	46
3.4.4	Nucleosynthesis and the age of the universe	51
3.5	Conclusions	57
4	Generalised cosmologies with Induced Gravity and Gauss-Bonnet terms	60
4.1	Introduction	60
4.2	Field Equations	60
4.3	Friedmann Equation Solutions	63
4.3.1	Minkowski bulk ($\phi = 0$) with brane tension	63
4.3.2	AdS bulk ($\phi \neq 0$) with brane tension	68
4.4	Conclusions	79
5	Conclusions	81
A	Conventions	86
	References	87

List of Figures

1.1	The RS1 configuration	3
1.2	The RS2 configuration	4
2.1	A plot of the potential in equation (2.70) with $\ell = 1$	17
2.2	A plot of equation (2.76) with $L/\ell = 1/4$, $1/2$ and $L/\ell = 1$ for the solid, dashed and pale solid lines respectively.	18
2.3	Determining the KK mass eigenvalues for two de Sitter branes with $L/\ell = 1/4$, $1/2$ and $L/\ell = 1$ for the solid, dashed and light solid lines respectively. The y-axis is the left-hand side of Eq. (2.116). $H\ell = 0.1$ in this plot.	24
2.4	A plot of the first massive mode as a function of L/ℓ (solid line), and the mass-gap (dashed line). We see that as we increase L/ℓ the first massive mode approaches $3H/2$. $H\ell = 1$ in this plot.	25
2.5	The KK mass eigenvalues for two de Sitter branes with different values of $H\ell$, i.e. different energy regimes. $H\ell = 0.1$, 1 and $H\ell = 10$ for the solid, dashed and light solid lines respectively. The y-axis is the left-hand side of Eq. (2.116). $L/\ell = 1$ in this plot.	26
2.6	A plot of the first massive mode as a function of $H\ell$ (solid line), and the mass-gap (dashed line). We see that as we increase $H\ell$ the first massive mode diverges from $3H/2$. $L/\ell = 1$ in this plot.	27
3.1	Solutions of the DGP Friedmann equation (h vs μ) with $\mathcal{C} = \Lambda_5 = \lambda = 0$. (Brane proper time τ flows from right to left, with $\tau = \infty$ at $\mu = 0$.) . . .	37
3.2	DGP and GB solutions of the Friedmann equation (H vs ρ) for a Minkowski bulk. (Brane proper time t flows from right to left, with $t = \infty$ at $\rho = 0$.) .	40
3.3	Solutions of the GBIG Friedmann equation ($h(\mu)$) with positive γ ($\gamma = 0.1$). On the left is the DGP (+) model and its Gauss-Bonnet corrections, GBIG 1 and GBIG 2. On the right is the DGP (−) model and its GB correction, GBIG 3. The curves are independent of the equation of state w . Brane proper time τ flows from right to left, with $\tau = \infty$ at $\mu = 0$. . .	42

3.4	Solutions of the GBIG Friedmann equation ($h(\mu)$) with negative γ ($\gamma = -0.1$). On the left is the DGP ($-$) model and its Gauss-Bonnet corrections, GBIG 1 and GBIG 2. On the right is the DGP ($+$) model and its GB correction, GBIG 3. The curves are independent of the equation of state w . Brane proper time τ flows from right to left, with $\tau = \infty$ at $\mu = 0$.	43
3.5	The dependence in GBIG 1–2 of the initial expansion rate and density on γ .	47
3.6	The GBIG 1–2 late-time asymptotic expansion rate as a function of γ .	47
3.7	The acceleration $f = a''/a$ vs $x = h^2$, for a GBIG 1 cosmology with inflation, followed by radiation domination, followed by late-time self-acceleration. Brane proper time flows from right to left. Here $\gamma = 1/12$, and $n = 0.8$ in Eq. (3.69).	51
3.8	The left plots use the plus branch of Eq. (3.83), the right plots use the negative branch. Values used are $\Omega_{rc} = 0.1$, $\Omega_m = 1/4$, $\Omega_\phi = 0$ and $\Omega_\lambda = 0$, so that $\Omega_{\alpha+} = 0.372$ and $\Omega_{\alpha-} = -4.372$. The top plots show the Hubble rates against redshift. The bottom two plots are the equivalent plots in h, μ .	54
3.9	The Ω_m, Ω_{rc} plane for GBIG 1. The central dashed line is for $\Omega_\alpha = 0$. On the left the dashed lines are $z_i = 10$ and the solid lines are $z_i = 2$. On the right the solid lines are $z_i = 1100$, the decoupling redshift. The lines above $\Omega_\alpha = 0$ have $\Omega_\alpha < 0$, while those below $\Omega_\alpha = 0$ correspond to $\Omega_\alpha > 0$. The magnitude of Ω_α increases as you move away from the $\Omega_\alpha = 0$ line.	56
3.10	The Ω_m, Ω_{rc} plane for $\Omega_{\alpha+}$ and $z_i = 1100$. The dotted line is for $\Omega_\alpha = 0$.	56
3.11	The age of the universe for $\Omega_{\alpha+}$.	57
3.12	As in Fig. 3.11, but viewed from above.	58
3.13	The age of the universe for $\Omega_{\alpha-}$.	58
3.14	As in Fig. 3.13, but viewed from above.	59
4.1	The effective bulk cosmological constant ϕ as a function of χ .	62
4.2	Solutions of the Friedmann equation (h vs μ) with negative brane tension ($\sigma = -4$) in a Minkowski bulk ($\phi = 0$) with $\gamma = 1/10$. The curves are independent of the equation of state w . The arrows indicate the direction of proper time on the brane.	63
4.3	Solutions of the Friedmann equation with positive brane tension ($\sigma = 2$) in a Minkowski bulk ($\phi = 0$) with $\gamma = 1/10$.	64

4.4	Plots of μ vs τ and h vs τ for GBIG 3 in a Minkowski bulk ($\phi = 0$) with negative brane tension ($\sigma = -1/4$). We see that GBIG 3 loiters around $\mu = \mu_l = -\sigma$, $h = 0$ before evolving towards a vacuum de Sitter solution ($\mu_e < 0$). (Here $\gamma = 1/10$. The solid line is $w = 1/3$. The dotted line is $w = 0$.)	65
4.5	Solutions of the Friedmann equation (h vs μ) in a Minkowski bulk ($\phi = 0$) with $\gamma = 1/7$. The vertical lines represent the $\mu = 0$ axis for the labeled brane tensions.	66
4.6	The (σ, γ) plane for solutions in a Minkowski ($\phi = 0$) bulk. The short dotted horizontal line is $\gamma_m = 1/3$. GBIG 1-2 exist with positive energy density in regions III, IV and V.	67
4.7	The plot on the left is h vs μ for three different solutions, all with $\phi = 0$. The plot on the right shows h' vs μ for the same solutions. (1): $\gamma = 1/3 - 0.1$, $\sigma = -3$. (2): $\gamma = 1/3$, $\sigma = -2.5$. (3): $\gamma = 1/3 + 0.1$, $\sigma = -2$. Different brane tensions are used purely for clarity.	67
4.8	h_∞ for solutions in a Minkowski ($\phi = 0$) bulk. The thin-dark line has $\sigma = -0.4$, thin-light line has $\sigma = -0.28$, thick-dark lines have $\sigma = -0.2$ and the thick-light lines have $\sigma = 0.2$	69
4.9	Solutions of the Friedmann equation (h vs μ) with negative brane tension ($\sigma = -3/4$) in an AdS bulk ($\phi = -0.01$) with $\gamma = 1/5$. The curves are independent of the equation of state w . The arrows indicate the direction of proper time on the brane.	70
4.10	In order for h_i to be real γ must lie beneath the solid line (γ_m). The region to the right of the vertical dotted line is where GBIG 4 ($h_e > 0$) is allowed (except where $\phi = 0$).	71
4.11	The (σ, γ) plane for solutions in a AdS ($\phi = -0.1$) bulk. The short dotted horizontal line is the maximum value of γ as obtained from Eq. (4.10). . .	72
4.12	The GBIG 4 solution in region I for $\phi = -0.1, \gamma = 0.4 > \gamma_m$ and $\sigma = -1/2$. The plot on the right is h'' vs μ for this solution. This shows the differences between this solution and the similar case when $\phi = -1$, where GBIG 4 is no longer allowed. Arrows denote proper time.	74
4.13	h_∞ for solutions in a AdS ($\phi = -0.1$) bulk. The thin-dark line has $\sigma = -1/2$, thin-light lines have $\sigma = -0.35$, thick-dark line has $\sigma = 0$ and the thick-light lines have $\sigma = 1/2$	75

4.14	Solutions of the Friedmann equation (h vs μ) with negative brane tension ($\sigma = -2$) in an AdS bulk ($\phi = -1$) with $\gamma = 1/10$. For this value of ϕ GBIG 4 no longer exists and GBIG 1 can collapse. The curves are independent of the equation of state w . The arrows indicate the direction of proper time on the brane.	75
4.15	The (σ, γ) plane for solutions in a AdS ($\phi = -1$) bulk. The short dotted horizontal line is the maximum value of γ as obtained from Eq. (4.26). The top horizontal line is from the initial bound in Eq. (4.10).	76
4.16	The GBIG 4 solution in region I for $\phi = -1, \gamma = 0.8 > \gamma_m$ and $\sigma = -1$. The plot on the right is h'' vs μ for this solution. This shows the differences between this solution and the case when $\phi = -0.1$. Arrows denote proper time.	77
4.17	h_∞ for solutions in a AdS ($\phi = -1$) bulk. The thin-dark line have $\sigma = -1.2$, thin-light lines have $\sigma = 0.8$, thick-dark line have $\sigma = 0$ and the thick-light lines have $\sigma = 1.2$	77
4.18	The (σ, γ) plane for solutions in a AdS ($\phi = -5$) bulk. The top horizontal line is the bound from the initial bound in Eq. (4.10).	78
4.19	h_∞ for solutions in a AdS ($\phi = -5$) bulk. The thin-dark line has $\sigma = -3$, thin-light lines have $\sigma = -1/2$, thick-dark lines has $\sigma = 1/2$ and the thick-light lines has $\sigma = 3$	79
5.1	The three GBIG models with zero brane tension in a Minkowski bulk. . .	82
5.2	Generalised GBIG models with negative brane tension in an AdS bulk. . .	83
5.3	Another example of generalised GBIG models with negative brane tension in an AdS bulk.	84

Chapter 1

Introduction

Quantum mechanics and General Relativity are two very successful and well validated theories within their own domains. The problem is that we have no way of unifying them into a single consistent theory. One of the most promising models of unification is String Theory (for an introduction to some of the concepts of String Theory see [1]). String Theories remove the infinities that are present in a classical unification by describing particles as extended 1-dimensional strings rather than point particles. These 1D strings live in a 10 dimensional space, or 11D for supergravity. The idea of extra dimensions was first put forward by Kaluza [2] and Klein [3] in order to unify general relativity and electromagnetism. A perturbative approach is usually applied when working in String Theory due to the complexity of the equations. It has been shown that there are five different formulations of perturbative String Theory and that these are dual to each other, under a certain set of transformations. It has been suggested that these five theories are aspects of one underlying theory, M Theory.

Two classes of strings are the closed and open strings. Gravity is described by closed strings and matter is described by open strings. In non-perturbative string theory there exist extended objects known as D (Dirichlet) branes. These are surfaces where the open strings must start and finish. This provides an alternative to the Kaluza-Klein approach, where matter penetrates the extra dimensions, leading to strong constraints from collider physics. If matter is confined to a 3-dimensional brane, the extra dimensions can be larger, since the constraints on gravity are weaker.

In this thesis we consider brane world models. These models are inspired by String Theory, in particular by the Hořava and Witten model [4]. Brane world models are characterized by the feature that standard model matter is confined to a 1+3 dimensional brane while gravity propagates in the higher dimensional bulk. This means that gravity is fundamentally a higher dimensional interaction and we only see the effective 4D theory on the brane. We can not see or measure (with existing technology) Planck scale compact

dimensions as they require Planck energy scales in order to probe them. But if an extra dimension is large (relative to the Planck scale) then there may be signatures of this in colliders and table-top experiments, as well as in cosmological observations.

In the model of Arkani-Hamed, Dimopoulos and Dvali (ADD) [5], the weakness of gravity on scales $\gtrsim 1\text{mm}$ (Newton's law has only been verified down to a scale of $\sim 0.1\text{mm}$ [6]) is due to the existence of $n \geq 2$ extra compact dimensions. This model can be embedded in String Theory [7] and has the advantage of putting forward a mechanism for explaining the hierarchy problem. The hierarchy problem is the discrepancy between the gravity scale ($M_{\text{Planck}} \sim 10^{19}\text{GeV}$) and the electro-weak scale ($M_{\text{EW}} \sim 10^3\text{GeV}$). The 10^{16} orders between these two scales is too vast to be considered natural. In the ADD model, length scales smaller than the scale of the extra dimensions ($r < L$) have a $4 + n$ dimensional gravitational potential:

$$V \sim r^{-(1+n)}. \quad (1.1)$$

On scales larger than L , $r \sim L$ in the n extra dimensions. Therefore the potential is given by:

$$V \sim L^{-n} r^{-1}, \quad (1.2)$$

on large scales. The observed Planck scale is then the product of the fundamental Planck scale and the volume of the extra dimensions [8]:

$$M_{\text{Planck}}^2 \sim M_{4+n}^{2+n} L^n. \quad (1.3)$$

Therefore in the ADD model the fundamental Planck scale could be much smaller than the Planck scale and the observed value is due to the size of the extra dimensions.

The Randall-Sundrum model of two, Z_2 symmetric, 3-branes living in an anti-de Sitter (AdS) spacetime provides an alternative to the ADD model for $n = 1$ [9] (see Fig. 1.1). The second Randall-Sundrum model has only one brane [10].

The Randall-Sundrum 2 Brane (RS1) Model

The RS1 model has two Minkowski branes living in a 5D AdS bulk, Fig. 1.1. The bulk metric is given, in a Gaussian normal coordinate system, by:

$$ds^2 = a^2(y) \eta_{\mu\nu} dx^\mu dx^\nu + dy^2, \quad (1.4)$$

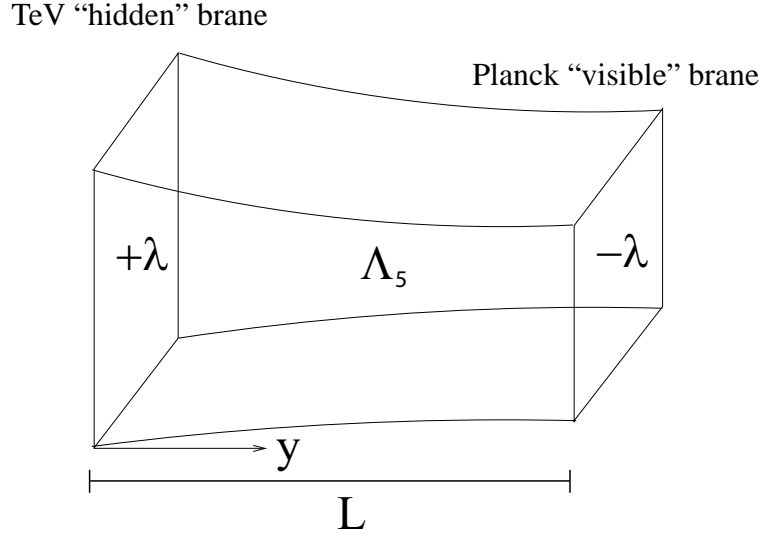


Figure 1.1: The RS1 configuration

where $\eta_{\mu\nu}$ is the Minkowski metric. We use Latin indices for 5D spacetime and Greek indices for 4D spacetime throughout this work. $a(y)$ is the warp factor, given by:

$$a(y) = e^{-|y|/\ell}, \quad (1.5)$$

where ℓ is the AdS curvature scale. The extra dimension is compact. In order for the bulk to be compact we invoke Z_2 symmetry so that:

$$y \leftrightarrow -y, \quad L + y \leftrightarrow L - y, \quad (1.6)$$

where L is the inter-brane separation.

As we shall see in the next chapter the branes have equal and opposite tensions. At $y = 0$ is the positive tension, ‘‘TeV’’ or ‘‘hidden’’ brane. At $y = L$ is the negative tension, ‘‘Planck’’ or ‘‘visible’’ brane. The brane tensions λ are given by:

$$\lambda_{y=0} = -\lambda_{y=L} = \frac{6}{\kappa_5^2 \ell} \equiv \lambda, \quad (1.7)$$

where $\kappa_5^2 = 8\pi G_5 = M_5^{-3}$. We reside on the negative tension brane in order to solve the hierarchy problem. The ‘‘hidden’’ brane has fundamental energy scale M_5 . Then due to the warping of the bulk the effective fundamental energy scale on the ‘‘visible’’ brane is M_{Planck} , where:

$$M_{Planck} = M_5^3 \ell [1 - e^{-2L/\ell}]. \quad (1.8)$$

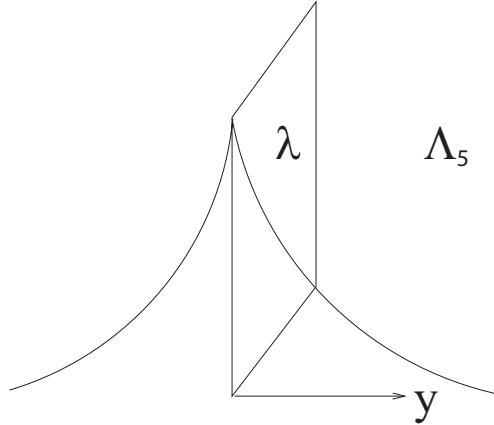


Figure 1.2: The RS2 configuration

The low energy effective theory on the branes is of Brans-Dicke type [11]. The Brans-Dicke parameter (ω) on each brane has the same sign as the brane tension [12]. Nucleosynthesis constrains $\omega \gtrsim 40000$ [13, 14]. This is a problem due to the fact that in this model we reside on the negative tension brane and as such we should measure a negative value of ω . A radion is required to stabilise the inter-brane separation in order for 4D General Relativity to be achieved at low energies [15].

The Randall-Sundrum 1 Brane (RS2) Model

The one brane (RS2) [10] model has a single positive tension brane at $y = 0$ as seen in Fig. 1.2. The bulk is infinite in extent. As there is only one brane there is no mechanism for solving the hierarchy problem but the low energy theory on the brane is general relativity [12]. Gravity is localised to the brane, in the low energy limit, via the warping of the bulk. At high energies the warping is insufficient to localise the gravity to the brane and observers on the brane perceive the 5D nature of gravity. The fundamental energy and the Planck scales are related by:

$$M_{Planck}^2 = M_5^3 \ell, \quad (1.9)$$

i.e. we have effectively sent the second brane off to infinity ($L = \infty$).

The Randall-Sundrum model exhibits its 5D nature, to a brane observer, at high energies, when the warp factor is insufficient to localise gravity to the brane. The deviation between the 4D and 5D nature can be seen in the gravitational potential. The modified gravitational potential is [12]:

$$V(r) \approx \frac{GM}{r} \left(1 + \frac{2\ell^2}{3r^2} \right). \quad (1.10)$$

In Ref. [10] this calculation was carried out with the result having a factor of 1 instead of $2/3$ in front of the r^{-2} term. The result in [12] was obtained by including the coupling of the graviton to matter on the brane.

At high energies we can not get away from the 5D nature of the universe but at low energies ($r \gg \ell$) we are given a constraint on the AdS curvature scale. As we have seen no deviation from Newton's laws down to $\approx 0.1\text{mm}$ in the lab, Eq. (1.10) gives us the constraint that $\ell \lesssim 0.1\text{mm}$. This constraint means that the brane tension, Eq. (1.7), and fundamental energy scale, Eq. (1.9), are also constrained. These constraints are:

$$\lambda > (1 \text{ TeV})^4, \quad M_5 > 10^5 \text{ TeV}. \quad (1.11)$$

In the RS models the 4-D cosmological constant on the brane is given by:

$$\Lambda_4 = \frac{1}{2} (\Lambda_5 + \kappa_4^2 \lambda). \quad (1.12)$$

Since the branes are Minkowski, we require the fine tuning:

$$\Lambda_5 + \kappa_4^2 \lambda = 0, \quad (1.13)$$

where $\kappa_4^2 = 8\pi G_4 = M_{Planck}^{-2}$, so that $\Lambda_4 = 0$. Breaking this fine tuning leads to different cosmologies on the branes [8]:

$$\lambda < -\frac{\Lambda_5}{\kappa_4^2} \Rightarrow \text{Anti-de Sitter}, \quad (1.14)$$

$$\lambda = -\frac{\Lambda_5}{\kappa_4^2} \Rightarrow \text{Minkowski}, \quad (1.15)$$

$$\lambda > -\frac{\Lambda_5}{\kappa_4^2} \Rightarrow \text{de Sitter}. \quad (1.16)$$

The bulk cosmological constant is given by:

$$\Lambda_5 = -\frac{6}{\ell^2}, \quad (1.17)$$

where ℓ is the AdS curvature scale.

The Randall-Sundrum models provides a simple way of investigating aspects of the phenomenology of the very complicated String Theories. In this thesis, we focus on brane world cosmological models based on generalisations of the RS scenario (see the

reviews [8, 16, 17, 18, 19, 20, 21]). These include models that can explain the late-time acceleration of the universe without the need for dark energy.

Chapter 2

RS Brane Worlds

2.1 Introduction

In this chapter we will look in some detail at the Randall-Sundrum (RS) model. We will start with the simplest model, the Minkowski brane. We shall then consider a de Sitter brane before looking at a cosmological solution (the Friedmann-Robertson-Walker brane). In the first two cases we will look at the equations in the bulk and on the brane. We will also look at the spectrum of Kaluza-Klein modes generated due to perturbations on the brane. For the cosmological brane we will only consider the equations on the brane and how they differ from the standard general relativity result. It is these brane Friedmann equations that will be of interest in the following chapters.

2.2 Minkowski Branes

Minkowski branes are the most simple branes possible. They are flat, empty and static. We start by obtaining the background form of the bulk Einstein field equations. Using the bulk field equations we can work out the induced equations on the brane. Later we shall consider bulk gravitational waves. These give rise to the Kaluza-Klein modes on the brane.

2.2.1 The background

The line element for Minkowski branes in an anti de Sitter bulk was considered in the previous chapter, Eq. (1.4). For simplicity we take $y \geq 0$ and implicitly assume Z_2 symmetry. We can write the metric for this model as:

$$g_{ab} = a^2(y)\eta_{\mu\nu}\delta_a^\mu\delta_b^\nu + \delta_a^y\delta_b^y. \quad (2.1)$$

This is a solution of the 5-dimensional Einstein equation:

$$G_{ab}^{(5)} = -\Lambda_5 g_{ab}^{(5)}. \quad (2.2)$$

Using Eq. (1.5) we can write out the following relationships for the warp factor:

$$a' = -\frac{a}{\ell}, \quad \Rightarrow \quad a'' = \frac{a}{\ell^2}, \quad (2.3)$$

where a prime represents differentiation with respect to y . This implies:

$$g_{ab,y} = g'_{ab} = -\frac{2}{\ell} (g_{ab} - \delta_a^y \delta_b^y), \quad (2.4)$$

and similarly:

$$g^{ab}{}_{,y} = g^{ab'} = \frac{2}{\ell} (g^{ab} - \delta_y^a \delta_y^b). \quad (2.5)$$

By Eq. (2.1):

$$g_{ay} = \delta_a^y, \quad \Rightarrow \quad g^{ay} = \delta_y^a. \quad (2.6)$$

These will be useful later.

In order to construct the Einstein field equations we require both the Ricci curvature tensor and the Ricci scalar. We start by obtaining the RS Riemann tensor. The only non-zero derivatives of g_{ab} are those with respect to y . Using Eq. (2.4) we can write the Christoffel symbols as:

$$\Gamma_{bc}^a = -\frac{1}{\ell} (\delta_c^y \delta_b^a + \delta_b^y \delta_c^a - \delta_y^a g_{bc} - \delta_y^a \delta_b^y \delta_c^y), \quad (2.7)$$

so that:

$$\Gamma_{bc,d}^a = -\frac{2}{\ell^2} \delta_y^a \delta_d^y (g_{bc} - \delta_b^y \delta_c^y). \quad (2.8)$$

The Riemann tensor is defined as:

$$R_{bcd}^a = \Gamma_{bd,c}^a - \Gamma_{bc,d}^a + \Gamma_{bd}^e \Gamma_{ec}^a - \Gamma_{bc}^e \Gamma_{ed}^a. \quad (2.9)$$

So for the Randall-Sundrum brane model the Riemann tensor has the anti de Sitter form:

$$R_{bcd}^a = -\frac{1}{\ell^2} (\delta_c^a g_{bd} - \delta_d^a g_{bc}). \quad (2.10)$$

The RS Ricci tensor and scalar are given by:

$$R_{ab} = -\frac{4}{\ell^2} g_{ab}, \quad (2.11)$$

and:

$$R = -\frac{20}{\ell^2}. \quad (2.12)$$

The Einstein tensor is given by:

$$G_{ab} = -\frac{4}{\ell^2} g_{ab} - \frac{1}{2} \left(-\frac{20}{\ell^2} \right) g_{ab} = \frac{6}{\ell^2} g_{ab}, \quad (2.13)$$

which satisfies the field equation:

$$G_{ab} = -\Lambda_5 g_{ab}, \quad (2.14)$$

where the 5D bulk cosmological constant is given by:

$$\Lambda_5 = -\frac{6}{\ell^2}. \quad (2.15)$$

This also means that we can write the Ricci tensor as:

$$R_{ab} = \frac{2}{3} \Lambda_5 g_{ab}. \quad (2.16)$$

Using the solution for the RS bulk cosmological constant in Eqs. (1.14) we find that in order for the brane(s) to have a Minkowski geometry we require the brane tension(s) to be finely tuned to:

$$\lambda_{\pm} = \pm \frac{6}{\ell^2 \kappa_4^2}, \quad (2.17)$$

where the \pm refer to the two different branes. The brane tensions can also be found from the extrinsic curvature of the brane. The extrinsic curvature depends on how the brane is embedded in the higher dimensional space. As we are working in Gaussian normal coordinates we can write the extrinsic curvature as [22]:

$$K_{\mu\nu} = \frac{1}{2} \partial_y g_{\mu\nu}. \quad (2.18)$$

For Minkowski branes we find that the extrinsic curvature is given by:

$$K_{\mu\nu} = \frac{g_{\mu\nu}}{\ell}. \quad (2.19)$$

The extrinsic curvature on the brane can also be obtained by considering the Israel-Darmois junction conditions [23]:

$$g_{\mu\nu}^+ - g_{\mu\nu}^- = 0, \quad (2.20)$$

$$K_{\mu\nu}^+ - K_{\mu\nu}^- = -\kappa_5^2 \left[T_{\mu\nu}^{brane} - \frac{1}{3} T^{brane} g_{\mu\nu} \right], \quad (2.21)$$

where:

$$T_{\mu\nu}^{brane} = T_{\mu\nu} - \lambda g_{\mu\nu}. \quad (2.22)$$

$T_{\mu\nu}^{brane}$ is the total energy-momentum tensor of the brane. This is the combination of the standard matter $T_{\mu\nu}$ on the brane and the brane tension λ which acts as a brane cosmological constant.

Using Z_2 symmetry, $K_{\mu\nu}^- = -K_{\mu\nu}^+$, the extrinsic curvature can be written as [8] (where we drop the \pm superscript):

$$K_{\mu\nu} = -\frac{1}{2} \kappa_5^2 \left[T_{\mu\nu} + \frac{1}{3} (\lambda - T) g_{\mu\nu} \right], \quad (2.23)$$

where $T = T^\mu_\mu$. Using Eq. (2.23) for a Minkowski brane i.e $T_{\mu\nu} = 0$ and Eq. (2.18) we find that the brane tension is given by:

$$\lambda_\pm = \pm \frac{6}{\kappa_5^2 \ell}. \quad (2.24)$$

Using this form of the brane tension with that in Eq. (2.17) gives us the following relationship for Minkowski branes:

$$\kappa_5^2 = \ell \kappa_4^2. \quad (2.25)$$

2.2.2 Field equations on the brane

For a general cosmological brane, in a general bulk, the 5-dimensional field equations are:

$$G_{ab}^{(5)} = \kappa_5^2 T_{ab}^{(5)}, \quad (2.26)$$

where the energy-momentum tensor is given by:

$$T_b^a{}^{(5)} = T_b^a|_{bulk} + T_b^a|_{brane}. \quad (2.27)$$

The bulk part of $T_{ab}^{(5)}$ is given by:

$$T_b^a|_{bulk} = -\frac{\Lambda_5}{\kappa_5^2} \delta_b^a, \quad (2.28)$$

which is just the 5D bulk cosmological constant.

The induced field equations on the brane are given by [8]:

$$G_{\mu\nu} = -\Lambda_4 g_{\mu\nu} + \kappa_4^2 T_{\mu\nu} + \frac{6\kappa_4^2}{\lambda} S_{\mu\nu} - \mathcal{E}_{\mu\nu} + 4\frac{\kappa_4^2}{\lambda} F_{\mu\nu}. \quad (2.29)$$

The first two terms on the right hand side are the standard GR contributions of the matter on the brane and the cosmological constant. Λ_4 and κ_4 are as defined in Chapter 1. The other terms are unique to brane models. The tensor $S_{\mu\nu}$ is the high-energy correction term and is quadratic in the energy-momentum tensor:

$$S_{\mu\nu} = \frac{1}{12} T T_{\mu\nu} - \frac{1}{4} T_{\mu\alpha} T_\nu^\alpha + \frac{1}{24} g_{\mu\nu} [3T_{\alpha\beta} T^{\alpha\beta} - T^2]. \quad (2.30)$$

The fourth term in the induced field equations, $\mathcal{E}_{\mu\nu}$, is the projection of the bulk Weyl tensor orthogonal to n^a :

$$\mathcal{E}_{\mu\nu} = C_{acbd}^{(5)} n^c n^d g_{\mu}^{(5)a} g_{\nu}^{(5)b}. \quad (2.31)$$

The Weyl tensor describes the free gravitational field. The $F_{\mu\nu}$ tensor is defined as:

$$F_{\mu\nu} = T_{ab}^{(5)} g_\mu^a g_\nu^b + \left[T_{ab}^{(5)} n^a n^b - \frac{1}{4} T^{(5)} \right] g_{\mu\nu}, \quad (2.32)$$

and includes contributions on the brane of the 5D energy-momentum tensor (if there is a bulk scalar field this is where it is felt). In the special case of Minkowski branes and an empty bulk, the Weyl tensor is zero, so that $\mathcal{E}_{\mu\nu} = 0$ and due to the empty bulk $F_{\mu\nu} = 0$. Also in Minkowski spacetime we have $T_{\mu\nu} = 0$ and therefore $S_{\mu\nu} = 0$, and $\Lambda_4 = 0$. The induced field equations on the brane are simply given by:

$$G_{\mu\nu} = 0. \quad (2.33)$$

2.2.3 Kaluza-Klein Modes

In this section we shall look at the Kaluza-Klein (KK) modes on the Minkowski brane. Before we look at the solutions we should consider the polarisations of the 5D graviton as this generalises the equivalent 4D polarisations.

Polarisations of the 5D graviton

The number of polarisations of the graviton is given by the number of degrees of freedom in the perturbation (h_{ab}) of the bulk metric tensor:

$$g_{ab}^{(5)} \rightarrow g_{ab}^{(5)} + h_{ab}. \quad (2.34)$$

The perturbation initially has 15 components since the metric is symmetric. We then apply the Randall-Sundrum gauge, which is the Gaussian normal and the transverse-traceless gauges combined. The Gaussian normal gauge ($h_{ay} = 0$) removes 5 degrees of freedom. The transverse-traceless gauge (after the application of the Gaussian normal gauge) is:

$$\nabla^\nu h_{\mu\nu} = 0 = g^{(5)\mu\nu} h_{\mu\nu}. \quad (2.35)$$

This removes another 5 degrees of freedom. This means that the 5D graviton has 5 degrees of freedom and therefore 5 polarisation states. These polarisation states (as felt on the brane) are decomposed into [8]:

- 2 polarisations in 4D spin-2 graviton modes.
- 2 polarisations in 4D spin-1 gravi-vector modes.
- 1 polarisation in 4D spin-0 gravi-scalar modes.

The normal 4D graviton is the massless spin-2 mode. The massive modes of the graviton are felt as massive modes in all of these fields on the brane, i.e massive graviton, gravi-vector and gravi-scalar.

Obtaining the gravitational wave equation

The perturbed line element is:

$$ds^2 = (a^2(y)\eta_{\mu\nu} + \varepsilon h_{\mu\nu}) dx^\mu dx^\nu + dy^2, \quad (2.36)$$

where $|\varepsilon| \ll 1$. The modified metric can be written as:

$$\begin{aligned} g_{ab}^{(5)} &= \bar{g}_{ab} + \delta g_{ab}, \\ &= \bar{g}_{ab} + \varepsilon h_{\mu\nu} \delta_a^\mu \delta_b^\nu, \end{aligned} \quad (2.37)$$

where \bar{g}_{ab} is the background metric (all subsequent barred terms are background quantities). Therefore for the inverse metric we have:

$$g^{(5)ab} = \bar{g}^{ab} - \varepsilon h^{\mu\nu} \delta_\mu^a \delta_\nu^b. \quad (2.38)$$

The perturbed Christoffel symbol is:

$$\delta\Gamma^{(5)a}_{bc} = \frac{\varepsilon}{2} \left\{ \bar{g}^{ad} (h_{bd,c} + h_{dc,b} - h_{bc,d}) - h^{ad} (\bar{g}_{bd,c} + \bar{g}_{dc,b} - \bar{g}_{bc,d}) \right\}. \quad (2.39)$$

The background Christoffel symbol is given by Eq. (2.7), $h_{ay} = 0$ and $\bar{g}_{ay,b} = 0$. This becomes:

$$\delta\Gamma^{(5)a}_{bc} = \frac{\varepsilon}{2} \left\{ \bar{g}^{a\nu} (h_{b\nu,c} + h_{\nu c,b} - h_{bc,\nu}) - g^{ay} h_{bc,y} h^{a\nu} (\bar{g}_{b\nu,c} + \bar{g}_{\nu c,b} - \bar{g}_{bc,\nu}) \right\}. \quad (2.40)$$

Then by using the relationships in Eqs. (2.4), (2.5) and defining $\tilde{h}_{\mu\nu} = a^{-2} h_{\mu\nu}$ this can be written as:

$$\begin{aligned} \delta\Gamma^{(5)a}_{bc} = & \frac{\varepsilon}{2} \left\{ \delta_\gamma^a \left[\tilde{h}_b{}^\gamma{}_{,c} + \tilde{h}^\gamma{}_{c,b} - \tilde{h}_{bc,}{}^\gamma - \frac{2}{\ell} \left(\delta_c^y \tilde{h}_b{}^\gamma + \delta_b^y \tilde{h}_c{}^\gamma \right) \right] \right. \\ & \left. + a^2 \delta_y^a \left(\frac{2}{\ell} \tilde{h}_{bc} - \tilde{h}_{bc,y} \right) + \frac{2}{\ell} \left(\delta_c^y \delta_b^\mu \tilde{h}^a{}_\mu + \delta_b^y \delta_c^\alpha \tilde{h}^a{}_\alpha \right) \right\}. \end{aligned} \quad (2.41)$$

In order to write out the perturbed Riemann tensor we need the explicit form of the derivative of Eq. (2.41). We find this to be:

$$\begin{aligned} \delta\Gamma^{(5)a}_{bc,d} = & \frac{\varepsilon}{2} \left\{ \delta_\gamma^a \left[\tilde{h}_b{}^\gamma{}_{,cd} + \tilde{h}^\gamma{}_{c,bd} - \tilde{h}_{bc,}{}^\gamma{}_d - \frac{2}{\ell} \left(\delta_c^y \tilde{h}_b{}^\gamma{}_d + \delta_b^y \tilde{h}_c{}^\gamma{}_d \right) \right] \right. \\ & + a^2 \delta_y^a \left(\frac{2}{\ell} \tilde{h}_{bc,d} - \tilde{h}_{bc,yd} \right) - \frac{2a^2}{\ell} \delta_y^a \delta_d^y \left(\frac{2}{\ell} \tilde{h}_{bc} - \tilde{h}_{bc,y} \right) \\ & \left. + \frac{2}{\ell} \left(\delta_c^y \delta_b^\mu \tilde{h}^a{}_{\mu,d} + \delta_b^y \delta_c^\alpha \tilde{h}^a{}_{\alpha,d} \right) \right\}. \end{aligned} \quad (2.42)$$

We now have all the required quantities for the perturbed Riemann tensor which is given by:

$$\delta R^{(5)a}_{bcd} = \delta\Gamma^{(5)a}_{bd,c} - \delta\Gamma^{(5)a}_{bc,d} + \bar{\Gamma}_{bd}^e \delta\Gamma^{(5)a}_{ec} + \bar{\Gamma}_{ec}^a \delta\Gamma^{(5)e}_{bd} - \bar{\Gamma}_{bc}^e \delta\Gamma^{(5)a}_{ed} - \bar{\Gamma}_{ed}^a \delta\Gamma^{(5)e}_{bc}. \quad (2.43)$$

In order for us to obtain the perturbed Einstein equations we do not need to explicitly write out the full perturbed Riemann tensor. We require the perturbed Ricci tensor so we can just consider each term and perform the Ricci contraction on each in turn.

We must also consider the Randall-Sundrum gauge requirements. We have already used $h_{ay} = 0$ but we also have $h^\nu_{\mu,\nu} = 0$ and $h^\mu_\mu = 0$. Using these and the Ricci contraction over the 1st and 3rd indices we find that Eq. (2.42) (the 2nd term in the perturbed Riemann tensor) has zero contribution to the Ricci tensor. Writing out Eq. (2.42) for the 1st term in the perturbed Riemann tensor and carrying out the same procedure we find the perturbed Ricci terms to be:

$$\frac{\varepsilon}{2} \left\{ -\tilde{h}_{bd, \gamma}^{\gamma} - \frac{4a^2}{\ell^2} \tilde{h}_{bd} + \frac{4a^2}{\ell} \tilde{h}_{bd,y} - a^2 \tilde{h}_{bd,yy} \right\}. \quad (2.44)$$

The 3rd term in the perturbed Riemann tensor ($\bar{\Gamma}_{bd}^e \delta \Gamma_{ec}^{(5)a}$) also gives us zero when we perform the Ricci contraction. The 4th term in the perturbed Riemann tensor ($\bar{\Gamma}_{ec}^a \delta \Gamma_{bd}^{(5)e}$) gives us the following components of the Ricci tensor:

$$-\frac{\varepsilon}{2} \left\{ \frac{8a^2}{\ell^2} \tilde{h}_{bd} - \frac{4a^2}{\ell} \tilde{h}_{bd,y} \right\}. \quad (2.45)$$

The 5th term in the Riemann tensor ($\bar{\Gamma}_{ed}^a \delta \Gamma_{bc}^{(5)e}$) gives us:

$$-\frac{\varepsilon}{2} \left\{ \frac{2a^2}{\ell^2} \tilde{h}_{bd} - \frac{2a^2}{\ell} \tilde{h}_{bd,y} \right\}. \quad (2.46)$$

The final term in the Riemann tensor ($\bar{\Gamma}_{bc}^e \delta \Gamma_{ed}^{(5)a}$) also gives us the following terms in the Ricci tensor:

$$-\frac{\varepsilon}{2} \left\{ \frac{2a^2}{\ell^2} \tilde{h}_{bd} - \frac{2a^2}{\ell} \tilde{h}_{bd,y} \right\}. \quad (2.47)$$

Then by combining Eqs. (2.44), (2.45), (2.46), (2.47) and making use of the fact that we can change the indices as long as the summations stay correct we find the perturbed Ricci tensor to be:

$$\delta R_{bd}^{(5)} = \frac{\varepsilon}{2} \left\{ -\tilde{h}_{bd, \gamma}^{\gamma} - \frac{8a^2}{\ell^2} \tilde{h}_{bd} + \frac{4a^2}{\ell} \tilde{h}_{bd,y} - a^2 \tilde{h}_{bd,yy} \right\}. \quad (2.48)$$

Using Eq. (2.11) we can write the following:

$$\delta R_{bd}^{(5)} = -\frac{4}{\ell^2} \varepsilon h_{bd}. \quad (2.49)$$

By combining these two forms of the Ricci tensor we find that the following wave equation must be satisfied:

$$-\tilde{h}_{bd,\gamma}{}^\gamma + \frac{4a^2}{\ell} \tilde{h}_{bd,y} - a^2 \tilde{h}_{bd,yy} = 0. \quad (2.50)$$

We can write the wave equation (2.50) as:

$$\left[a^{-2} \square + \partial_y^2 - \frac{4}{\ell} \partial_y \right] \tilde{h}_{\mu\nu} = 0, \quad (2.51)$$

where \square is the 4D Minkowski d'Alembertian operator. This can be equivalently written with \tilde{h}_{bd} instead of $\tilde{h}_{\mu\nu}$. The wave equation (2.51) is also:

$$\square^{(5)} \tilde{h}_{\mu\nu} = 0. \quad (2.52)$$

Using $h_{\mu\nu}$ the wave equation (2.51) becomes:

$$\left[a^{-2} \square + \partial_y^2 - \frac{4}{\ell^2} \right] h_{\mu\nu} = 0, \quad (2.53)$$

which agrees with the form given in [21]. The junction conditions can be enforced via a delta term which takes into account the presence of the brane at $y = 0$:

$$\left[a^{-2} \square + \partial_y^2 - \frac{4}{\ell^2} + \frac{4}{\ell} \delta(y) \right] h_{\mu\nu} = 0. \quad (2.54)$$

The two forms of the line element seen so far are written in Gaussian normal coordinates (the extra dimension is normal to a given hypersurface, the Minkowski spacetime brane in this case). Another coordinate system that can be used is the Poincaré system. This gives us a line element of the form:

$$ds^2 = \frac{\ell^2}{z^2} \left[dz^2 + \eta_{\mu\nu} dx^\mu dx^\nu \right], \quad (2.55)$$

where z is defined as:

$$z = \ell e^{y/\ell}. \quad (2.56)$$

The perturbed line element in these coordinates is given by:

$$ds^2 = \frac{\ell^2}{z^2} \left[dz^2 + \left(\eta_{\mu\nu} + \varepsilon \tilde{h}_{\mu\nu} \right) dx^\mu dx^\nu \right]. \quad (2.57)$$

Solving the wave equation

The solutions to the wave equation (2.53) can be written as the superposition of Fourier modes of the form:

$$h_{\mu\nu}(x^\lambda, y) = U_m(y) e^{ik_\lambda x^\lambda} \epsilon_{\mu\nu}, \quad (2.58)$$

where $\epsilon_{\mu\nu}$ is a (constant) polarisation tensor. We are interested in $U_m(y)$, the bulk gravitational wave part of the decomposition. By using Eq. (2.58) in Eq. (2.51) we find the y dependent wave equation to be:

$$\left[e^{2y/\ell} m^2 + \partial_y^2 - \frac{4}{\ell^2} \right] e^{-2y/\ell} U_m = 0, \quad (2.59)$$

where m can be interpreted as the 4D mass of the 5D graviton. The mass is due to the fact that an observer on the brane would measure the timelike 4D projection on the brane of the gravitons null 5-momentum:

$$-m^2 = k_\lambda k^\lambda. \quad (2.60)$$

The zero mode satisfies the boundary conditions given by $U_0 = C$ where C is a constant. For $m > 0$, we now define the function:

$$F_m(y) = e^{-2y/\ell} U_m(y), \quad (2.61)$$

and change variable to:

$$X = e^{y/\ell} m \ell, \quad (2.62)$$

to rewrite Eq. (2.59) as:

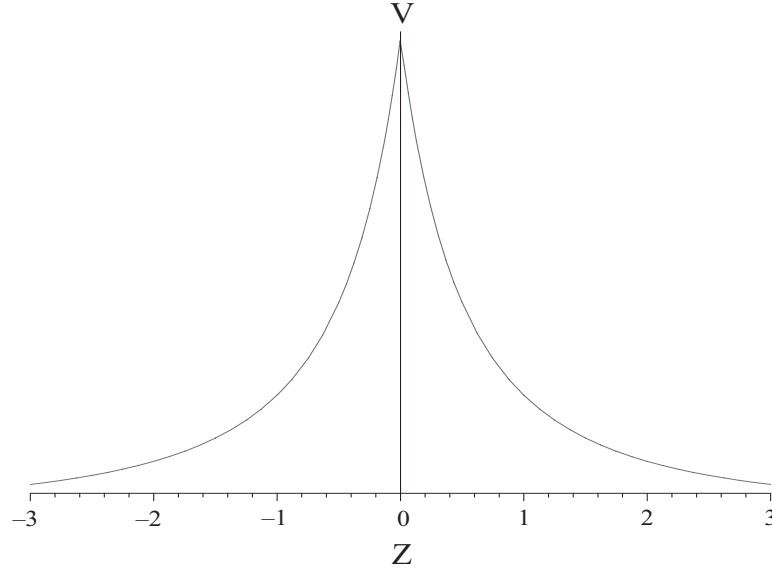
$$X^2 \frac{\partial^2 F_m}{\partial X^2} + X \frac{\partial F_m}{\partial X} + (X^2 - 4) F_m = 0. \quad (2.63)$$

This is a Bessel equation, with solution:

$$F_m = Z_2(e^{y/\ell} m \ell), \quad (2.64)$$

where:

$$Z_p(S) = A J_p(S) + B Y_p(S), \quad (2.65)$$

Figure 2.1: A plot of the potential in equation (2.70) with $\ell = 1$

with A and B constant and p is the order of the Bessel function. By Eq. (2.58) the full solution for $m > 0$ is:

$$h_{\mu\nu}(x^\lambda, y) = e^{2y/\ell} Z_2(e^{y/\ell} m \ell) e^{ik_\lambda x^\lambda} \epsilon_{\mu\nu}. \quad (2.66)$$

Schrödinger form of the wave equation

The wave equation (2.59) can be rewritten in a form similar to the Schrödinger wave equation. We define two new variables as:

$$\psi_m = a^{3/2} U_m, \quad (2.67)$$

$$Z = \ell(e^{y/\ell} - 1). \quad (2.68)$$

This gives:

$$-\frac{\partial^2 \psi_m}{\partial Z^2} + V(Z) \psi_m = m^2 \psi_m. \quad (2.69)$$

This is a Schrödinger equation with a potential $V(Z)$ given by:

$$V(Z) = \frac{15}{4(Z + \ell)^2}. \quad (2.70)$$

This is plotted in Fig. 2.1.

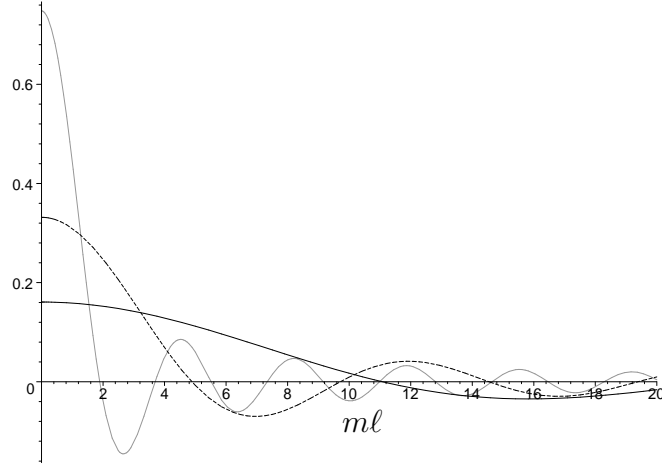


Figure 2.2: A plot of equation (2.76) with $L/\ell = 1/4$, $1/2$ and $L/\ell = 1$ for the solid, dashed and pale solid lines respectively.

Specific Solutions

In order to obtain specific solutions we must apply boundary conditions to the general solution. The boundary conditions for the perturbations are:

$$\left. \frac{\partial h_{\mu\nu}(y)}{\partial y} \right|_{brane} = 0. \quad (2.71)$$

This means RS1 has two boundary conditions whilst RS2 only has one. For RS1:

$$A \frac{\partial}{\partial y} (e^{2y/\ell} J_2(e^{y/\ell} m\ell))|_{(y=0)} + B \frac{\partial}{\partial y} (e^{2y/\ell} Y_2(e^{y/\ell} m\ell))|_{(y=0)} = 0, \quad (2.72)$$

$$A \frac{\partial}{\partial y} (e^{2y/\ell} J_2(e^{y/\ell} m\ell))|_{(y=L)} + B \frac{\partial}{\partial y} (e^{2y/\ell} Y_2(e^{y/\ell} m\ell))|_{(y=L)} = 0. \quad (2.73)$$

These can then be combined in the matrix equation:

$$\begin{bmatrix} J'_2(0) & Y'_2(0) \\ J'_2(L) & Y'_2(L) \end{bmatrix} \begin{bmatrix} A \\ B \end{bmatrix} = 0, \quad (2.74)$$

where $J'_2(0) = \frac{\partial}{\partial y} J_2(e^{y/\ell} m\ell)|_{(y=0)}$ and so on.

In order for us to obtain a unique and non-trivial solution we require that:

$$J'_2(0)Y'_2(L) - J'_2(L)Y'_2(0) = 0, \quad (2.75)$$

i.e.:

$$J_1(m\ell) Y_1(e^{L/\ell} m\ell) - J_1(e^{L/\ell} m\ell) Y_1(m\ell) = 0. \quad (2.76)$$

In Fig. 2.2 we see that for a particular value of L/ℓ we have a series of values of $m\ell$ that satisfy the above equation. We see that as we increase the brane separation the mode spacings decrease. We find that we have a zero mode solution with an infinite tower of discrete massive Kaluza-Klein modes. In the RS2 scenario we only have a single brane and therefore only one boundary condition. This means we can not solve for m independently of A and B and therefore obtain a specific solution. Thus RS2 has an infinite continuous tower of Kaluza-Klein modes. This is confirmed by taking the RS1 solution and sending the second brane off to infinity.

2.3 de Sitter Brane Worlds

The de Sitter brane is the simplest expanding solution. A de Sitter universe expands at a uniform rate given by the Hubble constant H .

2.3.1 The background

In Poincaré coordinates the spacetime is described by [11]:

$$ds^2 = A(z)^2 (dz^2 + \gamma_{\mu\nu} dx^\mu dx^\nu), \quad (2.77)$$

where:

$$\gamma_{\mu\nu} dx^\mu dx^\nu = -dt^2 + e^{2Ht} d\vec{x}^2. \quad (2.78)$$

and the warp factor is:

$$A(z) = \frac{\ell H}{\sinh(Hz)}. \quad (2.79)$$

On the visible (positive tension) brane, $z = z_+$, we need to have the standard de Sitter solution ($A(z_+) = 1$), so that:

$$z_+ = H^{-1} \sinh^{-1}(H\ell). \quad (2.80)$$

Let us consider the two brane case where the second brane is at $z = z_- > z_+$. The extrinsic curvature in this coordinate system is given by:

$$K_{\mu\nu} = -\frac{1}{2}A^{-1}\partial_z g_{\mu\nu}, \quad (2.81)$$

leading to:

$$K_{\mu\nu} = \left(\frac{\cosh(Hz)}{\ell} \right) g_{\mu\nu}. \quad (2.82)$$

The extrinsic curvature as found from the junction conditions, Eq. (2.23), is independent of the brane geometry. For de Sitter branes $T_{\mu\nu}^\pm = -\rho_\pm g_{\mu\nu}^\pm$ with ρ_\pm constant, unlike the Minkowski case, where $T_{\mu\nu}^\pm = 0$. The extrinsic curvature for a de Sitter brane can then be written as:

$$K_{\mu\nu} = -\frac{\kappa_5^2}{6}\sigma g_{\mu\nu}. \quad (2.83)$$

where $\sigma = \lambda + \rho$ is the total energy density on the brane. By Eq. (2.82) we obtain the following relationship:

$$\sigma_\pm = \pm \frac{6}{\kappa_5^2 \ell} \cosh(Hz_\pm). \quad (2.84)$$

There is some degeneracy in the brane tension and the energy density on the brane. We can rewrite the above equation in terms of the brane tensions as:

$$\lambda_\pm = \pm \frac{6}{\kappa_5^2 \ell} \cosh(Hz_\pm) - \rho_\pm. \quad (2.85)$$

Now if we evaluate the metric on each of the two branes:

- Positive tension brane:

$$ds^2|_{z_+} = -dt^2 + e^{2Ht} d\vec{x}^2. \quad (2.86)$$

This is just the standard de Sitter line element as we have set the observer on this brane.

- Negative tension brane:

$$\begin{aligned} ds^2|_{z_-} &= A^2(z_-) (-dt^2 + e^{2Ht} d\vec{x}^2), \\ &= -dt_-^2 + e^{2H-t_-} d\vec{x}^2, \end{aligned} \quad (2.87)$$

where we have defined the proper time on the negative tension brane as:

$$t_- = A(z_-)t + C, \quad (2.88)$$

with C constant. The Hubble rate on the negative brane is also modified by the warp factor:

$$H_- = \frac{H}{A(z_-)}. \quad (2.89)$$

This means that the warp factor on the negative tension brane is less than that on the positive tension brane [24].

The form of the Hubble rates given above means that the two are dependent only on the brane position (z). We can view the expansion of the brane as a consequence of the brane moving through the warped bulk. We can write the Hubble constant on each brane as:

$$H_{\pm} = \frac{\sinh H_+ z_{\pm}}{\ell}, \quad (2.90)$$

where $H_+ = H$ (the Hubble rate on the positive tension brane). Using this result in the brane tension, Eq. (2.84), we find that the tensions are given, as functions of the Hubble rate, by:

$$\lambda_{\pm} = \pm \frac{6}{\kappa_5^2 \ell} \sqrt{1 + (\ell H_{\pm})^2} - \rho_{\pm}. \quad (2.91)$$

High energy branes are characterised by $H\ell \gg 1$, so that:

$$\lambda_{\pm} \approx \pm \frac{6}{\kappa_5^2} H_{\pm} - \rho_{\pm}. \quad (2.92)$$

On low energy ($H\ell \ll 1$) branes:

$$\lambda_{\pm} \approx \pm \frac{6}{\kappa_5^2 \ell} - \rho_{\pm}. \quad (2.93)$$

This reduces to the Minkowski relation when $\rho_{\pm} = 0$.

In the de Sitter case:

$$S_{\mu\nu} = -\frac{1}{12} \rho^2 g_{\mu\nu}. \quad (2.94)$$

The bulk is still empty in this case so the other two terms ($\mathcal{E}_{\mu\nu}$ and $F_{\mu\nu}$) are still zero. The induced field equations on the brane are then given by:

$$G_{\mu\nu} = -\Lambda_4 g_{\mu\nu} - \kappa_4^2 \rho g_{\mu\nu} - \frac{\kappa_4^2}{2\lambda} \rho^2 g_{\mu\nu}, \quad (2.95)$$

where

$$\kappa_4^2 = \frac{\lambda}{6} \kappa_5^4. \quad (2.96)$$

Using Eqs. (1.12) and (2.15) we can write the field equations on the brane as:

$$G_{\mu\nu}^{\pm} = - \left\{ \frac{\lambda_{\pm} \kappa_5^4}{6} \rho_{\pm} + \frac{\kappa_5^4}{12} \rho_{\pm}^2 + \frac{1}{2} \left[\frac{\lambda_{\pm}^2 \kappa_5^4}{6} - \frac{6}{\ell^2} \right] \right\} g_{\mu\nu}^{\pm}. \quad (2.97)$$

2.3.2 Kaluza-Klein modes

In Gaussian normal coordinates, the metric for a de Sitter brane is:

$$ds^2 = dy^2 + w^2(y) \gamma_{\mu\nu} dx^{\mu} dx^{\nu}, \quad (2.98)$$

where warp factor is given by:

$$w(y) = H \ell \sinh(y/\ell). \quad (2.99)$$

If y_1 is the position of the visible brane then:

$$H = \frac{1}{\ell \sinh(y_1/\ell)}. \quad (2.100)$$

The perturbed metric is:

$$ds^2 = dy^2 + w^2(y) (\gamma_{\mu\nu} + f_{\mu\nu}) dx^{\mu} dx^{\nu}, \quad (2.101)$$

where:

$$\gamma^{\mu\nu} f_{\mu\nu} = 0 = \nabla^{\nu} f_{\mu\nu}. \quad (2.102)$$

The perturbation can be split into Fourier modes:

$$f_{\mu\nu}(t, \vec{x}, y) \rightarrow f_m(y) \psi_m(t, \vec{k}) e_{\mu\nu}(\vec{x}). \quad (2.103)$$

Using these in the perturbed field equations we obtain the following two wave equations [25]:

$$f_m'' + 4 \frac{w'}{w} f_m' + \left(\frac{m}{w} \right)^2 f_m = 0, \quad (2.104)$$

and

$$\ddot{\psi}_m + 3H \dot{\psi}_m + \left[\left(\frac{k}{e^{Ht}} \right)^2 + m^2 \right] \psi_m = 0, \quad (2.105)$$

where m is the separation constant and again can be considered as the effective mass of the 4D graviton. Eq. (2.104) becomes:

$$f_m''(y) + 4 \frac{\cosh(y/\ell)}{\ell \sinh(y/\ell)} f_m'(y) + \left(\frac{m}{H \ell \sinh(y/\ell)} \right)^2 f_m(y) = 0. \quad (2.106)$$

The zero-mode satisfying the boundary condition is given by:

$$f_0 = \text{constant}. \quad (2.107)$$

For the massive modes, $m > 0$, we rewrite Eq. (2.106) as:

$$\left[\frac{1}{\sinh^4(y/\ell)} \partial_y (\sinh^4(y/\ell) \partial_y) + \left(\frac{m}{H \ell \sinh(y/\ell)} \right)^2 \right] f_m(y) = 0. \quad (2.108)$$

The wave equation for (2.105) can be written as:

$$[\square - m^2] \psi_m = 0. \quad (2.109)$$

If we make the following substitutions:

$$U = \sinh^{3/2}(y/\ell) \psi(y), \quad Z = \cosh(y/\ell), \quad (2.110)$$

we can write Eq. (2.108) as:

$$(1 - Z^2) \frac{d^2 U}{dZ^2} - 2Z \frac{dU}{dZ} + \left[\nu(\mu + 1) - \frac{\mu^2}{1 - Z^2} \right] U = 0, \quad (2.111)$$

where $\nu = \frac{3}{2}$ and $\mu = i\sqrt{((m/H)^2 - 9/4)} = ip$. The solutions to this equation are associated Legendre functions. The general solution is a linear combination of the two associated Legendre functions P_ν^μ and Q_ν^μ . We find the profile for the KK modes are given by:

$$f_m(y) = \sinh^{-3/2}(y/\ell) \left\{ A_p P_{3/2}^{i\sqrt{(m/H)^2 - 9/4}}(\cosh(y/\ell)) + B_p Q_{3/2}^{i\sqrt{(m/H)^2 - 9/4}}(\cosh(y/\ell)) \right\}. \quad (2.112)$$

The two branes, at y_1 and y_2 , are related by:

$$y_2 - y_1 = L. \quad (2.113)$$

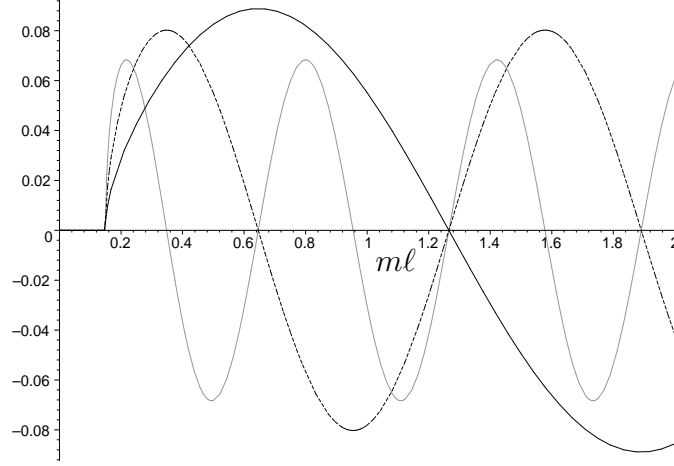


Figure 2.3: Determining the KK mass eigenvalues for two de Sitter branes with $L/\ell = 1/4$, $1/2$ and $L/\ell = 1$ for the solid, dashed and light solid lines respectively. The y-axis is the left-hand side of Eq. (2.116). $H\ell = 0.1$ in this plot.

We assume $y_1 > 0$, $y_2 > y_1$. The boundary conditions are the same as in Eq. (2.71). To obtain forms for the derivatives we use the following relationship [26]:

$$\frac{dP_\mu^\nu(Z)}{dZ} = (Z^2 - 1)^{-1} \{ \mu Z P_\mu^\nu(Z) - (\mu + \nu) P_{\mu-1}^\nu(Z) \}, \quad (2.114)$$

which is valid for $Re(Z) > 1$. $Q_\nu^\mu(Z)$ obeys the same relations. Then:

$$\begin{aligned} \frac{df_m(y)}{dy} = - \left\{ \frac{3/2 + i\sqrt{(m/H)^2 - 9/4}}{\ell \sinh^{5/2}(y/\ell)} \right\} & \left[A_m P_{1/2}^{i\sqrt{(m/H)^2 - 9/4}}(\cosh(y/\ell)) \right. \\ & \left. + B_m Q_{1/2}^{i\sqrt{(m/H)^2 - 9/4}}(\cosh(y/\ell)) \right]. \end{aligned} \quad (2.115)$$

We then obtain the specific solution to the boundary conditions:

$$P_{1/2}^{ip}(\cosh(y_1/\ell)) Q_{1/2}^{ip}(\cosh(y_2/\ell)) - P_{1/2}^{ip}(\cosh(y_2/\ell)) Q_{1/2}^{ip}(\cosh(y_1/\ell)) = 0, \quad (2.116)$$

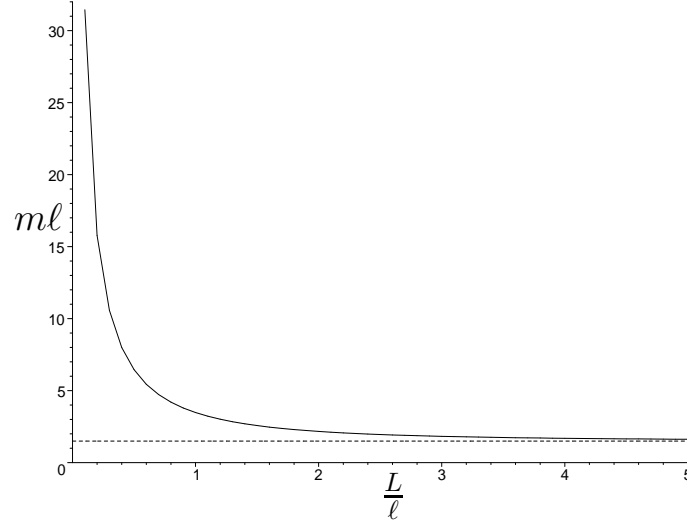


Figure 2.4: A plot of the first massive mode as a function of L/ℓ (solid line), and the mass-gap (dashed line). We see that as we increase L/ℓ the first massive mode approaches $3H/2$. $H\ell = 1$ in this plot.

where:

$$\frac{y_1}{\ell} = \operatorname{arcsinh} \left(\frac{1}{H\ell} \right), \quad \frac{y_2}{\ell} = \frac{y_1}{\ell} + \frac{L}{\ell}. \quad (2.117)$$

The KK mass eigenvalues defined by this equation are illustrated in Fig. 2.3. As far as we are aware, these eigenvalues have not previously been found.

By rewriting Eq. 2.108 in Schrödinger form, it is possible to show that for normalisable modes [25]:

$$m^2 > \frac{9}{4}H^2. \quad (2.118)$$

In the general solution, Eq. (2.112), the associated Legendre function $P_{3/2}^{i\sqrt{(m/H)^2 - 9/4}}$ diverges for large y if $i\sqrt{(m/H)^2 - 9/4}$ is real i.e. for $m^2 < \frac{9}{4}H^2$. There is a mass gap between the zero mode and the normalisable KK tower in both the one and two brane set-up.

As with the Minkowski solution if we increase the separation of the branes the mode separation decreases (see Fig. 2.3). In Fig. 2.4 we can see the spacing between the zero mode and the first massive mode as a function of L/ℓ . If we consider the RS2 model and send the second brane off to infinity we find that there is again a continuum of massive modes starting at $m^2 > \frac{9}{4}H^2$ ($m^2 = \frac{9}{4}H^2$ is not a solution).

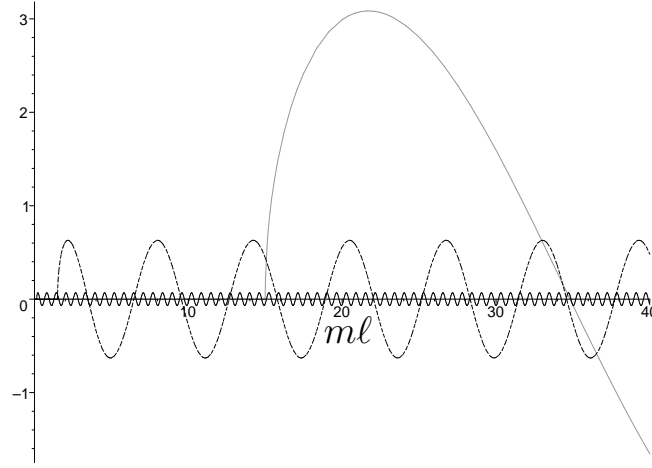


Figure 2.5: The KK mass eigenvalues for two de Sitter branes with different values of $H\ell$, i.e. different energy regimes. $H\ell = 0.1$, 1 and $H\ell = 10$ for the solid, dashed and light solid lines respectively. The y-axis is the left-hand side of Eq. (2.116). $L/\ell = 1$ in this plot.

In Fig. 2.5 we see the effect of going from the low to the high energy regime. At high energy the first KK modes are much more massive than in the low energy regime. The spacings are also much larger. Fig. 2.6 shows the spacing between the first massive mode and the mass gap as a function of $H\ell$. As we increase the energy ($H\ell$ increasing) the mass gap increases linearly. The mass of the first KK mode also increases linearly but at a faster rate than the mass gap. Therefore at higher energies we must put in even more energy, relative to the low energy regime, in order to excite the KK modes.

2.4 Friedmann Equations

Here we shall consider Friedmann-Robertson-Walker (FRW) branes. This is a general cosmological solution where the Hubble rate decreases as the energy density goes down. The FRW solution describes the uniform expansion of a homogenous and isotropic perfect fluid.

We shall derive the Friedmann equations, that govern the evolution of the model, for the standard GR case before we consider the brane results.

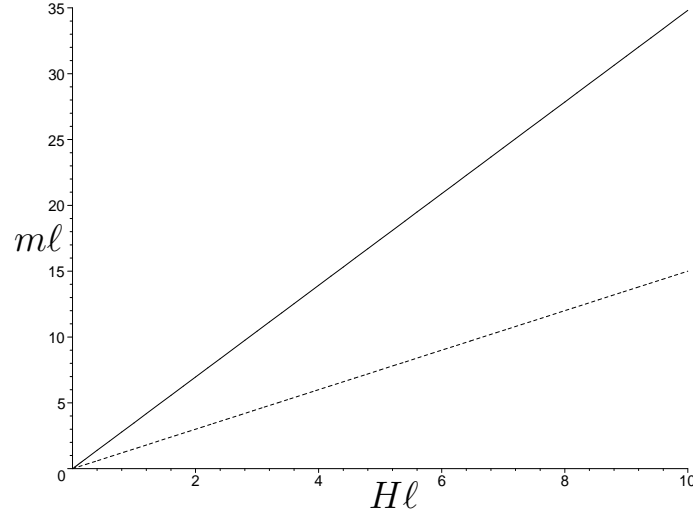


Figure 2.6: A plot of the first massive mode as a function of $H\ell$ (solid line), and the mass-gap (dashed line). We see that as we increase $H\ell$ the first massive mode diverges from $3H/2$. $L/\ell = 1$ in this plot.

2.4.1 The GR result

The FRW metric is:

$$ds^2 = -dt^2 + a^2(t) \left\{ \frac{dr^2}{1 - Kr^2} + r^2 d\theta^2 + r^2 \sin^2 \theta \right\}, \quad (2.119)$$

where $t = \text{constant}$ are maximally symmetric 3-spaces. The scale factor is $a(t)$ and K is the spatial curvature. We then use the Einstein Field equations:

$$G_{\mu\nu} = -\Lambda g_{\mu\nu} + \kappa^2 T_{\mu\nu}. \quad (2.120)$$

For $\Lambda = 0$, $\kappa^2 = 8\pi G$:

$$R_{\mu\nu} = 8\pi G \left(T_{\mu\nu} - \frac{1}{2} g_{\mu\nu} T \right). \quad (2.121)$$

We use the energy-momentum tensor for a perfect fluid:

$$T^{\mu\nu} = (\rho + P) U^\mu U^\nu + P g^{\mu\nu}, \quad (2.122)$$

where U^μ is the 4-velocity:

$$U^\mu = \frac{dx^\mu}{ds}, \quad U^\mu U_\mu = -1. \quad (2.123)$$

Therefore:

$$T = -\rho + 3P. \quad (2.124)$$

The spacetime is expanding but the fluid is at rest in a comoving frame i.e:

$$U^\mu = (1, 0, 0, 0). \quad (2.125)$$

The other ingredient that we need is the conservation of energy equation:

$$\nabla_\mu T^\mu_\nu = 0. \quad (2.126)$$

The time component gives:

$$\dot{\rho} = -3\rho H(1 + w), \quad (2.127)$$

where $w = P/\rho$ is the equation of state ($|w| \leq 1$). If w is constant then:

$$\rho \propto a^{-3(1+w)}. \quad (2.128)$$

Throughout this work we assume that w is constant. Physically this is not true as the effective equation of state will decrease from $w = 1/3$ to $w = 0$ as the universe evolves from radiation domination to matter domination. But is reasonable to assume w is constant as we either consider early time, radiation domination, or late time, matter domination.

By Eq. (2.121) we find the pure temporal component of the Ricci tensor to be:

$$R_{00} = 4\pi G(\rho + 3P). \quad (2.129)$$

From the metric we can show that:

$$R_{00} = -3\frac{\ddot{a}}{a}. \quad (2.130)$$

So we have:

$$\frac{\ddot{a}}{a} = -\frac{4}{3}\pi G(\rho + 3P), \quad (2.131)$$

which is one of the Friedmann equations. We now consider the spatial directions. In fact we only need to look at one as the expansion is isotropic. If we look at the $\theta\theta$ component, from the metric we have:

$$R_{\theta\theta} = r^2(a\ddot{a} + 2\dot{a}^2 + 2K). \quad (2.132)$$

Eq. (2.121) gives us:

$$R_{ij} = 4\pi G(\rho - P)g_{ij}, \quad (2.133)$$

so the $\theta\theta$ component is:

$$R_{\theta\theta} = 4\pi G(\rho - P)a^2r^2. \quad (2.134)$$

By Eqs. (2.132) and (2.134) we have:

$$\frac{\ddot{a}}{a} + 2\frac{\dot{a}^2}{a^2} + 2\frac{K}{a^2} = 4\pi G(\rho - P). \quad (2.135)$$

Using this with Eq. (2.131) we get the main Friedmann equation:

$$\left(\frac{\dot{a}}{a}\right)^2 = \frac{8\pi G}{3}\rho - \frac{K}{a^2}. \quad (2.136)$$

This is usually written in terms of the Hubble parameter which is defined as:

$$H \equiv \frac{\dot{a}}{a}. \quad (2.137)$$

If we include a cosmological constant in the field equations the Friedmann equations become:

$$\frac{\ddot{a}}{a} = -\frac{4}{3}\pi G(\rho + 3P) + \frac{\Lambda}{3}, \quad (2.138)$$

and:

$$H^2 = \frac{8\pi G}{3}\rho - \frac{K}{a^2} + \frac{\Lambda}{3}. \quad (2.139)$$

These are the standard GR Friedmann equations. When we consider the braneworld we will require the Israel junction conditions. This is because we now live on a hypersurface so the Friedmann equations only apply to a restricted part of the spacetime.

2.4.2 RS result

We consider a single Friedmann brane model (i.e RS2), so that gravity is described by General Relativity in the low energy limit (and not a Brans-Dicke theory). The line element is [27]:

$$ds_{(5)}^2 = -N(t, y)dt^2 + A^2(t, y)\gamma_{ij}dx^i dx^j + B^2(t, y)dy^2, \quad (2.140)$$

where γ_{ij} is the maximally symmetric space given by:

$$\gamma_{ij}dx^i dx^j = \frac{dr^2}{1 - Kr^2} + r^2 d\theta^2 + r^2 \sin^2 \theta d\phi^2. \quad (2.141)$$

The 5D field equations are:

$$G_{ab}^{(5)} = \kappa_5^2 T_{ab}^{(5)}, \quad (2.142)$$

where the energy-momentum tensor is given by:

$$T_b^{(5)a} = T_b^a|_{bulk} + T_b^a|_{brane}. \quad (2.143)$$

The bulk part of $T_{ab}^{(5)}$ is given by:

$$T_b^a|_{bulk} = -\frac{\Lambda_5}{\kappa_5^2} \delta_b^a, \quad (2.144)$$

which is just the 5D bulk cosmological constant. The brane term is given by:

$$T_b^a|_{brane} = \frac{\delta(y)}{b} \text{diag}(-\rho - \lambda, P - \lambda, P - \lambda, P - \lambda, 0), \quad (2.145)$$

where λ is the brane tension. The standard conservation of energy equation applies on the brane (only gravity can leak off the brane into the bulk). If we follow [27] and look at the non-zero components of the Einstein tensor we get for the tt component ($' = \partial/\partial y$ and $\dot{} = \partial/\partial t$):

$$G_{tt}^{(5)} = 3 \left\{ \frac{\dot{A}}{A} \left(\frac{\dot{A}}{A} + \frac{\dot{B}}{B} \right) - \frac{n^2}{b^2} \left(\frac{A''}{A} + \frac{A'}{A} \left(\frac{A'}{A} - \frac{B'}{B} \right) \right) + K \frac{N^2}{A^2} \right\}. \quad (2.146)$$

For the three brane dimensions we get:

$$\begin{aligned} G_{ij}^{(5)} = & \frac{A^2}{B^2} \gamma_{ij} \left\{ \frac{A'}{A} \left(\frac{A'}{A} + 2 \frac{N'}{N} \right) - \frac{B'}{B} \left(\frac{N'}{N} + 2 \frac{A'}{A} \right) + 2 \frac{A''}{A} + \frac{N''}{N} \right\} + \\ & \frac{A^2}{N^2} \gamma_{ij} \left\{ \frac{\dot{A}}{A} \left(2 \frac{\dot{N}}{N} - \frac{\dot{A}}{A} \right) - 2 \frac{\ddot{A}}{A} + \frac{\dot{B}}{B} \left(\frac{\dot{N}}{N} - 2 \frac{\dot{A}}{A} \right) - \frac{\ddot{B}}{B} \right\} - \gamma_{ij} K. \end{aligned} \quad (2.147)$$

For the bulk dimension we get two non-zero components:

$$G_{ty}^{(5)} = 3 \left\{ \frac{\dot{A}}{A} \frac{N'}{N} + \frac{A'}{A} \frac{\dot{B}}{B} - \frac{\dot{A}'}{A} \right\}, \quad (2.148)$$

and:

$$G_{yy}^{(5)} = 3 \left\{ \frac{A'}{A} \left(\frac{A'}{A} + \frac{N'}{N} \right) - \frac{B^2}{N^2} \left(\frac{\dot{A}}{A} \left(\frac{\dot{A}}{A} - \frac{N'}{N} \right) + \frac{\ddot{A}}{A} \right) - K \frac{B^2}{A^2} \right\}. \quad (2.149)$$

Since $T_{ty}^{(5)} = 0$ (and therefore $G_{ty}^{(5)} = 0$), this means that there is no flow of matter along the extra dimension. Therefore we get the following results from Eq. (2.148):

$$\frac{\dot{B}}{B} = \frac{\dot{A}'}{A'} - \frac{N'}{N} \frac{\dot{A}}{A}. \quad (2.150)$$

In Ref. [27] they have shown that if we define the function:

$$F(t, y) \equiv \frac{(A'A)^2}{B^2} - \frac{(\dot{A}A)^2}{N^2} - KA^2, \quad (2.151)$$

we can rewrite the Einstein equations in a simpler form. Using Eqs. (2.146), (2.150) and (2.151) we can show that:

$$F' = \frac{2A'A^3}{3} \kappa^2 T_t^t|_{bulk}. \quad (2.152)$$

Using Eqs. (2.149), (2.150) and (2.151) we can show that:

$$\dot{F} = \frac{2\dot{A}A^3}{3} \kappa^2 T_y^y|_{bulk}. \quad (2.153)$$

Thus:

$$F = \frac{2\kappa_5^2 T_t^t|_{bulk}}{3} \int A'A^3 dy = -\frac{A^4 \Lambda_5}{6} + \mathcal{C}. \quad (2.154)$$

So if we now use the form of F from Eq. (2.151) we get:

$$\left(\frac{\dot{A}}{AN} \right)^2 = \left(\frac{A'}{AB} \right)^2 - \frac{K}{A^2} + \frac{\Lambda_5}{6} + \frac{\mathcal{C}}{A^4} \quad (2.155)$$

We have the freedom in the coordinate system to redefine the extra dimension coordinate, so we set $B = 1$. We can also define t to be the proper time on the brane so we can set $N(t, 0) = 1$, which implies that:

$$\left(\frac{\dot{A}}{A} \right)^2 = \left(\frac{A'}{A} \right)^2 - \frac{K}{A^2} + \frac{\Lambda_5}{6} + \frac{\mathcal{C}}{A^4} \quad (2.156)$$

We must now consider the A'/A term, and we use the Israel junction conditions:

$$K_{\mu\nu} = -\frac{\kappa_5^2}{2} \left(T_{\mu\nu} - \frac{1}{3} T g_{\mu\nu} \right), \quad (2.157)$$

where:

$$K_{\mu\nu} = -\frac{1}{2} \partial_y g_{\mu\nu}. \quad (2.158)$$

Using this we can show that we can write the extrinsic curvature of the brane as:

$$K_\nu^\mu = \text{diag} \left(\frac{N'}{N}, \frac{A'}{A}, \frac{A'}{A}, \frac{A'}{A} \right). \quad (2.159)$$

By Eq. (2.157):

$$\left. \frac{A'}{A} \right|_{brane} = -\frac{\kappa_5^2}{6} (\rho + \lambda). \quad (2.160)$$

By Eqs. (1.12) and (2.17) we can write the Friedmann equation as:

$$H^2 = \frac{\kappa_4^2}{3} \rho \left(1 + \frac{\rho}{2\lambda} \right) - \frac{K}{a^2} + \frac{\Lambda_4}{3} + \frac{\mathcal{C}}{a^4}, \quad (2.161)$$

where \mathcal{C} is the constant of integration from Eq. (2.154) (it can also be obtained from the electric (Coulomb) part of the bulk Weyl tensor [28]). This term is called the dark radiation term from the bulk due to its a^{-4} behaviour. It can be shown that \mathcal{C} is the mass of the black hole in the Schwarzschild anti de Sitter bulk [29, 30]. The main differences between this Friedmann equation and the GR result is that we have a ρ^2 term driving the expansion. When $\rho \gg \lambda$, i.e. at early times (high energies), we see that $H \sim \rho$, unlike the GR case, $H \sim \sqrt{\rho}$. Therefore the scale factor evolves like (taking $\mathcal{C} = 0$):

$$a \propto t^{1/3(1+w)}, \quad (2.162)$$

rather than:

$$a \propto t^{2/3(1+w)}, \quad (2.163)$$

as it does in the standard GR case. In the low energy limit $\rho \ll \lambda$ (with $\mathcal{C} = 0$ again) the Friedmann equation gives us the same result as in the GR case.

The Raychaudhuri equation for the FRW brane follows from the Friedmann equation (2.161) and the conservation equation (2.127) as:

$$\dot{H} = -\frac{\kappa_4^2}{2} (\rho + p) \left(1 + \frac{\rho}{2\lambda} \right) + \frac{K}{a^2} - 2 \frac{\mathcal{C}}{a^4}. \quad (2.164)$$

The RS form of the Friedmann and Raychaudhuri equations are going to modify the predictions of primordial nucleosynthesis due to the presence of the ρ^2 and dark radiation terms. In order for the RS model to mimic the GR result at nucleosynthesis we require:

$$\lambda \gg \rho_{nuc} \gg \frac{C}{a^4}. \quad (2.165)$$

We shall consider the nucleosynthesis constraint further in Chapter 3.

2.5 Conclusions

In this chapter we have looked at the field equations in the bulk and how they are projected onto the brane for Minkowski and de Sitter brane worlds. These equations could be much more complicated if we had considered a scalar field to be present in the bulk. In general a scalar field should be present in order to stabilise the brane positions when there are two branes.

We have seen how the brane tensions are related on the two branes in both the Minkowski and de Sitter cases. The brane tensions are required to be fine tuned in order to obtain Minkowski or de Sitter branes. We have also seen how the Hubble rate on the two de Sitter branes are related.

We have looked at the Kaluza-Klein modes on Minkowski and de Sitter branes in both the RS1 and RS2 models. The Kaluza-Klein modes are decomposed into five different polarisations in three different fields (gravi-scalar, gravi-vector and the graviton). We have found the wave equation for bulk gravitational waves. We worked out the spectrum of the KK modes in both the Minkowski and de Sitter brane cases, the de Sitter case being a new result. In the RS1 case there is a discrete spectrum, described by associated Legendre functions, beginning above a mass gap. The spectrum is altered due to the curvature scale and the inter-brane separation. In the RS2 model, with an infinite brane separation, we obtain a continuum of massive KK modes, starting above the mass gap. The mass-gap is a function of the Hubble rate on the brane.

We then looked at a more general and physically relevant solution, that of the Friedmann-Robertson-Walker brane. We saw how the Friedmann equations were obtained in the standard GR setup and how we extend this to the brane world case. We saw that the brane setup modifies the high energy Hubble rate but at low energies we obtain the same result as in the GR case. In the next chapter we shall consider more complicated brane models which can give us more drastic modifications to GR.

Chapter 3

The DGP, GB and GBIG Brane World Cosmologies

3.1 Introduction

So far we have been considering the Randall-Sundrum brane models in which gravity appears 4D on the brane via the warping of the bulk dimension. This warping means that to a brane observer gravity appears 5D at high energy and 4D in the low energy regime. It is also possible to have 5D effects at low energy [31, 32]. The DGP (Dvali, Gabadadze and Porrati) model achieves this via a Einstein-Hilbert brane action; this brane Ricci scalar can be interpreted as arising from a quantum effect due to the interaction between the bulk gravitons and the matter on the brane [32] (see also [29, 33]). The induced gravity term on the brane dominates at higher energies, below a certain length scale r , so that gravity becomes 4D at high energy. As the bulk is no longer required to be warped, the DGP model lives in a Minkowski bulk. When a Friedmann brane is used within the DGP model it is possible to show that one of the solutions gives rise to late time acceleration without the presence of a dark energy field [34].

We can also construct brane models using the Gauss-Bonnet (GB) higher order curvature terms in the bulk action (see, e.g., [35, 36, 37, 38, 39, 40, 41, 42, 43, 44, 45, 46, 47]). These models modify gravity at high energy, unlike the DGP model. The Gauss-Bonnet term may be interpreted as a low-energy String Theory correction to the Einstein-Hilbert action. These models are akin to the Randall-Sundrum ones, in the sense that it is the nature of the bulk that gives rise to the 4D and 5D regimes on the brane, unlike the DGP model.

We would like to have a model that has 5D effects at both high energy and low energy but 4D gravity in between. This is because we would like a model that can modify the

early universe and explain the acceleration of the universe that we are currently experiencing. We require 4D gravity between these two limits in order for nucleosynthesis and other constraints to be obeyed.

In this chapter we shall start by taking a brief look at the DGP and GB models and see how they modify the cosmology on the brane. We shall then consider the effect of combining these two.

3.2 DGP Branes

In 2000 Dvali, Gabadadze and Porrati (DGP) [32] put forward a brane model that has low energy (infrared or IR) modifications through an induced gravity term. The induced gravity term (4D Ricci scalar term in the brane action) can be motivated by possible quantum effects of the interaction between matter on the brane and the bulk gravity. (String theories with a ghost free GB term in the bulk give rise to induced gravity terms on the brane [48].)

At early times, the 4D term dominates and General Relativity is recovered (in the background – note that the perturbations are not General Relativistic [49, 50, 51]). Gravity on the brane is 4D until the “cross-over” scale r is reached and we enter a 5D regime. At scales greater than r gravity “leaks” off the brane (the 5D Ricci term in Eq. (3.1) begins to dominate over the 4D Ricci term), and appears to observers on the brane to be 5D. As we have 4D gravity on the brane from the induced gravity we do not require the warping of the bulk space in order to recover 4D gravity. So the DGP model lives in a infinite Minkowski bulk. The DGP model has two branches, one of which is very interesting for cosmology as it ends with a phase of “self-acceleration” [34]. This is useful as we observe the universe to be in a period of acceleration which is usually explained via a dark energy field. The DGP model explains this with modified gravity. The DGP models are in some sense “unbalanced”, since they do not include ultra-violet modifications to cosmological dynamics. We would like a brane world model that modifies gravity at early times as this is where string and quantum effects must eventually dominate.

With induced gravity on the brane we have a gravitational action of the form [34]:

$$\begin{aligned}
 S_{grav} &= \frac{1}{2\kappa_5^2} \int d^5x \sqrt{-g^{(5)}} [R^{(5)} - 2\Lambda_5] \\
 &+ \frac{r}{\kappa_5^2} \int_{y=0} d^4x \sqrt{-g} [R - 2\kappa_4^2 \lambda],
 \end{aligned} \tag{3.1}$$

where r is the cross-over scale and is defined as:

$$r = \frac{\kappa_5^2}{2\kappa_4^2} = \frac{M_4^2}{2M_5^3}. \quad (3.2)$$

The sign of the induced gravity on the brane must be the same as the 5D part. We have an effective 4D gravitational constant which can be written as $\kappa_4^2 = \kappa_5^2/2r$.

The bulk field equations are of the same form as in the RS model. The 4D energy-momentum tensor is modified, in comparison to the RS model, as it includes the contribution from the induced gravity term in the action. By using the same assumptions and conditions as in the RS case (a perfect fluid undergoing isotropic and homogenous expansion) we obtain the induced gravity Friedmann equation to be [34]:

$$\epsilon \sqrt{H^2 - \frac{\mathcal{C}}{a^4} - \frac{\Lambda_5}{6} + \frac{K}{a^2}} = r \left(H^2 + \frac{K}{a^2} \right) - \frac{\kappa_5^2}{6}(\rho + \lambda), \quad (3.3)$$

where $\epsilon = \pm 1$ and \mathcal{C} is the bulk black hole mass (the DGP limit has a Minkowski bulk $\Lambda_5 = 0$ with $\mathcal{C} = 0$). If we consider a Minkowski bulk ($\Lambda_5 = 0$, $\mathcal{C} = 0$) with $\lambda = 0$ on a flat brane ($K = 0$) then we have:

$$H^2 = \pm \frac{H}{r} + \frac{\kappa_4^2}{3}\rho. \quad (3.4)$$

The two different solutions corresponding to the two different values of ϵ correspond to two different embeddings of the brane within the bulk. Both branches have a 4D limit at high energies:

$$\text{DGP}(\pm): H \gg r^{-1} \Rightarrow H^2 = \frac{\kappa_4^2}{3}\rho, \quad (3.5)$$

while at low energies both have modified 5D limits:

$$\text{DGP}(+): \quad \rho \rightarrow 0 \Rightarrow H \rightarrow \frac{1}{r}, \quad (3.6)$$

$$\text{DGP}(-): \quad \rho \rightarrow 0 \Rightarrow H = 0. \quad (3.7)$$

DGP(-) has a non-standard (and non-accelerating) late universe. The self-accelerating DGP(+) branch is of most interest for cosmology.

In dimensionless variables:

$$h = Hr, \quad \mu = \frac{r\kappa_5^2}{6}\rho, \quad \tau = \frac{t}{r}, \quad (3.8)$$

we can write the Friedmann equation (in the case $\mathcal{C} = \Lambda_5 = \lambda = 0$) as:

$$h^2 = \pm h + \mu. \quad (3.9)$$

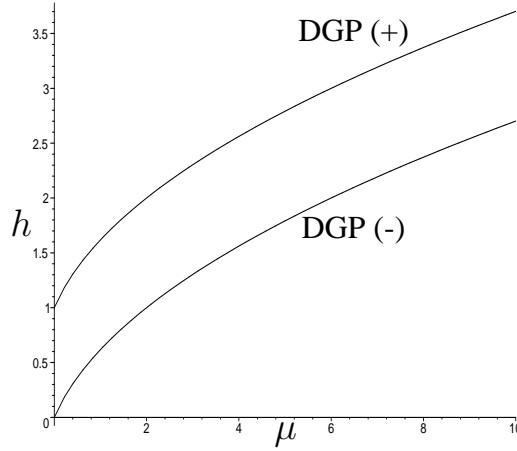


Figure 3.1: Solutions of the DGP Friedmann equation (h vs μ) with $\mathcal{C} = \Lambda_5 = \lambda = 0$. (Brane proper time τ flows from right to left, with $\tau = \infty$ at $\mu = 0$.)

The solutions for h can be written in terms of μ as:

$$h = \frac{\sqrt{1+4\mu}}{2} \pm \frac{1}{2}. \quad (3.10)$$

These solutions are shown in Fig. 3.1

In the $+$ branch we have late time self-acceleration ($H = 1/r$) i.e we end in a vacuum de Sitter state. In the $-$ branch we have $H = 0$ so we end up with a Minkowski state. The DGP(+) model gives us late time acceleration without dark energy with early universe dynamics that agrees with GR so we do not need to modify baryogenesis and other early universe events. The DGP late time acceleration has been tested against the supernova luminosity and baryon acoustic oscillations [52, 53, 54]. But the DGP is “unbalanced” as we would expect high energy (ultraviolet or UV) modifications as well. If we generalise the DGP model by introducing a negative bulk cosmological constant and a brane tension, so that the bulk is anti de Sitter, we do not get the desired results. It has been shown [55, 49, 56] that if we have an induced gravity brane in a warped bulk we either have 4D at early and late times with a period of 5D gravity in the middle or we have 4D gravity at all times. So we require another mechanism to modify early times in a induced gravity brane model.

3.3 Gauss-Bonnet Brane Worlds

The Gauss-Bonnet term added to the Einstein-Hilbert term, gives the most general action in 5D with 2^{nd} order field equations, as shown by Lovelock [57]. In four dimensions the

Gauss-Bonnet term is a topological invariant for compact manifolds without a boundary. Therefore Lovelock type gravity in 4D reduces to standard GR. The Gauss-Bonnet terms have also been shown to be a low order string correction to the action (see, e.g., [35, 36, 37, 38, 39, 40, 41, 42, 43, 44, 45, 46]). In a 5D theory the GB terms are only present in the bulk. The bulk action is [37]:

$$S_{grav} = \frac{1}{2\kappa_5^2} \int d^5x \sqrt{-g^{(5)}} \left[R^{(5)} - 2\Lambda_5 + \alpha \left(R^{(5)2} - 4R_{ab}^{(5)} R^{(5)ab} + R_{abcd}^{(5)} R^{(5)abcd} \right) \right], \quad (3.11)$$

where α is the Gauss-Bonnet coupling. In a classical Gauss-Bonnet theory α can be of either sign. It has been shown in Ref. [58] that for Gauss-Bonnet brane worlds a negative value of α gives rise to antigravity or tachyon modes on the brane. However if a bulk scalar field is present a negative α can be allowed without these effects occurring.

The field equations are much more complicated with the Gauss-Bonnet term in the action. The Friedmann equation that we obtain is of the form [39]:

$$H^2 = \frac{C_+ + C_- - 2}{8\alpha} - \frac{K}{a^2}, \quad (3.12)$$

where:

$$C_{\pm} = \left(\sqrt{\left(1 + \frac{4}{3}\alpha\Lambda_5 + 8\alpha\frac{\mathcal{C}}{a^4} \right)^{3/2} + \frac{\alpha\kappa_5^4(\rho + \lambda)^2}{2}} \pm \kappa_5^2(\rho + \lambda)\sqrt{\frac{\alpha}{2}} \right)^{2/3}. \quad (3.13)$$

The bulk cosmological constant Λ_5 has a modified relation to the curvature scale due to the GB gravity [59]:

$$\Lambda_5 = -\frac{6}{\ell^2} + \frac{12\alpha}{\ell^4}. \quad (3.14)$$

The first term is the standard RS result while the second is the Gauss-Bonnet contribution. This also gives us a constraint on α as Eq. (3.14) implies:

$$\frac{1}{\ell^2} = \frac{1}{4\alpha} \left[1 - \sqrt{1 + \frac{4}{3}\alpha\Lambda_5} \right]. \quad (3.15)$$

We have only one root here as this is the only one that gives the correct RS limit. The plus root could be written as:

$$\frac{4\alpha}{\ell^2} = 1 + \sqrt{1 + \frac{4}{3}\alpha\Lambda_5}. \quad (3.16)$$

The RS limit ($\alpha \rightarrow 0$) is not consistent with this solution.

From Eq. (3.15) we see that:

$$\alpha \leq \frac{\ell^2}{4}. \quad (3.17)$$

As $\sqrt{1 + \frac{4}{3}\alpha\Lambda_5} > 0$, this also ensures that $\Lambda_5 < 0$.

If we consider the case $\mathcal{C} = 0 = \Lambda_5$ and $\rho \gg \lambda$ for a flat brane ($K = 0$) we see, from Eq. (3.12), that $H \sim \rho^{1/3}$. The scale factor behaves as:

$$a \propto t^{1/(1+w)}. \quad (3.18)$$

So the Gauss-Bonnet bulk gravity effects the early universe. At late times \mathcal{C}/a^4 , $\rho \rightarrow 0$ with $\lambda = 0 = \Lambda_5$ we can show that we end with $H = 0$ so again we end with a Minkowski brane.

This GB Friedmann equation has no 4D limit:

$$\text{GB high energy: } H \gg \alpha^{-1/2} \Rightarrow H^2 \propto \rho^{2/3}, \quad (3.19)$$

$$\text{GB low energy: } H \ll \alpha^{-1/2} \Rightarrow H^2 \propto \rho^2. \quad (3.20)$$

The Friedmann equations for pure DGP and pure GB models with a Minkowski bulk are compared in Fig. 3.2. The GB Friedmann equation is a cubic, so has three roots. We can show that for $\rho > 0$ there is only one real root. This is shown in Fig. 3.2. When $\rho = 0$ there is the repeated root $H = 0$.

3.4 Gauss-Bonnet-Induced Gravity (GBIG) Branes

In this section and the next chapter we shall consider what happens when we combine the induced gravity terms of the DGP model with a Gauss-Bonnet bulk. We will start by presenting the model's governing equations in full generalisation. We shall then consider the modifications in relation to the pure DGP model. This means we shall only consider models with zero brane tension in a Minkowski bulk. In the next chapter we shall extend this to the non-zero brane tension in Anti-de Sitter bulk cases. We will see that even in the simplest case we get some striking new effects such as a finite density big bang. Some of the work in this section was first presented in [60].

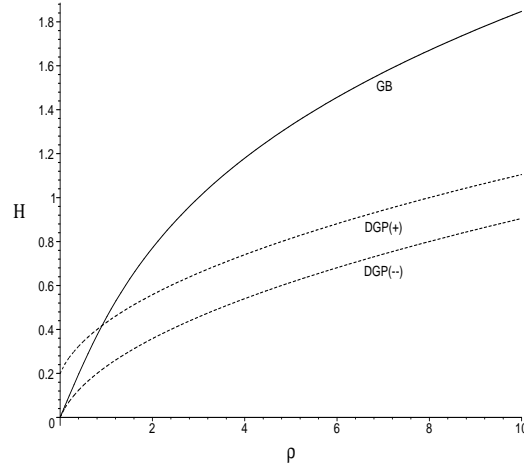


Figure 3.2: DGP and GB solutions of the Friedmann equation (H vs ρ) for a Minkowski bulk. (Brane proper time t flows from right to left, with $t = \infty$ at $\rho = 0$.)

3.4.1 Field Equations

The generalised gravitational action contains the Gauss-Bonnet (GB) term in the bulk and the induced gravity (IG) term on the brane:

$$\begin{aligned}
 S_{\text{grav}} = & \frac{1}{2\kappa_5^2} \int d^5x \sqrt{-g^{(5)}} \left\{ R^{(5)} - 2\Lambda_5 + \alpha \left[R^{(5)2} - 4R_{ab}^{(5)} R^{(5)ab} + R_{abcd}^{(5)} R^{(5)abcd} \right] \right\} \\
 & + \frac{r}{\kappa_5^2} \int_{\text{brane}} d^4x \sqrt{-g} \left[R - \frac{\kappa_5^2}{r} \lambda \right], \quad (3.21)
 \end{aligned}$$

where α (≥ 0) is the GB coupling constant and r (≥ 0)¹ is the IG cross-over scale and λ is the brane tension. As in the previous models we assume Z_2 symmetry about the brane.

The standard energy conservation equation holds on the brane,

$$\dot{\rho} + 3H(1+w)\rho = 0, \quad w = p/\rho. \quad (3.22)$$

The modified Friedmann equation was found in the most general case (where the bulk contains a black hole and a cosmological constant, and the brane has tension) in Ref. [62]:

$$\left[1 + \frac{8}{3}\alpha \left(H^2 + \frac{\Phi}{2} + \frac{K}{a^2} \right) \right]^2 \left(H^2 - \Phi + \frac{K}{a^2} \right) = \left[rH^2 + r\frac{K}{a^2} - \frac{\kappa_5^2}{6}(\rho + \lambda) \right]^2, \quad (3.23)$$

¹Note: the cross-over scale used is the one in Ref. [32] and is half that used in Refs. [60, 61].

where K is the brane curvature and Φ is determined by:

$$\Phi + 2\alpha\Phi^2 = \frac{\Lambda_5}{6} + \frac{\mathcal{C}}{a^4}, \quad (3.24)$$

where \mathcal{C} is the bulk black hole mass. In the correct limits this Friedmann equation reduces to forms equivalent to those previously seen.

In the rest of this chapter we shall only consider a Minkowski bulk ($\Lambda_5 = 0$) without a bulk black hole ($\mathcal{C} = 0$), so that Φ is a solution of:

$$\Phi + 2\alpha\Phi^2 = 0. \quad (3.25)$$

Equation (3.25) has solutions $\Phi = 0, -1/2\alpha$, but here we only consider $\Phi = 0$, since the second solution has no IG limit and thus does not include the DGP model. We shall consider $\Phi = -1/2\alpha$ in Chapter 4. In this bulk we shall consider a spatially flat brane ($K = 0$) without tension ($\lambda = 0$). Therefore the modified Friedmann equation is given by:

$$\left(1 + \frac{8}{3}\alpha H^2\right)^2 H^2 = \left(rH^2 - \frac{\kappa_5^2}{6}\rho\right)^2. \quad (3.26)$$

3.4.2 DGP brane with GB bulk gravity: combining UV and IR modifications of GR

By defining the dimensionless variables:

$$\gamma = \frac{8\alpha}{3r^2}, \quad h = Hr, \quad \mu = \frac{r\kappa_5^2}{6}\rho, \quad \tau = \frac{t}{r}, \quad (3.27)$$

the GBIG Friedmann equation becomes:

$$(\gamma h^2 + 1)^2 h^2 = (h^2 - \mu)^2, \quad (3.28)$$

while the conservation equation becomes:

$$\mu' + 3h(1 + w)\mu = 0, \quad (3.29)$$

where a dash denotes $d/d\tau$, and $h = a'/a$. In defining the variable γ as above, we have both the IG and GB contributions within one parameter. This reduces the dimensionality of the solution state space.

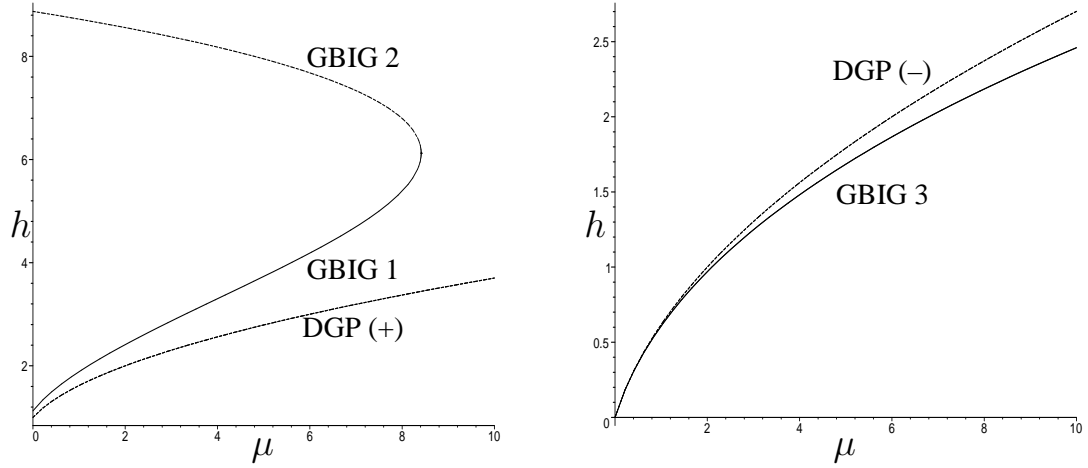


Figure 3.3: Solutions of the GBIG Friedmann equation ($h(\mu)$) with positive γ ($\gamma = 0.1$). On the left is the DGP (+) model and its Gauss-Bonnet corrections, GBIG 1 and GBIG 2. On the right is the DGP (-) model and its GB correction, GBIG 3. The curves are independent of the equation of state w . Brane proper time τ flows from right to left, with $\tau = \infty$ at $\mu = 0$.

Combining Eqs. (3.28) and (3.29), we find the modified Raychaudhuri equation:

$$h' = \frac{3\mu(1+w)(h^2 - \mu)}{(\gamma h^2 + 1)(3\gamma h^2 + 1) - 2(h^2 - \mu)}. \quad (3.30)$$

The acceleration $a''/a = h' + h^2$ is then given by:

$$\frac{a''}{a} = \frac{h^2(\gamma h^2 + 1)(3\gamma h^2 + 1) - (h^2 - \mu)[2h^2 - 3(1+w)\mu]}{(\gamma h^2 + 1)(3\gamma h^2 + 1) - 2(h^2 - \mu)}. \quad (3.31)$$

These shall be of use later.

The GB correction, via a non-zero value of γ , introduces significant complexity to the Friedmann equation, which becomes cubic in h^2 , as opposed to the quadratic DGP (\pm) case, $\gamma = 0$, for which:

$$h^2 = \frac{1}{2} \left\{ 1 + 2\mu \pm \sqrt{1 + 4\mu} \right\}, \quad (3.32)$$

as seen in Eq. (3.10). This additional complexity has a dramatic effect on the dynamics of the DGP (+) model, as shown in Fig. 3.3. The contribution of GB gravity at early times removes the infinite density big bang, and the universe starts at finite maximum density and finite pressure (but, as we show below, with infinite curvature). Furthermore, there are two such solutions, each with late-time self-acceleration, marked GBIG 1 and 2 on the plots. Since GBIG 2 is accelerating throughout its evolution (actually super-inflating, $h' > 0$), the physically relevant self-accelerating solution is GBIG 1.

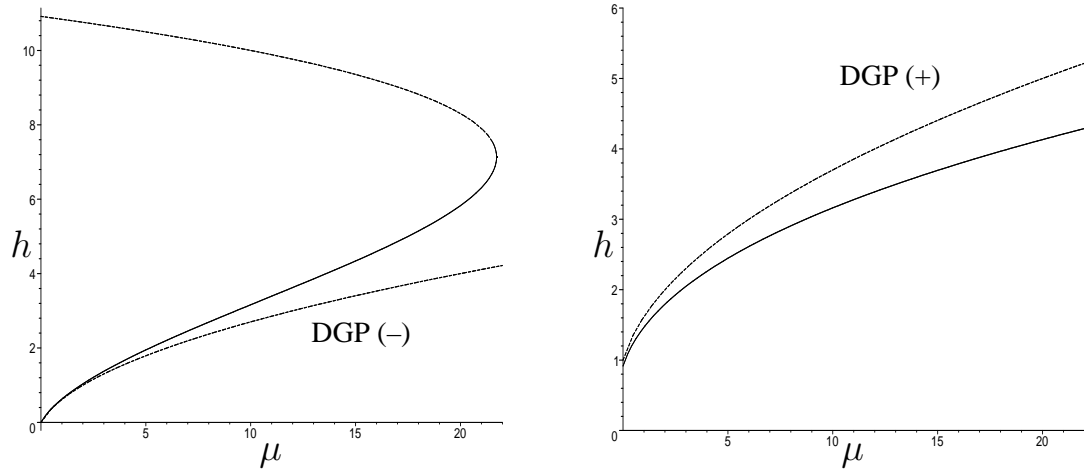


Figure 3.4: Solutions of the GBIG Friedmann equation ($h(\mu)$) with negative γ ($\gamma = -0.1$). On the left is the DGP $(-)$ model and its Gauss-Bonnet corrections, GBIG 1 and GBIG 2. On the right is the DGP $(+)$ model and its GB correction, GBIG 3. The curves are independent of the equation of state w . Brane proper time τ flows from right to left, with $\tau = \infty$ at $\mu = 0$.

In Ref. [58] it is shown that a negative value of α leads to antigravity or tachyon modes on the brane. A negative value of α can give regular solutions if a bulk scalar field is present. If we allow $\gamma < 0$ the effect of the GB terms is to produce a finite density big bang on the DGP $(-)$ branch, Fig. 3.4. The DGP $(-)$ branch is wrapped back on itself instead of the DGP $(+)$ branch as in the $\gamma > 0$ case. The DGP $(+)$ branch is now modified in a similar manner as the DGP $(-)$ was in the previous case. The consequence of this is that the finite density big bang model no longer self-accelerates. We could get acceleration at late times by including positive brane tension as we shall see later. In the rest of this chapter we shall confine ourselves to $\gamma > 0$.

The cubic in h^2 , Eq. (3.28), has three real roots when $0 < \gamma < 1/4$ (see below). Two of these roots correspond to GBIG 1 and GBIG 2, which are modifications of the DGP $(+)$ model. The third root GBIG 3 is a modification of the DGP $(-)$ model, as illustrated in Fig. 3.3. Note that the curves in these figures are independent of the equation of state w of the matter content of the universe – w will determine the time evolution of the universe along the curves, via the conservation equation (3.29).

The plots show that GBIG 3 starts with a hot big bang, $\rho = \infty$, in common with the DGP (\pm) and GB models in Fig. 3.2. By contrast, GBIG 1 and GBIG 2 have no big bang, since the density is bounded above:

$$\mu \leq \mu_i, \quad (3.33)$$

where μ_i (which is positive only for $\gamma < 1/4$), is found below, in Eq. (3.48).

The finite-density beginning was pointed out in Ref. [62], where the cubic for the general case (i.e., with brane tension, bulk cosmological constant and bulk black hole) was qualitatively analysed. The analysis shows that one solution, GBIG 3, is not bounded, which was not noticed in Ref. [62]. The numerical plots of the Friedmann equation in Fig. 3.3 are crucial to a proper understanding of the algebraic analysis of the cubic roots.

A detailed analysis [62, 63] of the cubic equation (3.28) confirms the numerical results, and shows that (for $\mu > 0$):

$$0 < \gamma < \frac{1}{4} : 3 \text{ real roots, GBIG 1-3,} \quad (3.34)$$

$$\gamma \geq \frac{1}{4} : 1 \text{ real root, GBIG 3.} \quad (3.35)$$

The real roots are given as follows:

- For $0 < \gamma < 1/4$: the roots GBIG 1-2 are

$$\gamma^2 h^2 = \frac{1-2\gamma}{3} + 2\sqrt{-Q} \cos\left(\theta + \frac{n\pi}{3}\right) \text{ for } \mu \leq \mu_i, \quad (3.36)$$

where $n = 4$ for GBIG 1, $n = 2$ for GBIG 2, and the root GBIG 3 is

$$\gamma^2 h^2 = \frac{1-2\gamma}{3} + \begin{cases} 2\sqrt{-Q} \cos \theta & \text{for } \mu \leq \mu_i, \\ S_+ + S_- & \text{for } \mu \geq \mu_i. \end{cases} \quad (3.37)$$

- For $\gamma \geq 1/4$: the only real root GBIG 3 is

$$\gamma^2 h^2 = \frac{1-2\gamma}{3} + S_+ + S_-. \quad (3.38)$$

In the above, S_{\pm}, Q, R, θ are defined by

$$S_{\pm} = \left[R \pm \sqrt{R^2 + Q^3} \right]^{1/3}, \quad (3.39)$$

$$Q = \frac{\gamma^2}{3}(1 + 2\mu) - \frac{1}{9}(2\gamma - 1)^2, \quad (3.40)$$

$$R = \frac{\gamma^4 \mu^2}{2} + \frac{\gamma^2}{6}(2\gamma - 1)(1 + 2\mu) - \frac{(2\gamma - 1)^3}{27}, \quad (3.41)$$

$$\cos 3\theta = R/\sqrt{-Q^3}. \quad (3.42)$$

The GBIG 1 and GBIG 2 solutions agree with those in Ref. [62] (where the roots are given in the fully general case, with brane tension and a bulk black hole and cosmological constant).

The explicit form of the solutions can be used to confirm the features in Figs. 3.3 and 3.4. Equations (3.37)–(3.42) show that GBIG 3 starts with a big bang, $h, \mu \rightarrow \infty$, with $h^2 \sim \mu^{2/3}$ near the big bang. This is the same as the high-energy behaviour of the pure GB model, as shown by Eq. (3.19) – the GB effect dominates at high energies in GBIG 3. This is not the case for GBIG 1–2, where the high energy behaviour is completely different from the pure GB model (and from the DGP(+) model).

The maximum density feature of GBIG 1–2 is more easily confirmed by analysing the turning points of μ as a function of h^2 . The GBIG Friedmann equation (3.28) gives

$$\frac{d\mu}{d(h^2)} = \frac{2(h^2 - \mu) - (\gamma h^2 + 1)(3\gamma h^2 + 1)}{2(h^2 - \mu)}. \quad (3.43)$$

Substituting $d\mu/d(h^2) = 0$ into Eq. (3.28), we find that

$$h_i = \frac{1 \pm \sqrt{1 - 3\gamma}}{3\gamma}, \quad (3.44)$$

$$\mu_i = \frac{2 - 9\gamma \pm 2(1 - 3\gamma)^{3/2}}{27\gamma^2}. \quad (3.45)$$

The second equation shows that positive maximum density only arises for the upper sign and with $\gamma < 1/4$, in agreement with the cubic analysis.

$$\infty > \mu_i > 0 \Rightarrow 0 < \gamma < \frac{1}{4}. \quad (3.46)$$

Thus the initial Hubble rate and density for GBIG 1–2 are

$$h_i = \frac{1 + \sqrt{1 - 3\gamma}}{3\gamma}, \quad (3.47)$$

$$\mu_i = \frac{2 - 9\gamma + 2(1 - 3\gamma)^{3/2}}{27\gamma^2}. \quad (3.48)$$

If $\gamma = 0$, then GBIG 1–2 reduce to DGP(+), and $h_i = \mu_i = \infty$. Note that

$$h_i \geq 2 \Leftrightarrow H_i \geq \frac{2}{r}. \quad (3.49)$$

The case $\gamma = 1/4, \mu_i = 0$ corresponds to a vacuum brane with de Sitter expansion, with $h = h_i = 2$, generalizing the DGP(+) vacuum de Sitter solution [34].

The late-time asymptotic value of the expansion rate, as $\mu \rightarrow 0$, is

$$h_\infty = \frac{1 \pm \sqrt{1 - 4\gamma}}{2\gamma}, \quad (3.50)$$

where the minus sign corresponds to GBIG 1 and the plus sign to GBIG 2. In the limit $\gamma \rightarrow 0$, GBIG 1 recovers the DGP(+) case, $h_\infty = 1$, while for GBIG 2, $h_\infty \rightarrow \infty$; the parabolic GBIG 1–2 curve in Fig. 3.3 “unwraps” and transforms into the DGP(+) curve. Equations (3.34) and (3.50) show that

$$1 \leq h_\infty < 2 \text{ for GBIG 1,} \quad (3.51)$$

while:

$$2 < h_\infty < \infty \text{ for GBIG 2.} \quad (3.52)$$

The behaviour of the key GBIG 1–2 parameters is illustrated in Figs. 3.5 and 3.6.

3.4.3 Cosmological Dynamics

The GBIG 1 model, which is the physically relevant generalisation of the DGP(+) model, exists if Eq. (3.34) holds. By Eq. (3.27), this means that the GB length scale $L_{\text{gb}} = \sqrt{\alpha}$ must be below a maximum threshold determined by the IG cross-over scale:

$$\gamma < \frac{1}{4} \Leftrightarrow L_{\text{gb}} \equiv \sqrt{\alpha} < \frac{1}{4} \sqrt{\frac{3}{2}} r. \quad (3.53)$$

If the GB term is taken as the correction term in certain string theories, then $L_{\text{gb}} \sim L_{\text{string}}$, while $r \sim H_0^{-1}$, so that this bound is easily satisfied.

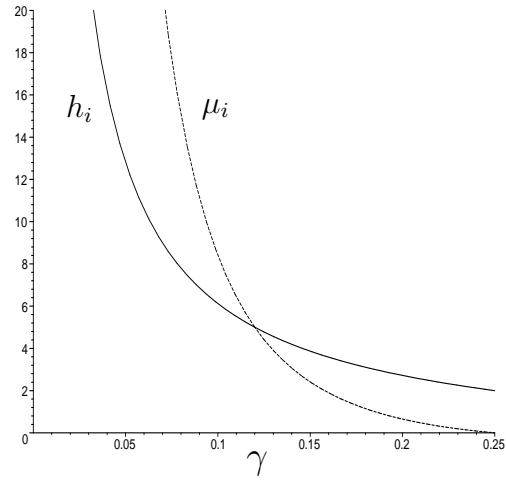


Figure 3.5: The dependence in GBIG 1–2 of the initial expansion rate and density on γ .

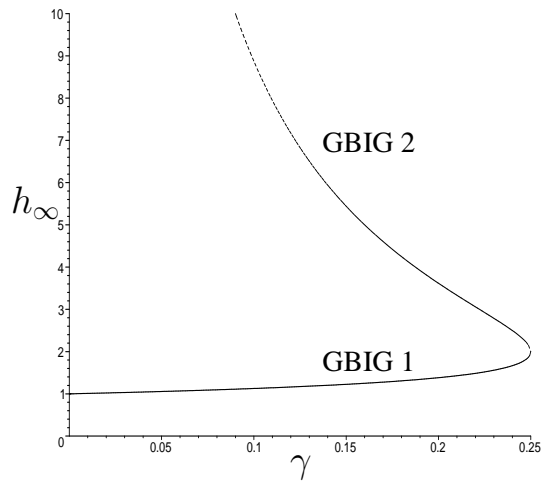


Figure 3.6: The GBIG 1–2 late-time asymptotic expansion rate as a function of γ .

When Eq. (3.53) holds, the universe starts with a maximum density ρ_i and maximum Hubble rate H_i , and evolves to an asymptotic vacuum de Sitter state:

$$0 < \rho < \rho_i = \frac{r^3}{16\kappa_5^2\alpha^2} \left\{ 1 - \frac{12\alpha}{r^2} + \left(1 - \frac{8\alpha}{r^2} \right)^{3/2} \right\}, \quad (3.54)$$

$$H_\infty < H < H_i = \frac{r}{8\alpha} \left(1 + \sqrt{1 - \frac{8\alpha}{r^2}} \right). \quad (3.55)$$

At any epoch t_0 , the proper time back to the beginning is:

$$t_0 - t_i = r \int_{a_i}^{a_0} \frac{da}{ah}. \quad (3.56)$$

Since a and h are nonzero on the interval of integration, the time back to the beginning is finite.

The current Hubble rate can be approximated by the final de Sitter Hubble rate, $H_0 \sim H_\infty$, so that by Eq. (3.51), the cross-over scale obeys:

$$H_0^{-1} \lesssim r \lesssim 2H_0^{-1}. \quad (3.57)$$

In the DGP(+) limit, $r \sim 1.2H_0^{-1}$ [64]. The effect of GB gravity is to allow for increased r but not beyond $r \sim 2H_0^{-1}$.

However, there is a UV-IR “bootstrap” operating to severely limit the GB effect at late times. The key point is that appreciable late-time GB effects require an increase in γ (see Fig. 3.6), whereas the primordial Hubble rate H_i is suppressed by an increase in γ – as shown in Fig. 3.5. Equations (3.47) and (3.50) imply that:

$$H_i \gg H_0 \Rightarrow \gamma \ll \frac{1}{4}. \quad (3.58)$$

Thus the GBIG 1 model does not alleviate the DGP(+) fine-tuning problem of a very large cross-over scale, $r \sim H_0^{-1} \sim (10^{-33} \text{ eV})^{-1}$.

The GBIG 1 Friedman equation (3.36) gives:

$$H^2 = \frac{3r^2}{64\alpha^2} \left\{ 1 - \frac{16\alpha}{3r^2} + 2\sqrt{\left(\frac{16\alpha}{3r^2} - 1 \right)^2 - \frac{64\alpha^2}{9r^4} (3 + 2r^2\kappa_4^2\rho)} \cos \left[\theta(\rho) + \frac{4\pi}{3} \right] \right\}, \quad (3.59)$$

where:

$$\cos 3\theta(\rho) = \frac{2048\alpha^4\mu^2 + 96\alpha^2r^4(1 + 2\mu) \left(\frac{16\alpha}{3r^2} - 1 \right) - 2 \left(\frac{16\alpha}{3r^2} - 1 \right)^3}{3r^8 \left[\left(\frac{16\alpha}{3r^2} - 1 \right)^2 - \frac{64\alpha^2}{9r^4} (1 - 2\mu) \right]^{3/2}}. \quad (3.60)$$

A more convenient form of the Friedmann equation follows from solving Eq. (3.28) for μ :

$$\mu = h^2 - h(\gamma h^2 + 1), \quad h_\infty \leq h < h_i. \quad (3.61)$$

By expanding to first order in $h^2 - h_\infty^2$, we find that at late times:

$$h^2 = h_\infty^2 + 2 \left(\frac{h_\infty}{2 - h_\infty} \right) \mu + O(\mu^2). \quad (3.62)$$

Taking the DGP(+) limit $h_\infty \rightarrow 1$, and comparing with Eqs. (3.4) and (3.32), we find that the effective Newton constant in GBIG 1 is:

$$G = \left(\frac{h_\infty}{2 - h_\infty} \right) \frac{G_5}{r}, \quad (3.63)$$

where $G_5 = \kappa_5^2/8\pi$ is the fundamental, 5D gravitational constant. In the DGP (+) case, $G = G_5/r$.

Equation (3.63) gives a relation for the fundamental Planck scale M_5 :

$$M_5^3 \sim \left(\frac{r H_0}{2 - r H_0} \right) \frac{M_p^2}{r}, \quad (3.64)$$

where M_p is the effective 4D Planck scale, and we used $H_\infty \sim H_0$. As $r \rightarrow 2H_0^{-1}$ (its upper limit), so M_5 increases. This is very different from the DGP(+) case, where:

$$M_5^3 = M_p^2/r, \quad (3.65)$$

so that M_5 is constrained to be very low, $M_5 \lesssim 100 \text{ MeV}$. In principle, GB gravity allows us to solve the problem of a very low fundamental Planck scale in DGP(+)- but in practice, the UV-IR bootstrap, Eq. (3.58), means that $\gamma \sim 0$ so that M_5 is effectively the same as in the DGP(+) case. Thus the GB modification of the DGP(+) does not change the fine tuning of the cross-over scale r , nor the consequent low value of M_5 . This is because γ is forced to be close to 0 if we want self-acceleration to replace dark energy, as in the DGP(+) case. However, no matter how small γ is, a nonzero γ dramatically alters the early universe, by removing the infinite-density big bang.

What is the nature of the beginning of the universe in GBIG 1? We can use Eq. (3.43) in Eq. (3.30), for matter with $w > -1$, to analyze the initial state, $d\mu/d(h^2) \rightarrow 0+$. We find that $h'_i = -\infty$, i.e., infinite deceleration:

$$a''_i = -\infty. \quad (3.66)$$

(For GBIG 2, with $d\mu/d(h^2) \rightarrow 0-$, we have $h'_i = +\infty$.) The initial state has no big bang, but it has infinite deceleration, and thus infinite Ricci curvature. The brane universe is born in a “quiescent” singularity. Although similar singularities may be found in induced gravity models [65], they arise from the special extra effect of a bulk black hole or a negative brane tension which is very different from the gravitational GB effect that is operating in the GBIG singularity. A key point is that neither the DGP(+) model nor the GB model avoid the big bang, as shown in Eqs. (3.5) and (3.19). But together, the IG and GB effects combine in a “nonlinear” way to produce entirely new behaviour. If we switch off either of these effects, the big bang reappears.

This singularity is reminiscent of the “sudden” (future) singularities in General Relativity [66] – but unlike those singularities, the GBIG 1–2 singularity has finite pressure. The initial curvature singularity signals a breakdown of the brane spacetime. The (Minkowski) bulk remains regular, but the imbedding of the brane becomes singular. Higher-order quantum-gravity effects will be needed to cure this singularity.

By performing an expansion near the initial state, using Eq. (3.61), we find that the primordial Hubble rate in GBIG 1, after the infinite deceleration at the birth of the universe, is given by:

$$H^2 \approx H_i^2 - \frac{r\kappa_4}{\sqrt{3}} \left[\frac{3H_i^2 - \kappa_4^2 \rho_i}{8\alpha(1 + 4\alpha H_i^2) - 1} \right]^{1/2} (\rho_i - \rho)^{1/2}. \quad (3.67)$$

This is independent of the equation of state w so that the universe decelerates for a finite time after its infinite-deceleration birth, regardless of the matter content. If there is primordial inflation in the GBIG 1 universe, then the acceleration a'' will become positive. For a realistic model (satisfying nucleosynthesis and other constraints), a'' must subsequently become negative, so that the universe decelerates during radiation- and early matter-domination. Finally, a'' will become positive again as the late universe self-accelerates due to the IG effects.

We can simplify the expression (3.31) for the acceleration in GBIG 1 via Eq. (3.61):

$$f = \frac{x(3\gamma x + 1 - 2\sqrt{x}) + 3(1 + w)[x\sqrt{x} - x(\gamma x + 1)]}{3\gamma x + 1 - 2\sqrt{x}}, \quad (3.68)$$

where $f \equiv a''/a$, $x \equiv h^2$. For a given $w(x)$, we can plot $f(x)$. We show an example in Fig. 3.7 of a simple model, with primordial inflation followed by radiation domination, followed by late-time self-acceleration. We have used the effective equation of state:

$$w = \begin{cases} -0.9 & n(h_i^2 - h_\infty^2) + h_\infty^2 < x < h_i^2, \\ 1/3 & h_\infty^2 < x < n(h_i^2 - h_\infty^2) + h_\infty^2. \end{cases} \quad (3.69)$$

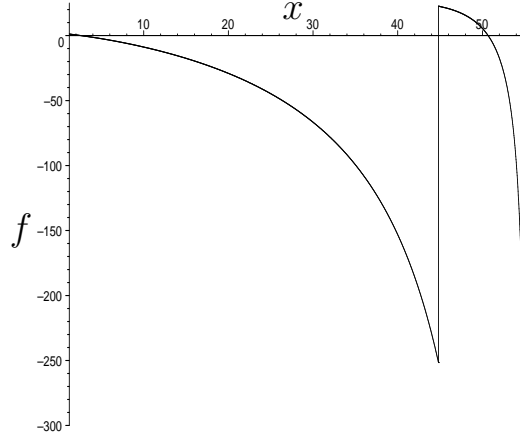


Figure 3.7: The acceleration $f = a''/a$ vs $x = h^2$, for a GBIG 1 cosmology with inflation, followed by radiation domination, followed by late-time self-acceleration. Brane proper time flows from right to left. Here $\gamma = 1/12$, and $n = 0.8$ in Eq. (3.69).

Here $0 < n < 1$ is a parameter determining the time of reheating (with $n = 0$ corresponding to no inflation and $n = 1$ to no reheating/ radiation). The values used for the equation of state are chosen in order to mimic slow-roll inflation in the first epoch ($w = -0.9$) and radiation in the second ($w = 1/3$).

3.4.4 Nucleosynthesis and the age of the universe

We have noted the UV-IR bootstrap, which enforces a very small value on γ if the universe is to be old enough. In order to make this more quantitative we impose constraints from nucleosynthesis and the age of the universe.

As already stated the DGP cross over-scale must be of the order of the Hubble scale or larger, therefore:

$$r \geq H_0^{-1} \Rightarrow Hr \geq \frac{H}{H_0}, \quad (3.70)$$

where H_0 is the current Hubble rate. Taking nucleosynthesis to have occurred at an energy scale of 1MeV and the observed universe to be at a scale of 10^{-33} eV we have the constraint that:

$$Hr \gtrsim \frac{1\text{MeV}}{10^{-33}\text{eV}} = 10^{39}. \quad (3.71)$$

We can also put a constraint on γ from requiring H_i to have occurred at an energy scale greater than 1TeV. This is in order to put it outside the range of collider experiments. Using the solution for h_i in Eq. (3.47) we can write γ as:

$$\gamma = \frac{2h_i - 1}{3h_i^2}, \quad (3.72)$$

where:

$$h_i = H_i r > 10^{45}. \quad (3.73)$$

Therefore γ is constrained by:

$$\gamma \lesssim 10^{-45}. \quad (3.74)$$

Taking $r \sim H_0^{-1} \sim (10^{-33} \text{ eV})^{-1}$ the above constraint gives:

$$\alpha \lesssim 10^{21} \text{ eV}^{-2}. \quad (3.75)$$

The string energy scale ($\alpha^{-1/2}$) is then constrained by:

$$\alpha^{-1/2} \gtrsim 10^{-10} \text{ eV}. \quad (3.76)$$

This is compatible with the constraint from proton decay which gives [67]:

$$\alpha^{-1/2} > 10^{17} \text{ eV}. \quad (3.77)$$

The GBIG Friedmann equation, in the case $\lambda = 0 = \Phi$, can be written as:

$$\left(H^2 - \frac{\kappa_4^2}{3} \rho \right)^2 = \frac{H^2}{r^2} \left(1 + \frac{8\alpha}{3} H^2 \right)^2, \quad (3.78)$$

where the left hand side is exactly zero in the GR limit. To see if the GBIG model approximates GR in the era of nucleosynthesis we write the above Friedmann equation in a dimensionless form and apply the constraints above. The dimensionless Friedmann equation, Eq. (3.78), can be written as:

$$\left(1 - \frac{\kappa_4^2 \rho}{3H^2} \right)^2 = \frac{1}{H^2 r^2} (1 + \gamma H^2 r^2)^2. \quad (3.79)$$

Expanding out the right hand side and using the constraints above we find:

$$\left(1 - \frac{\kappa_4^2 \rho}{3H^2} \right)^2 \lesssim 10^{-12}, \quad (3.80)$$

during nucleosynthesis. Thus the model will safely meet nucleosynthesis constraints if Eq. (3.73) holds.

In order to calculate the age of the universe we define a new set of dimensionless density parameters:

$$\Omega_\alpha = \frac{16}{3}\alpha H_0^2, \quad \Omega_{\text{rc}} = \frac{1}{4r^2 H_0^2}, \quad \Omega_\phi = \frac{\Phi}{2H_0^2}, \quad \Omega_{\text{m}} = \frac{\kappa_4^2}{3H_0^2}\rho, \quad \Omega_\lambda = \frac{\kappa_4^2}{3H_0^2}\lambda. \quad (3.81)$$

In terms of the Ω parameters the (general) GBIG Friedmann equation, Eq. (3.23), can be written as:

$$\Omega_{\text{rc}} \left\{ 2 + \Omega_\alpha (E^2 + \Omega_\phi) \right\}^2 (E^2 - 2\Omega_\phi) = [E^2 - \Omega_{\text{m}}(1+z)^3 - \Omega_\lambda]^2, \quad (3.82)$$

where $E = H/H_0$.

In order to reduce the number of free parameters in the model we consider the constraint on Ω_α at the present time ($z = 0$, $H = H_0$). This gives:

$$\Omega_{\alpha\pm} = \frac{1}{(1 + \Omega_\phi)} \left\{ \pm \frac{(1 - \Omega_{\text{m}} - \Omega_\lambda)}{\sqrt{\Omega_{\text{rc}}(1 - 2\Omega_\phi)}} - 2 \right\}. \quad (3.83)$$

With non-zero Φ and λ , E_i is given by:

$$E_i^2 = \frac{1}{9\Omega_\alpha^2\Omega_{\text{rc}}} \left\{ 2 - 6\Omega_\alpha\Omega_{\text{rc}} + 9\Omega_\alpha^2\Omega_{\text{rc}}\Omega_\phi \pm 2\sqrt{1 - 6\Omega_\alpha\Omega_{\text{rc}} - 9\Omega_\alpha^2\Omega_{\text{rc}}\Omega_\phi} \right\}. \quad (3.84)$$

By considering $dz/dE = 0$ in the Friedmann equation we get:

$$z_i = \left\{ \frac{\Omega_{\text{rc}} (4\Omega_\alpha\Omega_\phi + 3\Omega_\alpha^2\Omega_\phi^2 - 4) - 2\Omega_\lambda + 2(1 - 4\Omega_{\text{rc}}\Omega_\alpha) E_i^2 - 3\Omega_{\text{rc}}\Omega_\alpha^2 E_i^4}{2\Omega_{\text{m}}} \right\}^{1/3} - 1. \quad (3.85)$$

We will only consider the case of $\Phi = 0 = \lambda$, for which E_i and z_i reduce to:

$$E_i^2 = \frac{1}{9\Omega_\alpha^2\Omega_{\text{rc}}} \left\{ 2 - 6\Omega_\alpha\Omega_{\text{rc}} \pm 2\sqrt{1 - 6\Omega_\alpha\Omega_{\text{rc}}} \right\}, \quad (3.86)$$

and:

$$z_i = \left\{ \frac{2(1 - 4\Omega_{\text{rc}}\Omega_\alpha) E_i^2 - 3\Omega_{\text{rc}}\Omega_\alpha^2 E_i^4 - 4\Omega_{\text{rc}}}{2\Omega_{\text{m}}} \right\}^{1/3} - 1, \quad (3.87)$$

with:

$$\Omega_{\alpha\pm} = \pm \frac{(1 - \Omega_{\text{m}})}{\sqrt{\Omega_{\text{rc}}}} - 2. \quad (3.88)$$

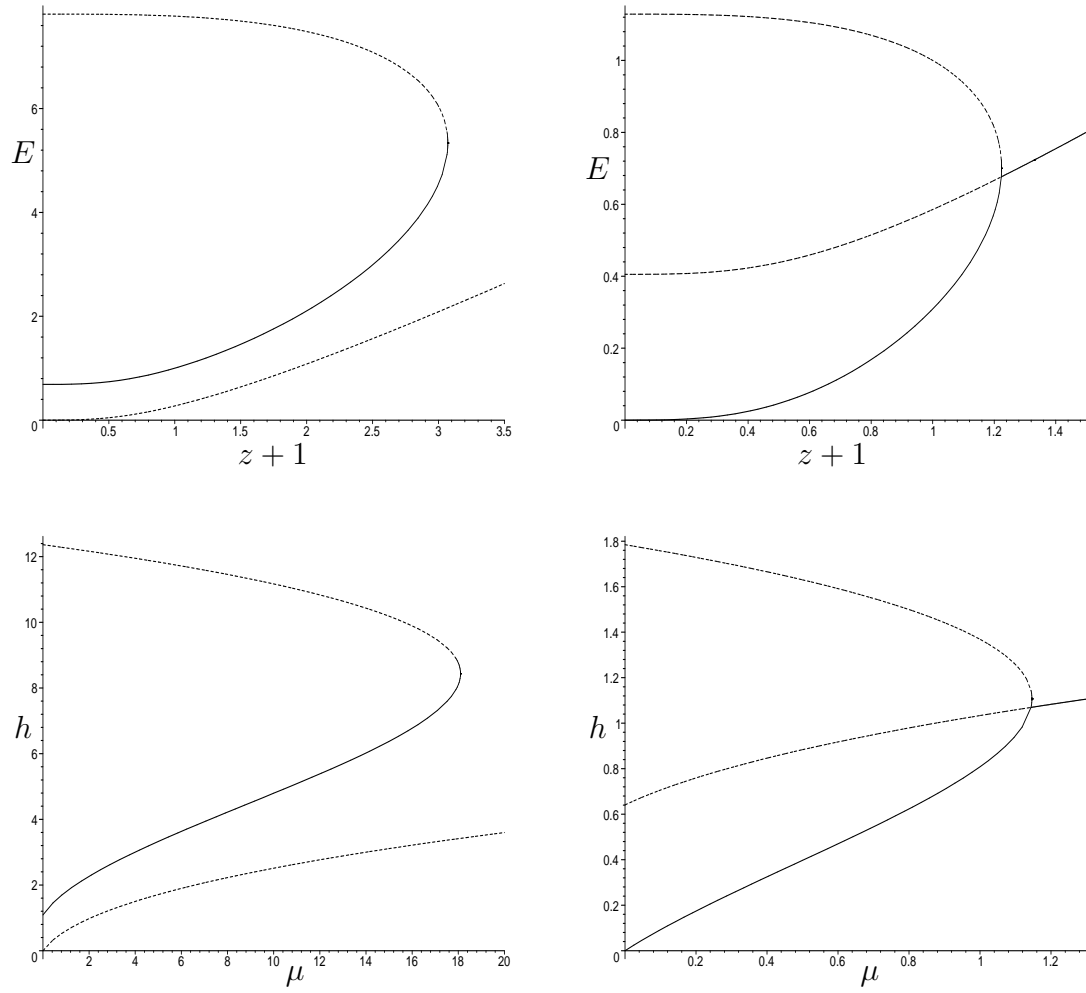


Figure 3.8: The left plots use the plus branch of Eq. (3.83), the right plots use the negative branch. Values used are $\Omega_{\text{rc}} = 0.1$, $\Omega_{\text{m}} = 1/4$, $\Omega_{\phi} = 0$ and $\Omega_{\lambda} = 0$, so that $\Omega_{\alpha+} = 0.372$ and $\Omega_{\alpha-} = -4.372$. The top plots show the Hubble rates against redshift. The bottom two plots are the equivalent plots in h, μ .

The DGP limit, $\Omega_\alpha \rightarrow 0$, gives $E_i = \infty$ due to the presence of Ω_α in the denominator, and thus of $z_i = \infty$.

We see, from Eq. (3.88), that when $\Omega_{\alpha\pm} = 0$:

$$\Omega_m = 1 \pm 2\sqrt{\Omega_{rc}}. \quad (3.89)$$

Therefore for $\Omega_{\alpha\pm}$ to be positive we require:

$$\Omega_m < 1 - 2\sqrt{\Omega_{rc}}, \quad \text{for } \Omega_{\alpha+}, \quad (3.90)$$

$$\Omega_m > 1 + 2\sqrt{\Omega_{rc}}, \quad \text{for } \Omega_{\alpha-}. \quad (3.91)$$

Since $\Omega_{\alpha\pm} > 0$ implies $\alpha > 0$, Eqs. (3.90) and (3.91) describe the GBIG 1 model. When $\Omega_{\alpha\pm} < 0$, we have $\alpha < 0$, and this corresponds to the non-self-accelerating GB modifications of the DGP(−) model, as discussed in section 3.4.2.

For $\Omega_{\alpha\pm}$ to be negative we require:

$$\Omega_m > 1 - 2\sqrt{\Omega_{rc}}, \quad \text{for } \Omega_{\alpha+}, \quad (3.92)$$

$$\Omega_m < 1 + 2\sqrt{\Omega_{rc}}, \quad \text{for } \Omega_{\alpha-}. \quad (3.93)$$

We only consider $0 < \Omega_m < 1$, therefore $\Omega_{\alpha-}$ is always negative and the solutions do not self-accelerate. $\Omega_{\alpha+}$ has two regions in the Ω_m, Ω_{rc} plane. One has solutions that self-accelerate ($\Omega_\alpha > 0$), one that does not ($\Omega_\alpha < 0$). If we included a non-zero Ω_λ or Ω_ϕ , self-acceleration would be possible on both branches. Fig. 3.8 illustrates the two branches for $\Omega_\lambda = 0 = \Omega_\phi$.

The initial redshift of the universe must be at least large enough to accommodate nucleosynthesis, i.e. $z_i > 10^{10}$. This enforces an extremely small value for Ω_α ($\Omega_\alpha \approx 5.5 \times 10^{-5}$), as illustrated in Fig. 3.9.

For each solution of z_i there is a region of the Ω_m, Ω_{rc} plane that is significantly different from the DGP model. This region, with small Ω_m and Ω_{rc} , is shown for the $z_i = 1100$ case in Fig. 3.10. This region, which is disallowed by observations, is present due to the form of the denominator in Eqs. (3.87) and (3.84). E_i becomes infinite when $\Omega_{rc} = 0$ and $z_i \rightarrow \infty$ for $\Omega_m = 0$.

We can work out the age (look-back time) of the universe by evaluating the following integral:

$$t_0 - t_i = H_0^{-1} \int_0^{z_i} \frac{dz}{(1+z)E(z)}. \quad (3.94)$$

Using $H_0 = 73 \text{ km s}^{-1} \text{ Mpc}^{-1}$ ($H_0 = 73 \pm 3 \text{ km s}^{-1} \text{ Mpc}^{-1}$ is the WMAP 3 year data result [68]) we can get the results in years, Figs. 3.11 and 3.12. In Fig. 3.11 we see a

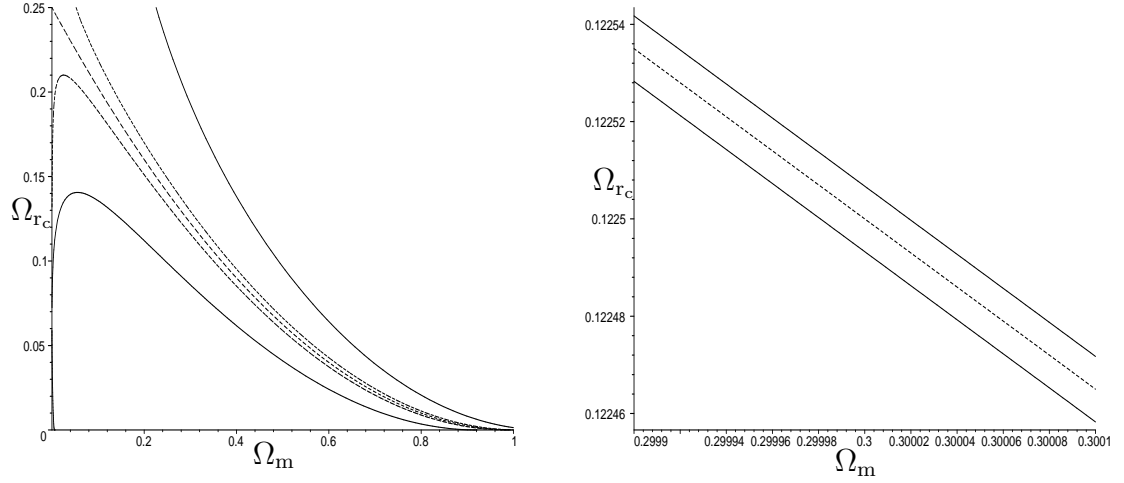


Figure 3.9: The Ω_m , Ω_{rc} plane for GBIG 1. The central dashed line is for $\Omega_\alpha = 0$. On the left the dashed lines are $z_i = 10$ and the solid lines are $z_i = 2$. On the right the solid lines are $z_i = 1100$, the decoupling redshift. The lines above $\Omega_\alpha = 0$ have $\Omega_\alpha < 0$, while those below $\Omega_\alpha = 0$ correspond to $\Omega_\alpha > 0$. The magnitude of Ω_α increases as you move away from the $\Omega_\alpha = 0$ line.

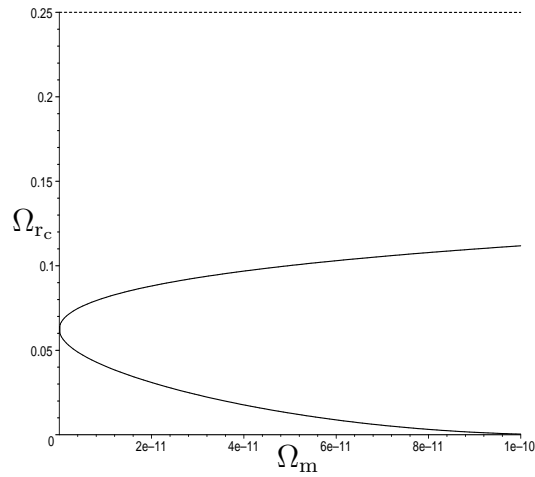
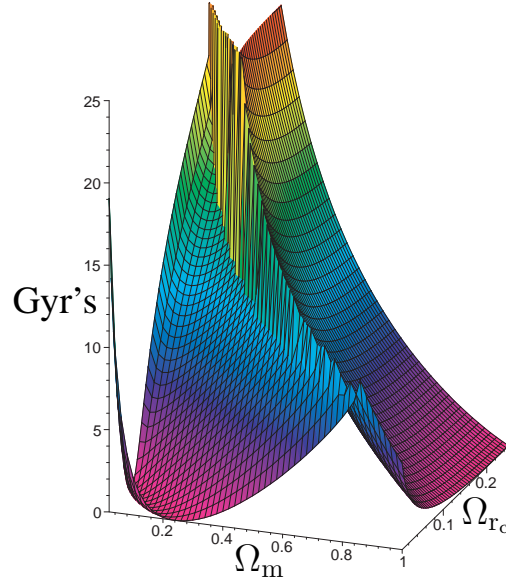


Figure 3.10: The Ω_m , Ω_{rc} plane for $\Omega_{\alpha+}$ and $z_i = 1100$. The dotted line is for $\Omega_\alpha = 0$.


 Figure 3.11: The age of the universe for $\Omega_{\alpha+}$.

sharp transition along the $\Omega_{\alpha} = 0$ ridge. This is because the $\Omega_{\alpha} > 0$ and $\Omega_{\alpha} < 0$ branches are disjoint. In the region where $\Omega_{\alpha} > 0$ (left hand side) z_i is for the self-accelerating branch. On the right hand side of the plot $\Omega_{\alpha} < 0$, so z_i is for the non-self-accelerating branch. From Fig. 3.12 we see that in general, solutions that lie in the $\Omega_{\alpha} < 0$ region will give us larger ages. If we considered solutions with a matter density less than that observed ($\Omega_m \approx 0.3$) it is possible to get a sufficiently large ages with Ω_{rc} measurably different from that of the DGP ($\Omega_{\alpha} = 0$) model. If we want to have self-acceleration and the finite density big bang ($\Omega_{\alpha} > 0$) and have enough time for the evolution of the universe we are restricted to solutions that lie along (or at least extremely close to) the DGP limit. This means that observationally the GBIG model will be indistinguishable from the DGP model even if the early universe is dramatically different.

In Figs. 3.13 and 3.14 we have the age results for the $\Omega_{\alpha-}$ case. As $\Omega_{\alpha-} < 0$ for all values for $\Omega_m < 1$ all the results are for the non-self-accelerating solution.

3.5 Conclusions

We have seen that by including the Gauss-Bonnet bulk term with the Induced gravity brane term in the gravitational action, we get some striking new features. The ultra-violet correction from the Gauss-Bonnet term in combination with the infra-red correction from the induced gravity term gives rise to a solution that starts with a finite density and ends with self-acceleration. We saw that the infra-red induced gravity term on its own can give a self-accelerating solution which is still present in the GBIG model. The GB term

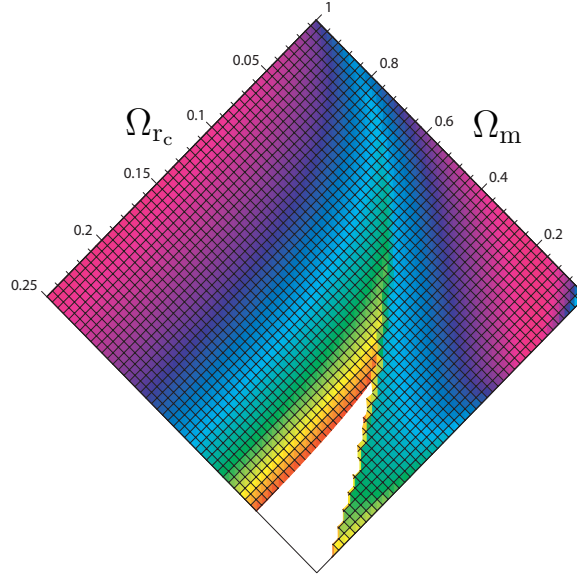
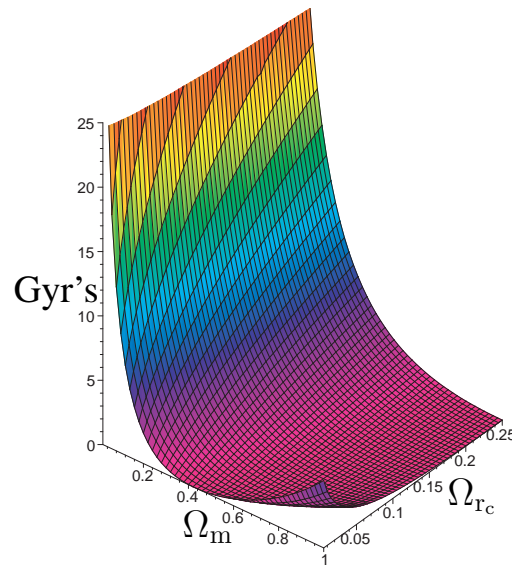


Figure 3.12: As in Fig. 3.11, but viewed from above.

Figure 3.13: The age of the universe for $\Omega_{\alpha-}$.

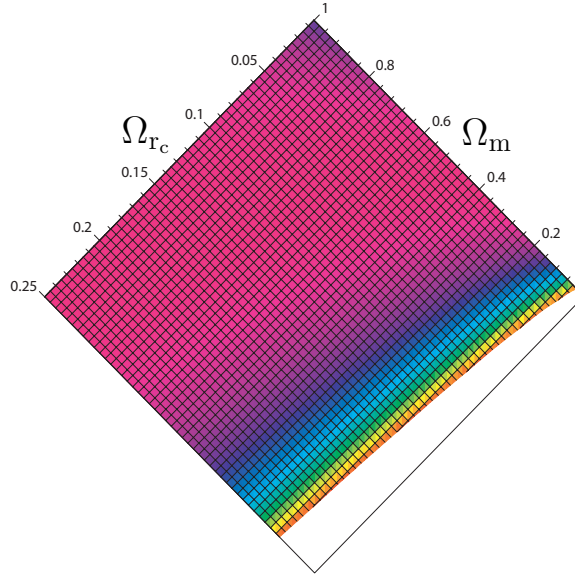


Figure 3.14: As in Fig. 3.13, but viewed from above.

modifies the early era but but does not produce the finite density big bang on its own. It is only the combination that does. There is no threshold for the finite density big bang to occur-the contributions from the GB and IG terms only need to be non-zero.

The density, pressure and temperature are finite but the big bang does have a curvature singularity at the beginning. This deserves further investigation.

We have seen that the UV-IR bootstrap confines γ to be very small i.e. the GBIG model is very close to the DGP(+) model for most of the history of the universe. This was also seen in the analysis of the age of the universe. In order for there to sufficient time for events such as nucleosynthesis to have taken place γ must be almost indistinguishable from the DGP(+) model ($\gamma = 0$).

Chapter 4

Generalised cosmologies with Induced Gravity and Gauss-Bonnet terms

4.1 Introduction

In this chapter we shall extend the work in Chapter 3 to models with non-zero brane tension and bulk curvature. We keep the assumptions that the bulk black hole mass is zero and the brane is spatially flat. We shall see that this leads to many more possible solutions, but not all of them are physically relevant.

4.2 Field Equations

The general form of the Friedmann equation in this case is:

$$\left[1 + \frac{8}{3}\alpha \left(H^2 + \frac{\Phi}{2}\right)\right]^2 (H^2 - \Phi) = \left[rH^2 - \frac{\kappa_5^2}{6}(\rho + \lambda)\right]^2, \quad (4.1)$$

where Φ is a solution to:

$$\Phi + 2\alpha\Phi^2 = \frac{\Lambda_5}{6}. \quad (4.2)$$

Due to the presence of the GB term in the bulk action, the bulk cosmological constant is given by:

$$\Lambda_5 = -\frac{6}{\ell^2} + \frac{12\alpha}{\ell^4}. \quad (4.3)$$

as seen in Chapter 3. Equations (4.2) and (4.3) give us two solutions for Φ :

$$\Phi_1 = -\frac{1}{\ell^2}, \quad \Phi_2 = \frac{1}{\ell^2} - \frac{1}{2\alpha}. \quad (4.4)$$

Φ_1 is the generalised form of the solution considered in the previous chapter.

We work with the Friedmann equation in dimensionless form. We shall use the same variables as defined in the previous chapter (Eq. 3.27) with the addition of:

$$\sigma = \frac{r\kappa_5^2}{6}\lambda, \quad \chi = \frac{r^2}{\ell^2}, \quad \phi = \Phi r^2. \quad (4.5)$$

Using these variables we can write the two solutions for Φ as:

$$\phi_1 = -\chi, \quad \phi_2 = \chi - \frac{4}{3\gamma}. \quad (4.6)$$

The bulk cosmological constant gives us an upper bound on the GB coupling constant α . Equation (4.3) gives us:

$$\frac{1}{\ell^2} = \frac{1}{4\alpha} \left[1 \pm \sqrt{1 + \frac{4}{3}\alpha\Lambda_5} \right]. \quad (4.7)$$

For a RS ($\alpha \rightarrow 0$) limit we take the minus branch. $\Lambda_5 > 0$ would imply $\ell^2 < 0$ and thus we must have $\Lambda_5 \leq 0$ and:

$$\alpha \leq \frac{\ell^2}{4}. \quad (4.8)$$

In dimensionless form this is given by:

$$\gamma \leq \frac{2}{3\chi}. \quad (4.9)$$

Maintaining a RS limit would also rule out the ϕ_2 branch. We would be restricted to the solutions lying along the line in the top left quadrant in Fig. 4.1. We are interested in the whole range of the model so we include the plus branch in Eq. (4.7). We assume $\Lambda_5 \leq 0$ therefore the constraint on α is given by:

$$\alpha \leq \frac{\ell^2}{2}, \quad \Rightarrow \quad \gamma \leq \frac{4}{3\chi}. \quad (4.10)$$

If we take $\chi = 0$ then we have no bound on γ (apart from being positive and real). This is the case considered in Chapter 3.

In Fig. 4.1 we have the two ϕ solutions plotted as functions of χ . The two solutions with $\phi = 0$ both live in a Minkowski bulk, all the rest live in an AdS bulk. Note that one of these AdS solutions ($\chi = 0, \phi = -4/3\gamma$) has $\Lambda_5 = 0$ but $\Phi = -1/2\alpha$ acting as an effective cosmological constant, Chapter 3. We see that for any allowed value of ϕ we can be on either of the two branches. This means that we need not consider the ϕ_1 and ϕ_2 solutions to the Friedmann equation separately. We therefore consider Eq. (4.10) in

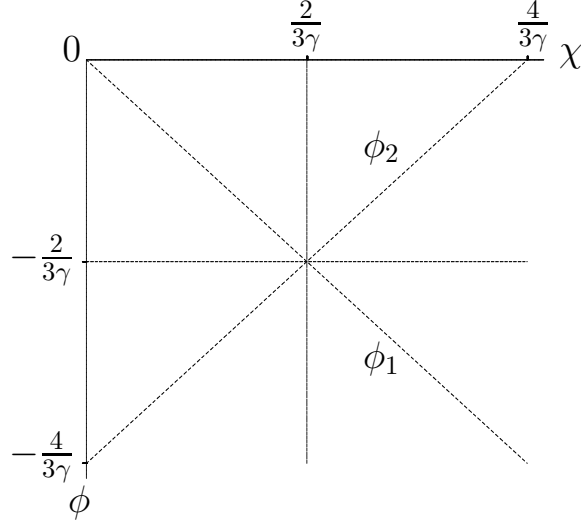


Figure 4.1: The effective bulk cosmological constant ϕ as a function of χ .

terms of ϕ . We define the maximum value of γ , for a particular value of ϕ , that is allowed by the constraint equation:

$$\gamma_M = -\frac{4}{3\phi}. \quad (4.11)$$

The dimensionless Friedmann equation is:

$$\left[1 + \gamma \left(h^2 + \frac{\phi}{2}\right)\right]^2 (h^2 - \phi) = [h^2 - (\mu + \sigma)]^2. \quad (4.12)$$

with the conservation equation now given by:

$$\mu' + 3h(1 + w)\mu = 0, \quad (4.13)$$

where $' = d/d\tau$ and $h = a'/a$. The Raychaudhuri and acceleration equations are given by:

$$h' = \frac{3\mu(1 + w)[h^2 - (\mu + \sigma)]}{(\gamma h^2 + 1)(3\gamma h^2 + 1) - 2[h^2 - (\mu + \sigma)] - \phi\gamma(1 + \frac{3}{4}\phi\gamma)}, \quad (4.14)$$

and:

$$\frac{a''}{a} = \frac{h^2(\gamma h^2 + 1)(3\gamma h^2 + 1) - [h^2 - (\mu + \sigma)][2h^2 - 3\mu(1 + w)] - h^2\phi\gamma(1 + \frac{3}{4}\phi\gamma)}{(\gamma h^2 + 1)(3\gamma h^2 + 1) - 2[h^2 - (\mu + \sigma)] - \phi\gamma(1 + \frac{3}{4}\phi\gamma)}. \quad (4.15)$$

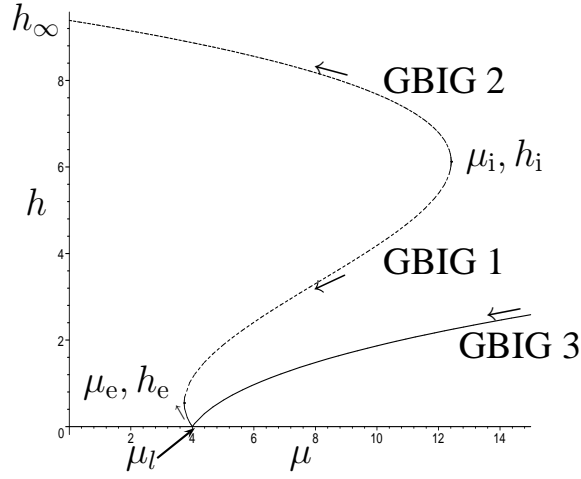


Figure 4.2: Solutions of the Friedmann equation (h vs μ) with negative brane tension ($\sigma = -4$) in a Minkowski bulk ($\phi = 0$) with $\gamma = 1/10$. The curves are independent of the equation of state w . The arrows indicate the direction of proper time on the brane.

4.3 Friedmann Equation Solutions

The model we considered in Chapter 3 is the Minkowski bulk limit ($\chi = 0$) of the ϕ_1 case, which we now see to be equivalent to $\chi = \frac{4}{3\gamma}$ in the ϕ_2 case. The results we present below are in terms of ϕ and thus include both ϕ_1 and ϕ_2 . We will consider the effect of including brane tension in a Minkowski bulk before we look at the AdS bulk cases. The Minkowski bulk case is given by $\phi = 0$, since Eqs. (4.3) and (4.2) imply $\Lambda_5 = 0$.

4.3.1 Minkowski bulk ($\phi = 0$) with brane tension

In Figs. 4.2 and 4.3 we can see the solutions to the Friedmann equation in a Minkowski bulk for both positive and negative brane tensions. By introducing brane tension into the model we are effectively adding a brane cosmological constant. These solutions are therefore less desirable than the zero brane tension, self-accelerating ones. For both negative and positive brane tensions there are three solutions (this is not always true as we will show later) denoted GBIG 1-3. There are four points of interest in Figs. 4.2 and 4.3, these are:

- (μ_i, h_i) and (μ_e, h_e) : The initial density for GBIG 1 and GBIG 2 (μ_i) and the final density for GBIG 1 and 3 (μ_e), found by considering $d\mu/d(h^2) = 0$, are given by:

$$\mu_{i,e} = \frac{2 - 9\gamma \pm 2(1 - 3\gamma)^{3/2}}{27\gamma^2} - \sigma, \quad (4.16)$$

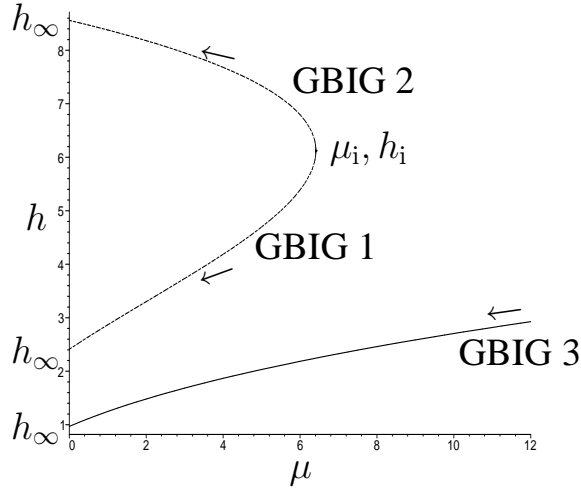


Figure 4.3: Solutions of the Friedmann equation with positive brane tension ($\sigma = 2$) in a Minkowski bulk ($\phi = 0$) with $\gamma = 1/10$.

where the plus sign is for μ_i and the negative sign is for μ_e . The Hubble rates for these two densities are given by:

$$h_{i,e} = \frac{1 \pm \sqrt{1 - 3\gamma}}{3\gamma}, \quad (4.17)$$

where the sign convention is the same as above. The points $(\mu_{i,e}, h_{i,e})$ have $h' = |\infty|$. Therefore cosmologies that evolve to μ_e , h_e end in a “quiescent” (finite density) future singularity. This singularity is of type 2 in the notation of Ref. [65].

- $(\mu_l, 0)$: This is the density at which GBIG 3 “loiters”. The point was found by considering $h = 0$ and is given by :

$$\mu_l = -\sigma. \quad (4.18)$$

In the case considered in Chapter 3 we had $\sigma = 0$ so $\mu_l = 0$. We can show that for $\sigma < 0$ GBIG 3 will not collapse but will loiter at a density of $\mu = -\sigma$ before evolving towards (μ_e, h_e) , by considering h'_l . At $\mu = -\sigma$, $h = 0$ we get $h'_l = 0$ from Eq. (4.14). In a standard expanding or collapsing cosmology $h' < 0$ at all times. The evolution for radiation and dust dominated universes can be seen in Fig. 4.4. A dust dominated universe loiters for longer than the radiation dominated universe. The length of time a universe will loiter for is also dependent on γ in a non-trivial way. This dependence is a matter for further investigation. In Ref. [69] they consider a loitering braneworld model. An important difference between the two models is that in Ref. [69] they require negative dark radiation, i.e. a naked

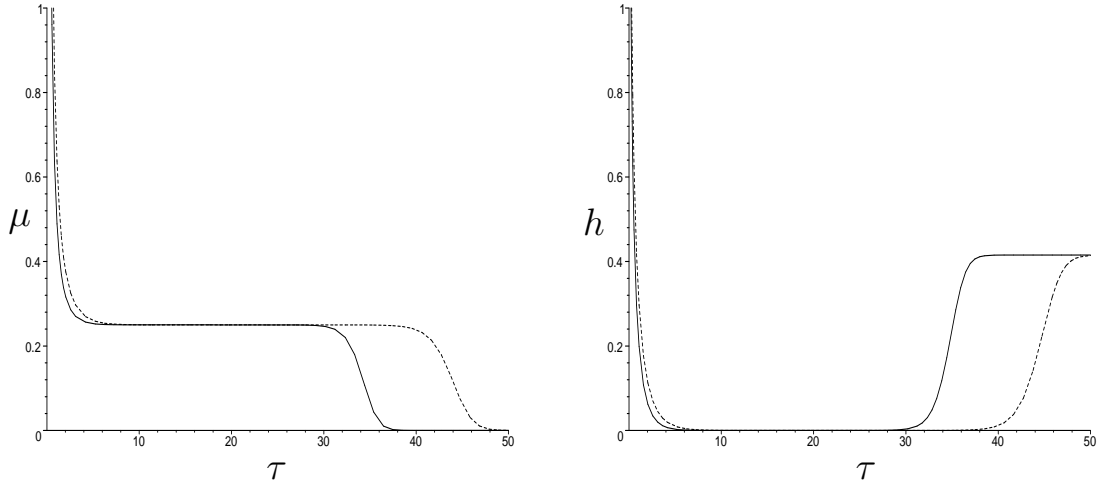


Figure 4.4: Plots of μ vs τ and h vs τ for GBIG 3 in a Minkowski bulk ($\phi = 0$) with negative brane tension ($\sigma = -1/4$). We see that GBIG 3 loiters around $\mu = \mu_l = -\sigma$, $h = 0$ before evolving towards a vacuum de Sitter solution ($\mu_e < 0$). (Here $\gamma = 1/10$. The solid line is $w = 1/3$. The dotted line is $w = 0$.)

singularity in the bulk or a de Sitter bulk. Also in the model the Hubble rate at the loitering phase is exactly zero. The time spent at this point is only dependent on w and the density of the loitering phase is only dependent on the brane tension.

- $(0, h_\infty)$: This is the asymptotic value of the Hubble rate as $\mu \rightarrow 0$. For the value of the parameters used in Fig. 4.2, GBIG 2 is the only case with this limit. In general any of the models can end in a similar state (Fig. 4.3). The different values of h_∞ are given by the solutions to the cubic:

$$h_\infty^6 + \frac{(2\gamma - 1)}{\gamma^2} h_\infty^4 + \frac{2\sigma}{\gamma^2} h_\infty^2 - \frac{\sigma^2}{\gamma^2} = 0. \quad (4.19)$$

In the case we considered in Chapter 3 ($\sigma = 0$) the last term in the above cubic is zero. Therefore we have $h_\infty = 0$ for GBIG 3 while the solutions for GBIG 1 and GBIG 2 are given by:

$$h_\infty = \frac{1 \pm \sqrt{1 - 4\gamma}}{2\gamma}, \quad (4.20)$$

where the minus sign corresponds to GBIG 1 and the plus sign to GBIG 2. This is the only case where we can write simple analytic solutions as in all other cases we have to solve the cubic.

The two Hubble rates, h_i and h_e , are independent of the brane tension which simply shifts the $\mu = 0$ axis. Therefore μ_e only corresponds to a physical (positive) energy

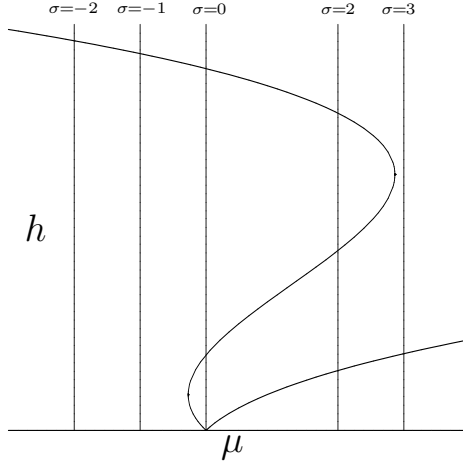


Figure 4.5: Solutions of the Friedmann equation (h vs μ) in a Minkowski bulk ($\phi = 0$) with $\gamma = 1/7$. The vertical lines represent the $\mu = 0$ axis for the labeled brane tensions.

density when $\sigma < \sigma_e < 0$, see Eq. (4.21). The effect of the brane tension on the $\mu = 0$ axis is illustrated in Fig. 4.5.

We showed in Chapter 3 that for $\phi = 0 = \sigma$ we require $\gamma \leq 1/4$ for GBIG 1 and GBIG 2 solutions to exist within the positive energy density region (if $\gamma = 1/4$ GBIG 1 and GBIG 2 reduce to the same vacuum de Sitter universe). If we have some non-zero brane tension this constraint is modified. The maximum value of γ , for GBIG 1 and GBIG 2 to exist with positive energy density, as a function of σ can be seen in Fig. 4.6. We have defined new quantities, $\sigma_{e,i}$ and σ_l , for which $\mu_{e,i,l} = 0$. We can see from Eq. (4.18) that $\sigma_l = 0$. $\sigma_{e,i}$ are given in terms of γ by:

$$\sigma_{i,e} = \frac{2 - 9\gamma \pm 2(1 - 3\gamma)^{3/2}}{27\gamma^2}. \quad (4.21)$$

The maximum value of γ (γ_m) for GBIG 1 and GBIG 2 to exist (i.e. for Eqs. (4.16) and (4.17) to have real solutions) is $\gamma_m = 1/3$. Actually for $\gamma = 1/3$, GBIG 2 exists but GBIG 1 is lost. This is since $h_i = h_e$ at $\gamma = 1/3$. The point $h_i = h_e$ is now a point of inflection and Eq. (4.17) is still valid and therefore $|h'| = \infty$. For values of $\gamma > 1/3$, $h_{i,e}$ and $\mu_{i,e}$ become complex, it is no longer a point of inflection. Therefore $|h'| \neq \infty$ and GBIG 3 can continue its evolution through this point to h_∞ . In Fig. 4.7 we show results for h and h' for three values of γ , $\gamma = 1/3 - 0.01$, $1/3$, $1/3 + 0.01$. In the top plot we see that the solution denoted (1) has GBIG 1-3 present as $\gamma < 1/3$, we have two real and different values for h_i and h_e . This solution in the bottom plot has three parts (GBIG 1 has negative values not shown in Fig. 4.7), GBIG 2 is the dotted solution and the solid is GBIG 3. As (1) approaches $h_{i,e}$ $|h'| \rightarrow \infty$. Solution (2) has $\gamma = 1/3$, in

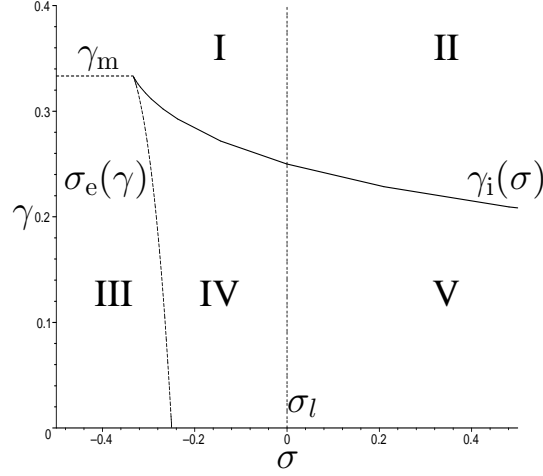


Figure 4.6: The (σ, γ) plane for solutions in a Minkowski ($\phi = 0$) bulk. The short dotted horizontal line is $\gamma_m = 1/3$. GBIG 1-2 exist with positive energy density in regions III, IV and V.

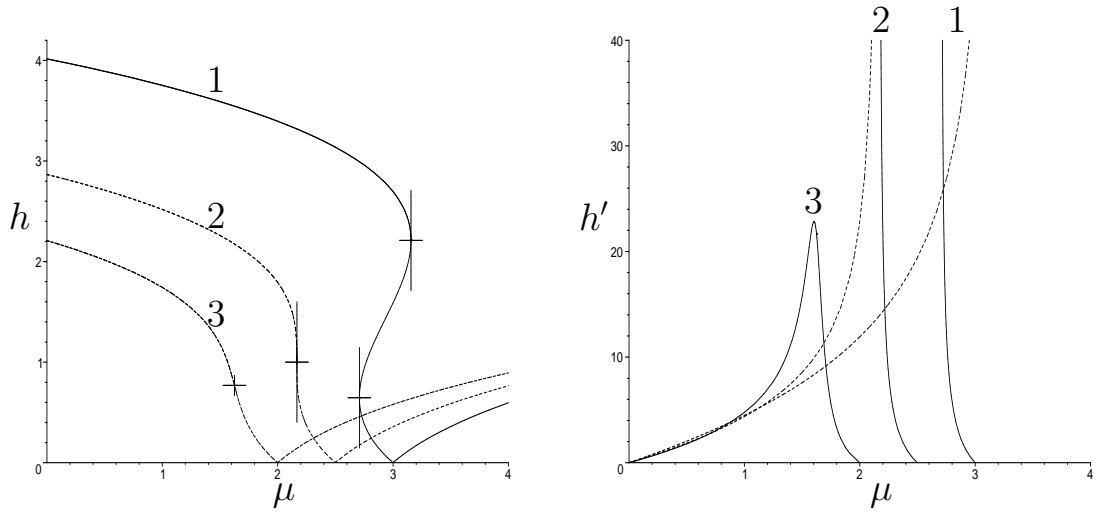


Figure 4.7: The plot on the left is h vs μ for three different solutions, all with $\phi = 0$. The plot on the right shows h' vs μ for the same solutions. (1): $\gamma = 1/3 - 0.1$, $\sigma = -3$. (2): $\gamma = 1/3$, $\sigma = -2.5$. (3): $\gamma = 1/3 + 0.1$, $\sigma = -2$. Different brane tensions are used purely for clarity.

the top plot we see that GBIG 1 now no longer exists as $h_i = h_e$. In the bottom plot GBIG 3 (solid) and GBIG 2 (dotted) solutions both go to $h' = \infty$ at the point $h_i = h_e$. Solution (3) has $\gamma > 1/3$. Now $h_{i,e}$ does not represent $d\mu/dh = 0$, therefore h' stays well behaved throughout the evolution (bottom plot). GBIG 3 moves seamlessly onto GBIG 2 making a single solution. As GBIG 2 super-accelerates this new solution will show late time phantom-like behaviour ($h' > 0 \rightarrow w < -1$).

Solutions that lie along the σ_l line in Fig. 4.6 are those considered in Chapter 3. Regions I and II in Fig. 4.6 extend up to $\gamma_M = \infty$. Solutions in each region of Fig. 4.6 have the following properties:

- *I* : $\sigma_e(\gamma_m) < \sigma < 0$, $\gamma > \gamma_i$ and $\sigma < \sigma_e(\gamma_m)$, $\gamma > \gamma_m$. GBIG 1 and GBIG 2 do not exist. GBIG 3 loiters at μ_l before evolving to a vacuum de Sitter universe.
- *II* : $\sigma > 0$, $\gamma > \gamma_i$. GBIG 1 and GBIG 2 do not exist. GBIG 3 evolves to a vacuum de Sitter universe.
- *III* : $\sigma \leq \sigma_e$, $\gamma \leq \gamma_m$. GBIG 1 will evolve to (μ_e, h_e) . GBIG 2 evolves to $(0, h_\infty)$. GBIG 3 loiters at μ_l before evolving towards (μ_e, h_e) . When $\sigma = \sigma_e$ GBIG 1 and 3 evolve to $(0, h_e)$. When $\gamma = \gamma_m$, GBIG 1 ceases to exist ($h_i = h_e$).
- *IV* : $\sigma_e < \sigma < 0$, $\gamma \leq \gamma_i$. GBIG 1 and GBIG 2 both evolve to vacuum de Sitter states. GBIG 3 loiters before evolving to a vacuum de Sitter universe. Each vacuum de Sitter state has a different value of h_∞ . When $\gamma = \gamma_i$ GBIG 1 and GBIG 2 live at $(0, h_i)$.
- *V* : $\sigma \geq 0$, $\gamma \leq \gamma_i$. GBIG 1-3 all end in vacuum de Sitter states. With $\gamma = \gamma_i$ GBIG 1-2 live at $(0, h_i)$. When $\sigma = 0$ GBIG 3 ends in a Minkowski state.

In Fig. 4.8 we can see how solutions in each of the regions mentioned above affect h_∞ . The thin-dark line ($\sigma = -0.4$) lies in III and I in Fig. 4.6. Only GBIG 2 exists for $0 \leq \gamma < 1/3$. For $\gamma > 1/3$ we've seen that GBIG 3 and GBIG 2 connect to make a single solution, which is why the line is continuous through $\gamma = 1/3$. The thin-light line ($\sigma = -0.28$) has an interesting feature due to the solutions lying on a line that cuts through both region III and IV as well as I. Both the thick lines have GBIG 1-3 ending at h_∞ . The thick-dark solution loiters before evolving to h_∞ , but this has no effect upon the results in Fig. 4.8.

4.3.2 AdS bulk ($\phi \neq 0$) with brane tension

When $\phi = 0$, we have $\Lambda_5 \neq 0$, with one exception: the ϕ_2 solution with $\chi = 0$, i.e. $\phi_2 = -4/3\gamma$, has $\Lambda_5 = 0$, but the bulk is AdS. For $\chi > 0$, $\Lambda_5 \neq 0$. Thus in all cases, $\phi \neq 0$ implies an AdS bulk.

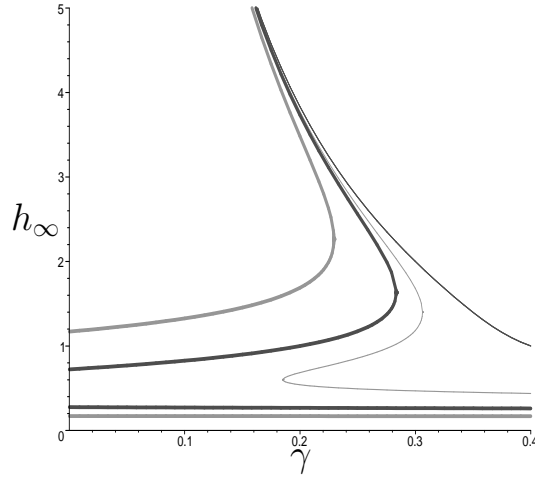


Figure 4.8: h_∞ for solutions in a Minkowski ($\phi = 0$) bulk. The thin-dark line has $\sigma = -0.4$, thin-light line has $\sigma = -0.28$, thick-dark lines have $\sigma = -0.2$ and the thick-light lines have $\sigma = 0.2$.

When we allow the bulk to be warped ($\phi \neq 0$) we open up another possible solution, denoted GBIG 4. There is a maximum value of ϕ for which GBIG 4 can exist as we shall see later. The nature of GBIG 3 is also changed. These solutions, for a negative brane tension, can be seen in Fig. 4.9. Brane tension affects the solutions in the same manner as in $\phi = 0$ case. The qualitative effect of the warped bulk is to make GBIG 3 collapse and to introduce the new bouncing branch GBIG 4. This is due to $h = 0$ now giving two solutions:

$$\mu_{c,b} = \pm \sqrt{-\phi} \left(1 + \frac{\gamma\phi}{2} \right) - \sigma, \quad (4.22)$$

where the plus sign is for the GBIG 3 collapse (μ_c) and the minus for the GBIG 4 bounce (μ_b). Effectively the loitering point in the Minkowski bulk is split into the max/min densities of the bouncing/collapsing cosmologies of GBIG 3-4. The other points in Fig. 4.9 are modified by the warped bulk; they are now given by:

$$\mu_{i,e} = \frac{4 - 18\gamma + 27\gamma^2\phi \pm \sqrt{2}(2 - 6\gamma - 9\gamma^2\phi)^{3/2}}{54\gamma^2} - \sigma, \quad (4.23)$$

with the plus sign for μ_i and the negative sign for μ_e . The Hubble rates $h_{i,e}$ are given by:

$$h_{i,e} = \frac{\sqrt{2}}{6\gamma} \sqrt{4 - 6\gamma + 9\gamma^2\phi \pm 2\sqrt{4 - 12\gamma - 18\gamma^2\phi}}, \quad (4.24)$$

with the same sign convention. h_∞ is given by a similarly modified equation:

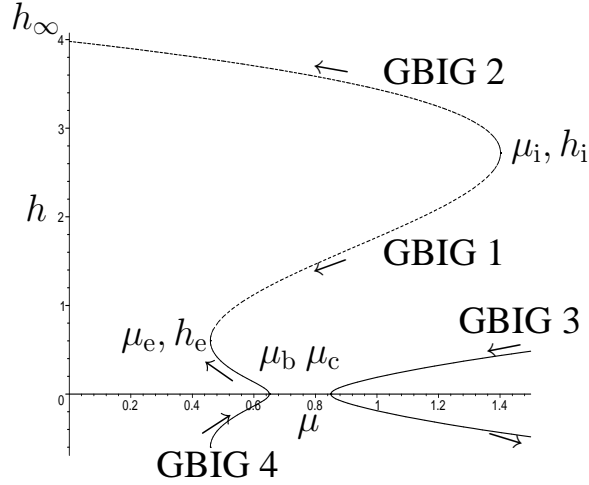


Figure 4.9: Solutions of the Friedmann equation (h vs μ) with negative brane tension ($\sigma = -3/4$) in an AdS bulk ($\phi = -0.01$) with $\gamma = 1/5$. The curves are independent of the equation of state w . The arrows indicate the direction of proper time on the brane.

$$h_\infty^6 + \frac{(2\gamma - 1)}{\gamma^2} h_\infty^4 + \frac{[1 + 2\sigma - \phi\gamma(1 + \frac{3}{4}\phi\gamma)]}{\gamma^2} h_\infty^2 - \frac{[\phi(1 + \frac{\phi\gamma}{2})^2 + \sigma^2]}{\gamma^2} = 0. \quad (4.25)$$

With a warped bulk the constraint from h_i ($\gamma \leq 1/3$ in the Minkowski case) is modified. In the equation for h_i we effectively have two bounds from the two square root terms. In the $\phi = 0$ case only the inner term is of any consequence (giving rise to the bound $\gamma \leq 1/3$). When $\phi \neq 0$ there are two bounds which are applicable in different regimes. If we consider the bound from the inner square root we get:

$$\gamma \leq \frac{\sqrt{1 + 2\phi} - 1}{3\phi}. \quad (4.26)$$

This is valid for $\phi \geq -1/2$. Considering the outer square root term we get the bound:

$$\gamma \leq \frac{2(1 - 2\sqrt{-\phi})}{3\phi}. \quad (4.27)$$

This bound becomes negative when $\phi > -1/4$ which is disallowed as this prevents self-acceleration. The bound on γ is given by the lower of the two constraints when

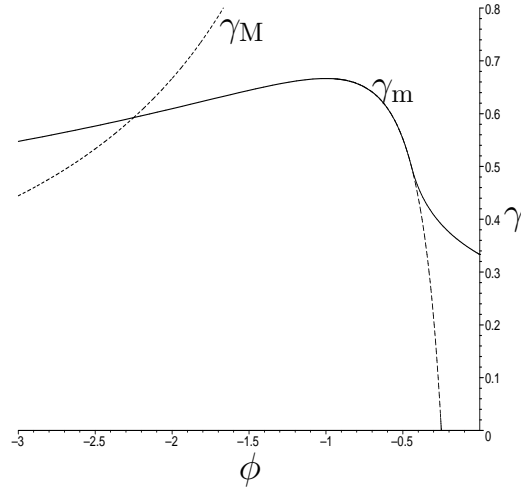


Figure 4.10: In order for h_i to be real γ must lie beneath the solid line (γ_m). The region to the right of the vertical dotted line is where GBIG 4 ($h_e > 0$) is allowed (except where $\phi = 0$).

$-1/2 < \phi < -1/4$ i.e. when in the range where both exists. Therefore the bound on γ for h_i to be real is given by (see Fig. 4.10):

$$\gamma \leq \begin{cases} \frac{\sqrt{1+2\phi}-1}{3\phi} & -\frac{4}{9} \leq \phi \leq 0 \\ \frac{2(1-2\sqrt{-\phi})}{3\phi} & \phi \leq -\frac{4}{9} \end{cases} \quad (4.28)$$

For a particular value of ϕ the maximum value of γ allowed by this constraint is denoted γ_m . When $\phi < -9/4$ the constraint in Eq. (4.10) is tighter than that in Eq. (4.27) ($\gamma_M < \gamma_m$). This means that for $\phi \leq -9/4$, h_i is always real for allowed values of γ .

There is a bound for GBIG 4 to exist, found by considering $h_e = 0$. This bound is given by:

$$\phi > -\frac{2}{9\gamma^2} \left\{ 4 - 3\gamma - 2\sqrt{4 - 6\gamma} \right\}. \quad (4.29)$$

This is a solution to the quadratic obtained from $h_e = 0$, the other root of the quadratic does not obey the constraint $\phi \leq -4/3\gamma$ so it is ignored. The minimum value for GBIG 4 to exist will be denoted $\phi_{GBIG4Lim}$. Using the constraints we can split the γ, ϕ plane into three sections, see Fig. 4.10. The solid line is constructed from the bounds in Eq. (4.28). For h_i to be real we must choose values below this line. The area to the right of the vertical dotted line (but excluding $\phi = 0$) allows GBIG 4. Points to the left of this line have GBIG 1 collapsing after a minimum energy density (μ_b) is reached. The dotted curve on the left comes from initial constraint $\gamma \leq -4/3\phi$.

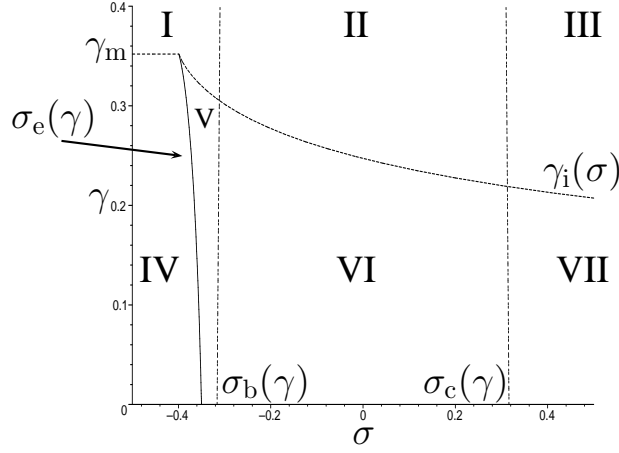


Figure 4.11: The (σ, γ) plane for solutions in a AdS ($\phi = -0.1$) bulk. The short dotted horizontal line is the maximum value of γ as obtained from Eq. (4.10).

In order to consider the σ, γ plane as we did in the $\phi = 0$ Minkowski case, we need the modified $\sigma_{i,e}$ equations:

$$\sigma_{i,e} = \frac{4 - 18\gamma + 27\gamma^2\phi \pm \sqrt{2}(2 - 6\gamma - 9\gamma^2\phi)^{3/2}}{54\gamma^2}. \quad (4.30)$$

We now have two more formulas for the collapse density of GBIG 3 and the bounce density of GBIG 4:

$$\sigma_{c,b} = \pm \sqrt{-\phi} \left(1 + \frac{\gamma\phi}{2} \right), \quad (4.31)$$

with the plus sign corresponding to the collapse and the minus to the bounce.

We shall consider the σ, γ plane for three different values of ϕ corresponding to three distinct regions in Fig. 4.10. We shall first consider $\phi = -0.1$.

Typical example $\phi = -0.1$

If we take $\phi = -0.1$, we are in the region where GBIG 4 is allowed. The σ, γ plane can be seen in Fig. 4.11. The regions I, II and III in Fig. 4.11 extend up to $\gamma_M = 40/3$.

In each region we have the following cosmologies.

- *I* : $\sigma_e(\gamma_m) < \sigma < 0$, $\gamma > \gamma_i$ and $\sigma \leq \sigma_e(\gamma_m)$, $\gamma > \gamma_m$. GBIG 1-2 do not exist. GBIG 3 reaches a minimum energy density (μ_c) and then evolves back to $\mu = \infty$. GBIG 4 starts at $(0, -h_\infty)$ then bounces at $(\mu_b, 0)$ before evolving to $(0, +h_\infty)$. When $\sigma = \sigma_b$, GBIG 4 exists as a Minkowski universe.

- *II* : $\sigma_b \leq \sigma < \sigma_c$, $\gamma > \gamma_i$. Only GBIG 3 exists. GBIG 3 reaches a minimum energy density (μ_c) and then evolves back to $\mu = \infty$. When $\sigma = \sigma_c$ GBIG 3 ends in a Minkowski universe.
- *III* : $\sigma > \sigma_c$, $\gamma > \gamma_i$. Only GBIG 3 exists and evolves to a vacuum de Sitter universe.
- *IV* : $\sigma \leq \sigma_e < 0$, $\gamma \leq \gamma_m$. GBIG 1 evolves to (μ_e, h_e) . GBIG 2 evolves to h_∞ . GBIG 3 reaches a minimum energy density (μ_c) and then evolves back to $\mu = \infty$. GBIG 4 starts at $(\mu_e, -h_e)$, bounces at $(\mu_b, 0)$ before evolving to $(\mu_e, +h_e)$. When $\sigma = \sigma_e$ GBIG 1 and 3 evolve to $(0, h_e)$. GBIG 4 starts at $(0, -h_e)$ and bounces before evolving to $(0, h_e)$. When $\gamma = \gamma_m$ GBIG 1 ceases to exist ($h_i = h_e$).
- *V* : $\sigma_e < \sigma \leq \sigma_b$, $\gamma \leq \gamma_i$. GBIG 1 and GBIG 2 both end in vacuum de Sitter universes with different values of h_∞ . GBIG 3 reaches a minimum energy density (μ_c) and then evolves back to $\mu = \infty$. GBIG 4 starts at $(0, -h_\infty)$ then bounces at $(\mu_b, 0)$ before evolving back to $(0, +h_\infty)$. When $\sigma = \sigma_b$ GBIG 4 exists as a Minkowski universe $(0, 0)$.
- *VI* : $\sigma_b < \sigma \leq \sigma_c$, $\gamma \leq \gamma_i$. GBIG 1 and GBIG 2 both end in vacuum de Sitter universes with different values of h_∞ . GBIG 3 reaches a minimum energy density (μ_c) and then evolves back to $\mu = \infty$. GBIG 4 does not exist. When $\sigma = \sigma_c$ GBIG 3 ends in a Minkowski universe. When $\gamma = \gamma_i$ GBIG 1 and GBIG 2 live at $(0, h_i)$.
- *VII* : $\sigma > \sigma_c$, $\gamma \leq \gamma_i$. GBIG 1-3 all end in vacuum de Sitter universes with different values of h_∞ . GBIG 4 does not exist. When $\gamma = \gamma_i$ GBIG 1 and GBIG 2 live at $(0, h_i)$.

In region I there is a GBIG 4 solution, which is modified in the same way as the GBIG 3 solution in the Minkowski bulk. As $h_{i,e}$ are no longer valid in region I GBIG 4 joins onto GBIG 2, see Fig. 4.12. The plot on the right in this figure shows h'' , in order to clearly distinguish this solution from the one in the $\phi = -1$ case where GBIG 4 is no longer allowed.

In Fig. 4.13 are the results for h_∞ with $\phi = -0.1$. The thin-dark line ($\sigma = -1/2$) lies in regions I and IV. Therefore we have only one solution for h_∞ , which corresponds to GBIG 2 for $\gamma \leq \gamma_m$. For $\gamma_m < \gamma < \gamma_M$ this root now corresponds to the end point for GBIG 3 as in the $\phi = 0$ case. The thin-light lines ($\sigma = -0.35$) lie in regions I and V. There are the two GBIG 1 and GBIG 2 solutions and the GBIG 4 solution which converges with the light-thick line at the bottom. The thick-dark line ($\sigma = 0$) lies in regions II and VI, so only has GBIG 1 and GBIG 2 present. The thick-light lines

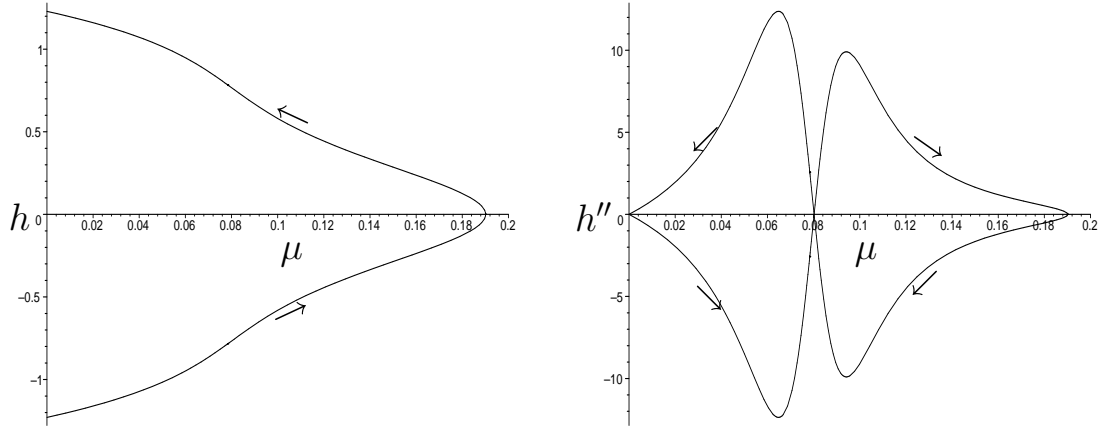


Figure 4.12: The GBIG 4 solution in region I for $\phi = -0.1, \gamma = 0.4 > \gamma_m$ and $\sigma = -1/2$. The plot on the right is h'' vs μ for this solution. This shows the differences between this solution and the similar case when $\phi = -1$, where GBIG 4 is no longer allowed. Arrows denote proper time.

($\sigma = 1/2$) lie in regions III and VII, so has GBIG 1 and GBIG 2 and the GBIG 3 solution (the horizontal line).

Typical example: $\phi = -1$

We now consider $\phi = -1$ which is in the region where GBIG 4 no longer exists (see Fig. 4.14), as $h_e = 0$. Therefore μ_e is not relevant and GBIG 1 bounces at μ_b . This means that the (σ, ϕ) plane, Fig. 4.15, is simpler. The regions in Fig. 4.15 are:

- *I* : $\sigma \leq \sigma_b, \gamma_m < \gamma \leq \gamma_M$. GBIG 1 does not exist. GBIG 2 starts at $(0, -h_\infty)$, collapses to $(\mu_b, 0)$ and then expands back to $(0, h_\infty)$. GBIG 3 expands to $(\mu_c, 0)$ and then collapses. When $\sigma = \sigma_b$ GBIG 2 exists as a Minkowski universe.
- *II* : $\sigma_b < \sigma \leq \sigma_c, \gamma_i < \gamma \leq \gamma_M$. GBIG 1 and GBIG 2 do not exist. GBIG 3 expands to μ_c and then collapses. When $\sigma = \sigma_c$ GBIG 3 evolves to a Minkowski universe.
- *III* : $\sigma > \sigma_c, \gamma_i < \gamma \leq \gamma_M$. GBIG 1 and GBIG 2 do not exist. GBIG 3 evolves to h_∞ .
- *IV* : $\sigma \leq \sigma_b, \gamma \leq \gamma_m$. GBIG 1 evolves from μ_i to μ_b and then expands back to μ_i . GBIG 2 evolves to h_∞ . GBIG 3 expands to μ_c and then collapses. When $\gamma = \gamma_m$ GBIG 1 ceases to exist, GBIG 2 expands from $(\mu_b, 0)$. When $\sigma = \sigma_b$ GBIG 1 evolves to a Minkowski universe.

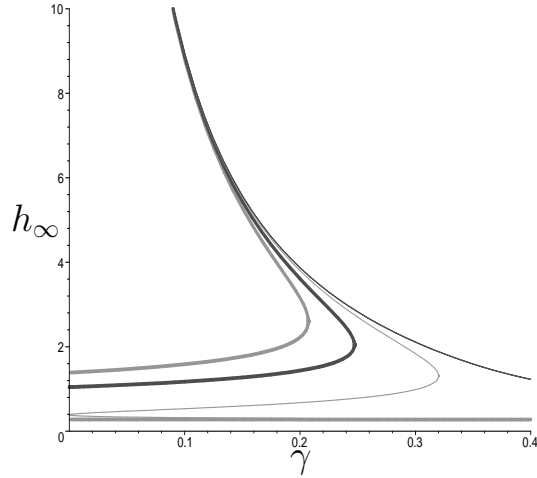


Figure 4.13: h_∞ for solutions in a AdS ($\phi = -0.1$) bulk. The thin-dark line has $\sigma = -1/2$, thin-light lines have $\sigma = -0.35$, thick-dark line has $\sigma = 0$ and the thick-light lines have $\sigma = 1/2$.

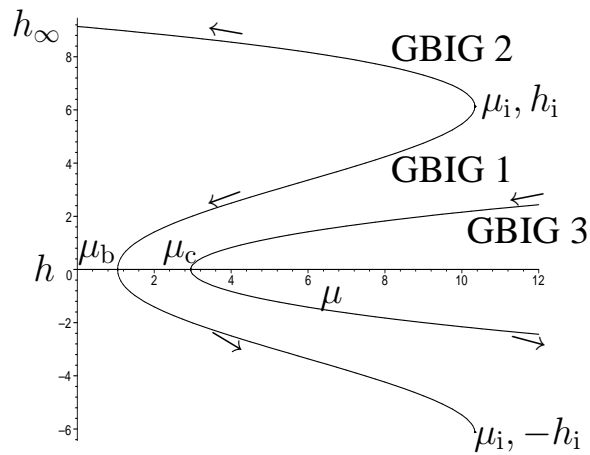


Figure 4.14: Solutions of the Friedmann equation (h vs μ) with negative brane tension ($\sigma = -2$) in an AdS bulk ($\phi = -1$) with $\gamma = 1/10$. For this value of ϕ GBIG 4 no longer exists and GBIG 1 can collapse. The curves are independent of the equation of state w . The arrows indicate the direction of proper time on the brane.

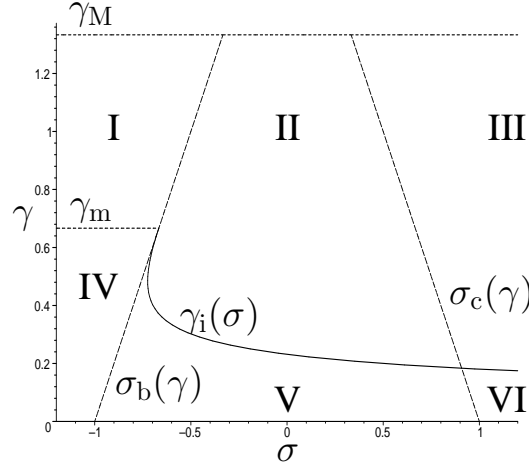


Figure 4.15: The (σ, γ) plane for solutions in a AdS ($\phi = -1$) bulk. The short dotted horizontal line is the maximum value of γ as obtained from Eq. (4.26). The top horizontal line is from the initial bound in Eq. (4.10).

- V : $\sigma_b < \sigma \leq \sigma_c$, $\gamma \leq \gamma_i$. GBIG 1 and GBIG 2 evolve to h_∞ . GBIG 3 expands to μ_c and then collapses. When $\gamma = \gamma_i$, GBIG 1 and GBIG 2 exist as the same de Sitter universe with $(0, h_\infty)$. When $\sigma = \sigma_c$, GBIG 3 ends as a Minkowski universe.
- VI : $\sigma > \sigma_c$, $\gamma \leq \gamma_i$. GBIG 1-3 evolve to h_∞ . When $\gamma = \gamma_i$, GBIG 1-2 live at $(0, h_\infty)$.

In region I we again have a combined solution as GBIG 1 has vanished. As GBIG 4 is not allowed ($h_e = 0$) when we take $\gamma > \gamma_m$, which causes $h_i = 0$, GBIG 2 matches up with its negative counterpart. We see the bouncing GBIG 2 solution in Fig. 4.16. Note the nature of h'' is very different to that of the GBIG 2, 4 bounce in the $\phi = -0.1$ case. In Fig. 4.17 we present results for h_∞ for $\phi = -1$.

Typical example: $\phi = -5$

Here we shall present results for $\phi = -5$ for completeness. This value of ϕ lives in the region of Fig. 4.10 where h_i is always real. This means that the σ, γ plane is much simpler, Fig. 4.18.

The regions in Fig. 4.18 are:

- I : $\sigma \leq \sigma_b$, $\gamma \leq \gamma_m$. GBIG 1 evolves from μ_i to μ_b and back. GBIG 2 evolves to h_∞ . GBIG 3 expands to μ_c and then collapses. When $\sigma = \sigma_b$, GBIG 1 ends in a Minkowski universe.

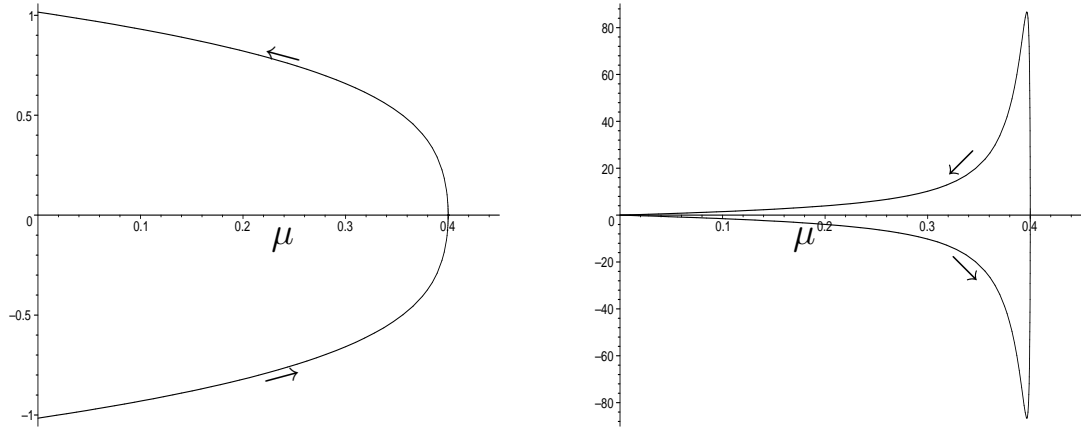


Figure 4.16: The GBIG 4 solution in region I for $\phi = -1, \gamma = 0.8 > \gamma_m$ and $\sigma = -1$. The plot on the right is h'' vs μ for this solution. This shows the differences between this solution and the case when $\phi = -0.1$. Arrows denote proper time.

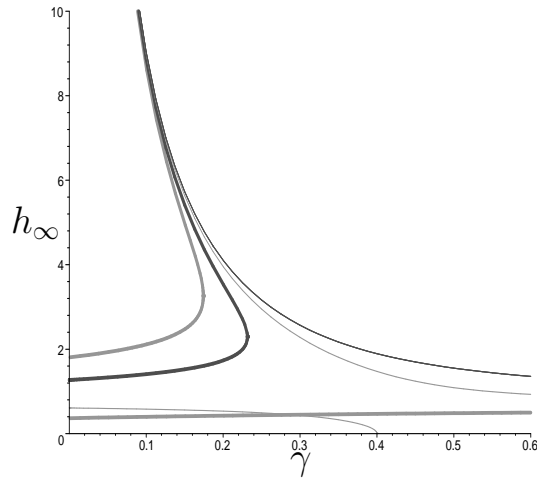


Figure 4.17: h_∞ for solutions in a AdS ($\phi = -1$) bulk. The thin-dark line have $\sigma = -1.2$, thin-light lines have $\sigma = 0.8$, thick-dark line have $\sigma = 0$ and the thick-light lines have $\sigma = 1.2$.

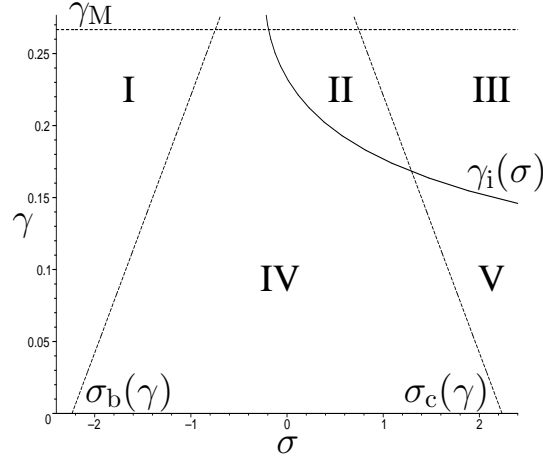


Figure 4.18: The (σ, γ) plane for solutions in a AdS ($\phi = -5$) bulk. The top horizontal line is the bound from the initial bound in Eq. (4.10).

- *II* : $\sigma_i < \sigma \leq \sigma_c$, $\gamma_i < \gamma \leq \gamma_M$. GBIG 1 and GBIG 2 do not exist. GBIG 3 expands to μ_c and then collapses. When $\sigma = \sigma_c$ GBIG 3 evolves to a Minkowski universe.
- *III* : $\sigma > \sigma_c$, $\gamma_i < \gamma \leq \gamma_M$. GBIG 1 and GBIG 2 do not exist. GBIG 3 evolves to h_∞ .
- *IV* : $\sigma_b < \sigma \leq \sigma_i$ and $\sigma_b < \sigma \leq \sigma_c$; $\gamma \leq \gamma_M$ and $\gamma \leq \gamma_i$. GBIG 1 and GBIG 2 do not exist. GBIG 3 expands to μ_c and then collapses. When $\gamma = \gamma_i$ (and for $\sigma = \sigma_i$) GBIG 1 and GBIG 2 both live at $(0, h_\infty)$. When $\sigma = \sigma_c$ GBIG 3 evolves to a Minkowski universe.
- *V* : $\sigma > \sigma_c$, $\gamma \leq \gamma_i$. GBIG 1-3 evolve to h_∞ . When $\gamma = \gamma_i$, GBIG 1-2 both live at $(0, h_\infty)$.

As we decrease the value of ϕ , region II in Fig. 4.18 shrinks (the point $\sigma_i(\gamma_M)$ becomes increasingly positive). For $\phi \leq -64/9$ region II no longer exists. The nature of the solutions in the other regions are unaffected.

There are no bouncing solutions in this case (in fact for any case with $\phi \leq -9/4$) as GBIG 4 is unallowed and $\gamma_M < \gamma_m$ (which rules out the combined solutions). In Fig. 4.19 we show the h_∞ results for $\phi = -5$.

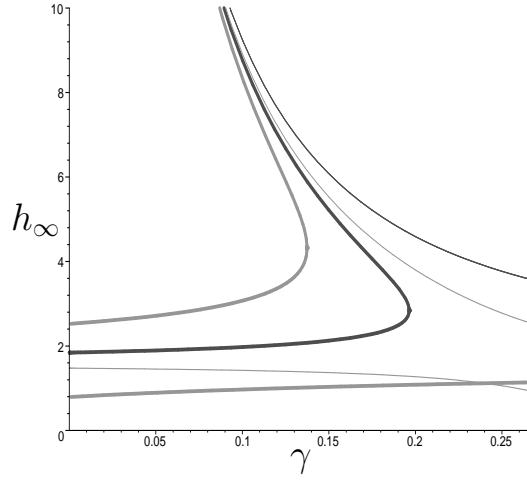


Figure 4.19: h_∞ for solutions in a AdS ($\phi = -5$) bulk. The thin-dark line has $\sigma = -3$, thin-light lines have $\sigma = -1/2$, thick-dark lines has $\sigma = 1/2$ and the thick-light lines has $\sigma = 3$.

4.4 Conclusions

In this chapter we have looked at the general GBIG model. We have seen that there is a range of possible dynamics that can be achieved depending on the parameters in the model. The main model of interest is still GBIG 1 as this is the one that starts in a finite density “quiescent” singularity and evolves to a de Sitter universe. If we warp the bulk enough, GBIG 1 can be allowed to collapse back to its initial density, provided there is sufficient negative brane tension. If the bulk is warped enough to allow GBIG 1 to collapse this means that the bouncing cosmology GBIG 4 can no longer exist. The exact nature of the late time dynamics can be changed by including a non-zero brane tension. A negative brane tension can reduce the Hubble rate at late time and a positive tension will increase it. GBIG 1 can end in a future “quiescent” singularity with a non-zero density if we have an appropriate (negative) brane tension present. As the solution of interest is GBIG 1 and we want it to provide the late time acceleration that we are experiencing it needs to end as a vacuum de Sitter universe. Therefore if there is some brane tension it must take values $\sigma_i > \sigma > \sigma_e$.

GBIG 2 also starts in a “quiescent” singularity but it super-accelerates so it is unphysical and of little interest.

GBIG 3 still starts in an infinite density big-bang but has a number of possible late time dynamics. In a Minkowski bulk GBIG 3 can either evolve to a Minkowski state, as shown in Chapter 3, a vacuum de Sitter state or even loiter around $\mu = -\sigma$ before ending in a vacuum de Sitter state or a “quiescent” singularity. This loitering cosmology

is different from that in Ref. [69], as we do not require a naked bulk singularity or a de Sitter bulk. If we warp the bulk then GBIG 3 will generally collapse, unless there is sufficient (positive) brane tension to allow the solution to end in a vacuum de Sitter state.

GBIG 4 can only ever exist in a mildly warped bulk with negative brane tension. So it can be said that GBIG 4 is unphysical due to the requirement that $\sigma < 0$.

There are a number of bouncing cosmologies within this set-up, in addition to the GBIG 4. There are also the solutions where GBIG 4 and 2 match up ($\gamma_m < \gamma \leq \gamma_M$ with $\phi_{\text{GBIG4Lim}} < \phi < 0$) and the GBIG 2 bouncing cosmologies ($\gamma_m < \gamma \leq \gamma_M$ with $-9 < \phi \leq \phi_{\text{GBIG4Lim}}$). Each of these have different dynamics so would produce different evolutionary histories. The solutions that spend time on the GBIG 2 branch will experience phantom-like behaviour during this period.

Chapter 5

Conclusions

In this thesis we have looked at some brane world cosmological models. The Randall-Sundrum is an interesting toy model of the universe in which we are able to investigate some of the phenomenological properties of string theory ideas. The idea that everything apart from gravity is confined to a four dimensional hypersurface leads to some striking new features.

In chapter 2 we looked at the Kaluza-Klein modes of the graviton in Randall-Sundrum models. We considered the nature of these modes for both Minkowski and de Sitter branes in the Randall-Sundrum one and two-brane models. For two Minkowski branes there is a zero mode and then a series of massive modes. The spacings of these modes are governed by Bessel functions, dependent on the AdS length scale of the bulk and the inter-brane distance. When we send the second brane out to infinity we obtain a continuum of massive Kaluza-Klein modes. In the investigation of two de Sitter branes we saw that there is a zero mode and a mass gap, which is a function of the Hubble rate on the brane, to the first massive mode. We derived a new expression for the mode spacing as a function of associated Legendre functions, dependent on the AdS length scale and the inter-brane distance but also on the Hubble rate on the brane. Therefore they differ in the low energy and high energy limits. Taking the one brane limit we again find a continuum of massive modes.

In chapter 2 we reviewed the 5D bulk equations and how these are projected onto the brane in Randall-Sundrum models. It is the projected equations that are used when we want to understand the cosmological dynamics in these models.

In chapter 3 we briefly reviewed the DGP and GB models before combining the two into GBIG model. The DGP is a very interesting brane world model that much work has been done on, because of the late time acceleration in the DGP(+) branch. This is a very interesting result as the observed acceleration of the universe is usually interpreted via the introduction of a “dark energy” field. The DGP model explains this phenomenon via

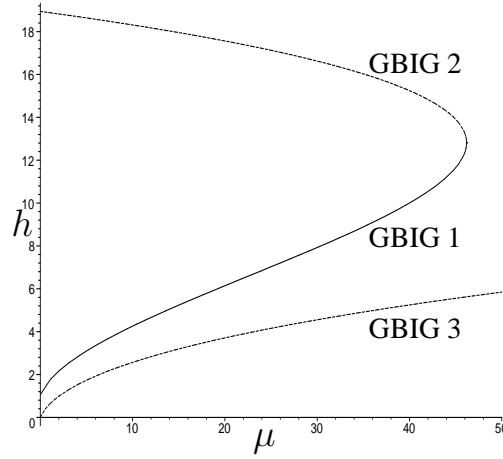


Figure 5.1: The three GBIG models with zero brane tension in a Minkowski bulk.

modified gravity. In the GBIG model we have included the Gauss-Bonnet term in order to modify the high energy dynamics of the universe. The GB term has been shown to arise naturally within a string theory context. Therefore we investigated a model where both the induced gravity on the brane and Gauss-Bonnet terms in the bulk are present. Note, in the context of string theory terms of higher order than the GB term will need to be incorporated at even higher energies, and earlier times.

We have shown that the GBIG model gives some intriguingly distinct phenomenology from that of the DGP and GB models. With a non-zero contribution from both the GB and IG terms we find we have three solutions (in the zero brane tension case), as shown in Fig. 5.1. We have a solution that starts in a finite density big bang and then self accelerates in the future. This is the solution of most interest. The DGP and GB terms do not remove the initial singularity on their own. Only when both sets of terms are present that this feature occurs. It has been shown that a 4D heterotic string using a one loop corrected superstring effective action with GB terms and dilaton and modulus fields can avoid the initial singularity [70].

There is a second GBIG solution which also starts with the finite big bang but then super accelerates. This solution is therefore less relevant. The third solution which starts with a standard big bang singularity evolves to a Minkowski universe. The GBIG model has finite density, pressure and temperature but it does have a curvature singularity at the birth of the universe.

The GBIG model has a severe UV-IR bootstrap which forces γ to be very small in order to have high enough initial redshift. The analysis of Big Bang nucleosynthesis gives us the constraint that γ must be very small. This also means that observations of Big Bang

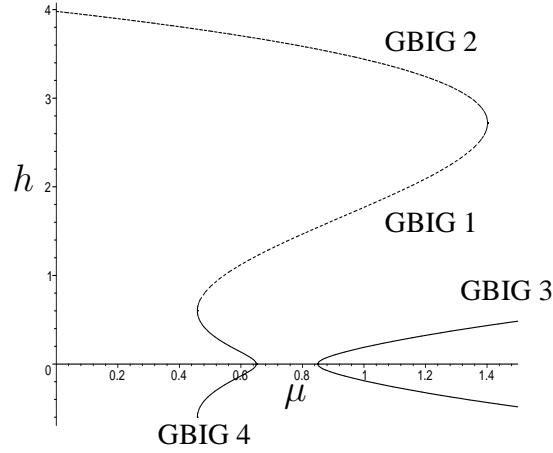


Figure 5.2: Generalised GBIG models with negative brane tension in an AdS bulk.

nucleosynthesis are incapable of discriminating between the GBIG and DGP(+) models. In order to discern between the two models we need to consider the earlier universe where the GBIG model is substantially different from the DGP(+). These differences will be apparent in the analysis of inflation dynamics + perturbations giving rise to formation of structure. The problem of structure formation in the DGP model has been investigated in Ref. [71]. Inflation with Gauss-Bonnet terms in the bulk has been considered in Ref. [59]. In both cases there are substantial unresolved problems to be tackled. Combining the two in the GBIG model will be a difficult but important future line of research.

In chapter 4 we looked at the GBIG model in more generality by including both brane tension and a non zero effective cosmological constant ϕ . We saw that the effect of including brane tension was to shift the solutions (of Fig. 5.1) along the μ axis. The consequence of this is that by including positive brane tension it is possible to make the GBIG 1-2 start at lower densities and end with greater acceleration. It is also possible to make the GBIG 1-2 branches inaccessible. GBIG 3 can now accelerate at late time i.e. the brane tension acts as an effective cosmological constant. Including a negative brane tension causes GBIG 1-2 to start at higher densities and end with less acceleration. If enough tension is added the GBIG 1 model ends in a “quiescent” singularity. GBIG 3 now loiters at a density given by an absolute value of the brane tension. After loitering at this density it will either evolve to a de Sitter solution or the “quiescent” singularity. The time GBIG 3 loiters for is a function of the equation of state w and γ . The exact solution for this time requires further investigation. This loitering solution is of interest as it does not require the presence of a naked bulk singularity or a de Sitter bulk, as other loitering brane cosmologies require.

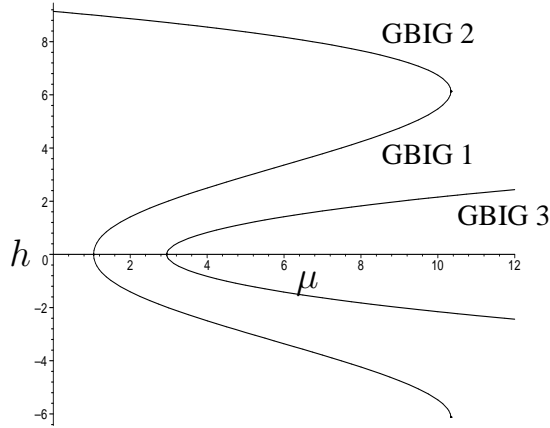


Figure 5.3: Another example of generalised GBIG models with negative brane tension in an AdS bulk.

The effective cosmological constant ϕ modifies the solutions in a more complex way. GBIG 1-2 are not altered in nature only in size. GBIG 3 is the most affected. The GBIG 3 branch is now split in two, as seen in Fig. 5.2. GBIG 3 can now collapse after a minimum density is reached, as long as sufficient brane tension is present. GBIG 4 is a new solution which is only present for a non-zero ϕ which is below a certain threshold. For values of ϕ above this threshold GBIG 4 vanishes and GBIG 1 is allowed to collapse, with sufficient brane tension, Fig. 5.3. GBIG 4 is only accessible with negative brane tension present.

There are a number of constraints on γ . The most important is imposed by the fact that $\Lambda_5 \leq 0$. Another constraint is imposed by requiring GBIG 1 to exist. In the $\sigma = 0$ cases we are constrained by the density of the big bang being greater than zero. With the presence of brane tension we can always have this density greater than zero. Now the constraint on γ comes from the fact that as we increase γ , the GBIG 1 density range decreases. At a certain point GBIG 1 disappears and GBIG 3 ends at a “quiescent” singularity of the same density as the GBIG 2 big bang (this is in the $\phi = 0$ cases; if $\phi \neq 0$ then GBIG 2 meets up with GBIG 4). Increasing γ further allows evolution to continue through this point causing GBIG 2 and 3 to become a single solution.

We have seen that the GBIG model has many possible evolutionary histories depending on the values of the effective cosmological constant ϕ , the brane tension σ and most importantly the contribution of the IG and GB terms in γ . Not all the solutions are physical. Our comprehensive analysis of the dynamics is the starting point for further investigations into the GBIG model, including inflation and structure formation.

The work on the GBIG model in chapter 3 has been cited in a number of papers including [72, 73, 74, 75, 76, 77, 78, 79, 80, 81]. The work in chapter 4 has been cited in [76, 77, 79, 80].

Appendix A

Conventions

The conventions used in this thesis are as follows:

- Greek letters are used for 4D indices.
- Roman letters are used for 5D indices.
- 5D tensor are denoted by superscript (5) with Roman indices.
- The extra dimension is denoted by index y when in a Gaussian-normal coordinate system.
- The extra dimension is denoted by index z when in a Poincaré coordinate system.
- The metric signature is:

$$(-, +, +, +). \tag{A.1}$$

- The Riemann tensor is defined such that for AdS spacetime we have:

$$R_{cd}^{ab} = -\frac{1}{\ell^2} \left(\delta_c^a \delta_d^b - \delta_d^a \delta_c^b \right). \tag{A.2}$$

References

- [1] A. Sevrin, (2004), hep-th/0407023.
- [2] T. Kaluza, Sitzungseber. Press. Akad. Wiss. Phys. Math. Klasse K1 (1921) 966.
- [3] O. Klein, Z. Phys. 37 (1926) 895.
- [4] P. Horava and E. Witten, Nucl. Phys. B460 (1996) 506, hep-th/9510209.
- [5] N. Arkani-Hamed, S. Dimopoulos and G.R. Dvali, Phys. Lett. B429 (1998) 263, hep-ph/9803315.
- [6] D.J.H. Chung, L.L. Everett and H. Davoudiasl, Phys. Rev. D64 (2001) 065002, hep-ph/0010103.
- [7] I. Antoniadis et al., Phys. Lett. B436 (1998) 257, hep-ph/9804398.
- [8] R. Maartens, Living Rev. Rel. 7 (2004) 7, gr-qc/0312059.
- [9] L. Randall and R. Sundrum, Phys. Rev. Lett. 83 (1999) 3370, hep-ph/9905221.
- [10] L. Randall and R. Sundrum, Phys. Rev. Lett. 83 (1999) 4690, hep-th/9906064.
- [11] U. Gen and M. Sasaki, Prog. Theor. Phys. 105 (2001) 591, gr-qc/0011078.
- [12] J. Garriga and T. Tanaka, Phys. Rev. Lett. 84 (2000) 2778, hep-th/9911055.
- [13] B. Bertotti, L. Iess and P. Tortora, Nature 425 (2003) 374.
- [14] A. De Felice, G. Mangano and M. Trodden, (2005), astro-ph/0510359.
- [15] W.D. Goldberger and M.B. Wise, Phys. Rev. Lett. 83 (1999) 4922, hep-ph/9907447.
- [16] A. Perez-Lorenzana, (2004), hep-ph/0406279.
- [17] C. Csaki, (2004), hep-ph/0404096.
- [18] D. Langlois, Astrophys. Space Sci. 283 (2003) 469, astro-ph/0301022.

- [19] P. Brax and C. van de Bruck, *Class. Quant. Grav.* 20 (2003) R201, hep-th/0303095.
- [20] Y.b. Kim et al., *J. Kor. Astron. Soc.* 37 (2004) 1, hep-th/0307023.
- [21] D. Langlois, (2002), gr-qc/0207047.
- [22] R.M. Wald, *General Relativity* (The University of Chicago Press, Chicago, US, 1984).
- [23] W. Israel, *Nuovo Cim.* B44S10 (1966) 1.
- [24] G.N. Felder, A.V. Frolov and L. Kofman, *Class. Quant. Grav.* 19 (2002) 2983, hep-th/0112165.
- [25] D. Langlois, R. Maartens and D. Wands, *Phys. Lett.* B489 (2000) 259, hep-th/0006007.
- [26] I. Gradshteyn and I. Ryzhik, *Table of Integrals, Series, and Products* (Academic Press, London, UK, 1994).
- [27] P. Binetruy et al., *Phys. Lett.* B477 (2000) 285, hep-th/9910219.
- [28] D. Ida, *JHEP* 09 (2000) 014, gr-qc/9912002.
- [29] H. Collins and B. Holdom, *Phys. Rev.* D62 (2000) 105009, hep-ph/0003173.
- [30] C. Barcelo and M. Visser, *Phys. Lett.* B482 (2000) 183, hep-th/0004056.
- [31] R. Gregory, V.A. Rubakov and S.M. Sibiryakov, *Phys. Rev. Lett.* 84 (2000) 5928, hep-th/0002072.
- [32] G.R. Dvali, G. Gabadadze and M. Porrati, *Phys. Lett.* B485 (2000) 208, hep-th/0005016.
- [33] Y.V. Shtanov, (2000), hep-th/0005193.
- [34] C. Deffayet, *Phys. Lett.* B502 (2001) 199, hep-th/0010186.
- [35] J.E. Kim, B. Kyae and H.M. Lee, *Nucl. Phys.* B582 (2000) 296, hep-th/0004005.
- [36] Y.M. Cho and I.P. Neupane, *Int. J. Mod. Phys.* A18 (2003) 2703, hep-th/0112227.
- [37] C. Charmousis and J.F. Dufaux, *Class. Quant. Grav.* 19 (2002) 4671, hep-th/0202107.
- [38] S. Nojiri, S.D. Odintsov and S. Ogushi, *Int. J. Mod. Phys.* A17 (2002) 4809, hep-th/0205187.

- [39] S.C. Davis, Phys. Rev. D67 (2003) 024030, hep-th/0208205.
- [40] E. Gravanis and S. Willison, Phys. Lett. B562 (2003) 118, hep-th/0209076.
- [41] J.E. Lidsey and N.J. Nunes, Phys. Rev. D67 (2003) 103510, astro-ph/0303168.
- [42] K.i. Maeda and T. Torii, Phys. Rev. D69 (2004) 024002, hep-th/0309152.
- [43] M. Sami and V. Sahni, Phys. Rev. D70 (2004) 083513, hep-th/0402086.
- [44] S. Tsujikawa, M. Sami and R. Maartens, Phys. Rev. D70 (2004) 063525, astro-ph/0406078.
- [45] S. Nojiri and S.D. Odintsov, Gen. Rel. Grav. 37 (2005) 1419, hep-th/0409244.
- [46] T.G. Rizzo, JHEP 01 (2005) 028, hep-ph/0412087.
- [47] P. Brax, N. Chatillon and D.A. Steer, Phys. Lett. B608 (2005) 130, hep-th/0411058.
- [48] N.E. Mavromatos and E. Papantonopoulos, Phys. Rev. D73 (2006) 026001, hep-th/0503243.
- [49] T. Tanaka, Phys. Rev. D69 (2004) 024001, gr-qc/0305031.
- [50] C. Deffayet, Phys. Rev. D71 (2005) 103501, gr-qc/0412114.
- [51] K. Koyama and K. Koyama, Phys. Rev. D72 (2005) 043511, hep-th/0501232.
- [52] J.S. Alcaniz and N. Pires, Phys. Rev. D70 (2004) 047303, astro-ph/0404146.
- [53] M. Fairbairn and A. Goobar, (2005), astro-ph/0511029.
- [54] R. Maartens and E. Majerotto, Phys. Rev. D74 (2006) 023004, astro-ph/0603353.
- [55] E. Kiritsis, N. Tetradis and T.N. Tomaras, JHEP 03 (2002) 019, hep-th/0202037.
- [56] E. Papantonopoulos and V. Zamarias, JCAP 0410 (2004) 001, gr-qc/0403090.
- [57] D. Lovelock, J. Math. Phys. 12 (1971) 498.
- [58] S.C. Davis, Phys. Rev. D72 (2005) 024026, hep-th/0410065.
- [59] J.F. Dufaux et al., Phys. Rev. D70 (2004) 083525, hep-th/0404161.
- [60] R.A. Brown et al., JCAP 0511 (2005) 008, gr-qc/0508116.
- [61] R.A. Brown, (2006), gr-qc/0602050.

- [62] G. Kofinas, R. Maartens and E. Papantonopoulos, JHEP 10 (2003) 066, hep-th/0307138.
- [63] M. Bouhmadi-Lopez, unpublished notes. .
- [64] C. Deffayet et al., Phys. Rev. D66 (2002) 024019, astro-ph/0201164.
- [65] Y. Shtanov and V. Sahni, Class. Quant. Grav. 19 (2002) L101, gr-qc/0204040.
- [66] J.D. Barrow, Class. Quant. Grav. 21 (2004) L79, gr-qc/0403084.
- [67] P. Burikham, JHEP 02 (2005) 030, hep-ph/0502102.
- [68] D.N. Spergel et al., (2006), astro-ph/0603449.
- [69] V. Sahni and Y. Shtanov, Phys. Rev. D71 (2005) 084018, astro-ph/0410221.
- [70] I. Antoniadis, J. Rizos and K. Tamvakis, Nucl. Phys. B415 (1994) 497, hep-th/9305025.
- [71] K. Koyama and R. Maartens, JCAP 0601 (2006) 016, astro-ph/0511634.
- [72] J.E. Lidsey and D. Seery, Phys. Rev. D73 (2006) 023516, astro-ph/0511160.
- [73] E. Papantonopoulos, (2006), gr-qc/0601011.
- [74] E.J. Copeland, M. Sami and S. Tsujikawa, (2006), hep-th/0603057.
- [75] T.G. Rizzo, (2006), hep-ph/0603242.
- [76] P.S. Apostolopoulos and N. Tetradis, (2006), hep-th/0604014.
- [77] C. de Rham and A.J. Tolley, JCAP 0607 (2006) 004, hep-th/0605122.
- [78] G. Panotopoulos, (2006), astro-ph/0606249.
- [79] L. Fernandez-Jambrina and R. Lazkoz, (2006), gr-qc/0607073.
- [80] E. Papantonopoulos and V. Zamarias, (2006), gr-qc/0608026.
- [81] K. Farakos and P. Pasipoularides, (2006), hep-th/0610010.